Republic of Iraq

Ministry of Higher Education and Scientific Research

University of Kerbala /College of Engineering

Civil Engineering Department

Structural Behaviour of Damaged High Strength Reinforced Concrete Short Columns Rehabilitated by CFRP Under Eccentric Loading

A Thesis
Submitted to the College of Engineering at the University of Kerbala
for the Partial Requirements for the Degree of Master of Science in
General Civil Engineering

Prepared by:

Ahmed Hassan Jabbar

(B. Sc. in Civil Engineering-2003)

Supervised by:

Assist Prof. Dr. Sadjad Amir Hemzah

Assist Prof. Dr. Wajde Shobar Saheb

2021 AD   **1443 AH**

بِسْمِ اللَّهِ الرَّحْمَٰنِ الرَّحِيمِ

وَقُلِ ٱعْمَلُوا۟ فَسَيَرَى ٱللَّهُ عَمَلَكُمْ وَرَسُولُهُۥ وَٱلْمُؤْمِنُونَ ۖ وَسَتُرَدُّونَ إِلَىٰ عَٰلِمِ ٱلْغَيْبِ وَٱلشَّهَٰدَةِ فَيُنَبِّئُكُم بِمَا كُنتُمْ تَعْمَلُونَ

صدق الله العلي العظيم

ACKNOWLEDGEMENTS

In the name of ALLAH, the most compassionate, the most merciful.

Supervisor certificate

I certify that this thesis entitled "Structural Behaviour of Damaged High Strength Reinforced Concrete Short Columns Rehabilitated by CFRP under eccentric Loading", which is prepared by " Ahmed Hassan Jabbar ", is under our supervision at University of Kerbala in partial fulfilment of the requirements for the degree of Master of Science in Civil Engineering (Structure Engineering).

Signature:

Asst. Prof. Dr. Sadjad Amir

Hemzah

(Supervisor)

Signature:

Assist Prof. Dr. Wajde Shober

Alyhya

(Supervisor)

Linguistic certificate

I certify that this thesis entitled "Structural Behaviour of Damaged High Strength Reinforced Concrete Short Columns Rehabilitated by CFRP under eccentric Loading", which is prepared by " Ahmed Hassan Jabbar ", is under my linguistic supervision. It was amended to meet the English style.
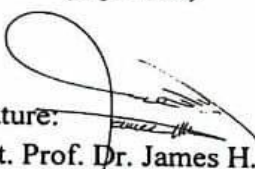
Signature: 2021 \10\24
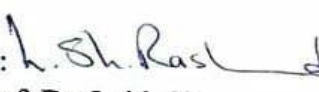
Name: Dr. Muhammad Abdulredha
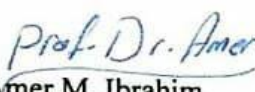
Examination committee certification

We certify that we have read the thesis entitled " Structural Behaviour of Damaged High Strength Reinforced Concrete Short Columns Rehabilitated by CFRP under eccentric Loading" and as an examining committee, we examined the student "Ahmed Hassan Jabbar" in its content and in what is connected with it and that in our opinion it is adequate as a thesis for the degree of Master of Science in Civil Engineering (Structural Engineering).

Signature:

Assist. Prof. Dr. Sadjad Amir Hemzah

(Supervisor)

Signature:

Assist. Prof. Dr. James H. Haido

(Member)

Signature:

Assist Prof. Dr. Wajde Shober Alyhya

(Supervisor)

Signature: L. Sh. Rasl

Assist. Prof. Dr. Laith Sh. Rasheed

(Member)

Signature: Prof. Dr. Amer

Prof. Dr. Amer M. Ibrahim

(Chairman)

Approval of the Department of Civil Engineering	Approval of Deanery of the College of Engineering -University of Karbala
Signature: Name: Dr. Raid R. A. Almuhanna (Head of civil Engineering Dept.) Date 26 /10/ 2021	Signature: L. Sh. Ras Name: Assist. Prof. Dr. Laith Sh. Rasheed (Dean of the College of Engineering). Date: / / 2021

Abstract

The strengthening process for any structural member, such as columns, has become one of the most standard solutions for building restoration in the world, which might be carried out for several reasons, including: change in use, failure in steel, over loads and/or cruel weather conditions. This research aims to investigate experimentally and numerically the structural behaviour of partially loaded high strength short concrete columns strengthened with CFRP strips. In this study, Nine columns with a square cross-section (100×100) mm and height of 800 mm with two corbel heads were prepared and tested under eccentric load with an eccentricity of 50 mm from the center (e/h=0.5). One column, which is designated by CC, was tested to failure and considered as a control column. In contrast, the other eight columns were divided into two groups of four identical columns. The first group of columns was loaded by 25% of their ultimate design loads, while the second group was loaded by 50%. Then, all the partially loaded specimens in the two groups were strengthened with various schemes of CFRP based on the initial loading ratios, which is represented as follows: full by direction longitudinal wrapping with CFRP in all sides of the column, full longitudinal wrapping with CFRP for tension side only, full by direction horizontal wrapping with CFRP for clear column height and partial horizontal wrapping with CFRP for 250 mm length at column mid-height.

The experimental results for specimens strengthened with a full by longitudinal direction wrapping on all sides and for the tension side only of the columns in group one recorded the ultimate load capacity increases by 65.55% and 44.82 %, respectively, compared to CC. In addition, the ultimate load capacity for the strengthened columns in the second group With the same strengthened schemes increased by 44.83%, 37.93 %, respectively, compared to CC. Further, the ultimate load capacity for the specimens strengthened with full or partial

horizontal encapsulation increased of the two groups by 24.14, 20.69, 13.79, and 10.34 %, respectively.

The finite element method (ABAQUS) was used to verify the structural behaviour of partially loaded high strength short square columns strengthened with CFRP strips, which were experimentally tested earlier. Results showed a good agreement between the experimental and numerical results regarding the ultimate load capacity and load-horizontal and vertical deflection curves. The mean difference in the ultimate load capacity and maximum deflection horizontal and vertical were (6.28%, 7.38%, 6.24 %), respectively, which ensure the accuracy of the numerical solution.

Additional parameters were suggested to be investigated numerically by the verified model: the effect of increasing CFRP layers, the impact of different load eccentricities (e/h), the effect of various initial loading rates, and the effect of increasing the width for CFRP. The numerical results illustrated that Increasing the number of CFRP layers to two or three layers, presented in full longitudinal wrapping with CFRP for all column faces increased significantly the ultimate load capacity by 83.08% and 109.45%, respectively, compared with CC. Furthermore, decreasing in the deflection for eccentricity load (e/h) from (0.5 to 0.35) led to obtained high ultimate load by 54.62% for specimens fully longitudinal strengthened. On the other hand, increasing the percentage of initial loading from 50% to 80% caused a slight reduction in the ultimate load by 9.23% and 11.92%, respectively, for control column and specimens fully longitudinal strengthened with CFRP sheets. Moreover, increasing the width for CFRP sheets for partial horizontal wrapping caused a slight increase in the ultimate load.

List of Contents

List of Figures

List of Plates

List of Tables

Notation

Symbol	Description
Ag	Cross-sectional area of a section (mm^2)
Ac	The cross-sectional area of the concrete (mm^2)
As	The cross-sectional area of steel reinforcement (mm^2)
$A\bar{s}$	The cross-sectional area of steel reinforcement (mm^2)
E_c	Concrete modulus of elasticity (GPa)
E_s	Steel modulus of elasticity (GPa)
f_{cu}	Concrete compressive strength (MPa)
f_y	Yield strength of steel reinforcement (MPa)
f_{sy}	Strength of steel reinforcement (MPa)
f_{su}	The ultimate strength of steel reinforcement(MPa)
f_{st}	Splitting tensile strength of concrete(MPa)
a	The total length of column (mm)
b	Total width of column (mm)
db	Dimeter of steel reinforcement
P	Maximum applied load (kN)
P_u	Ultimate load (kN)
ϕ	Size of bar diameter (mm)

Abbreviations

Symbol	Description
HSC	High-strength concrete
CFRP	Carbon fibre reinforcement polymer
ABAQUS	Finite element package
NC	Normal concrete
ACI	American concrete institute
ASTM	American society for testing and materials
BS	British standard
et al.	Others
FRP	Fibre reinforcement polymer
FEA	Finite element analysis
IQS	Iraqi specification
MPa	Mega Pascal (N/mm^2)
No.	Number
mm	Millimetre
NSM	Near-surface mounted
RC	Reinforced concrete
GFRP	Glass fibre reinforcement polymer

Chapter one
Introduction

1.1   Introduction

Columns are structural elements designed to withstand internal loads and transfer them to the foundations for any existing building. They usually have strong properties such as excellent strength, stiffness and ability. However, over design loads and unfavourable weather conditions surrounding the columns may cause deterioration, especially exterior columns. These deteriorations include cracks, concrete peeling off, internal reinforcement deterioration and loss of properties of some materials used in concrete. These can lead to column collapse resulting in a significant risk to the structure **(Olivova and Bilcik, 2009)**. The potentially damaged columns require repairing to improve their structural properties such as strength, ductility and stiffness.

1.2 Damaged Columns

In general, various structural members are exposed to several conditions that might cause losing their functionality, including **(Parvin and Brighton, 2014)**:

1. Natural disasters like earthquakes and hurricanes can damaged the building, as shown in the Fig. (1. 1).

2. Over design loads and fire can cause damage to the columns.

3. Ancient buildings were built in the past and constructed according to non-replaced codes and not concerning new updates. Such buildings should thus be renovated, particularly if there are specific issues, following the current design criteria.

4. Exposure to salt water, aggressive solutions, and/or freezing-thawing cycles on buildings for an extended period.

Generally, columns are exposed to different loads, including axial compression load and bending moments that could cause various failure modes such as inclusive flexural failure and/or shear failure before or after yielding the primary reinforcement **(Yoshikawa and Miyagi, 2001)**.

Fig 1.1 Samples of damaged columns caused by earthquakes

1.3 Columns Rehabilitation

The rehabilitation process for any structural member, such as columns in an existing building, has become one of the most widely standard solutions for building restoration in the world. However, most structural members, such as columns, in particular, might require enhancement for several reasons, including:

1. Increase the number of floors of a specific building or the vehicle loads of a particular bridge (i.e. increasing the live loads);
2. Strengthen structural members, which are constructed and/or designed in compliance with old codes;

2

3. Increase building's vulnerability to the intensity caused by earthquakes and wind;

4. Replace damaged or corrosive reinforcing steel;

5. Strengthen joints between structural components, especially in precast concrete **(Ibrahim and Mahmood, 2009)**.

Several techniques were used to restore and strengthen damaged columns and/or increase their structural behaviours in the last centuries. These techniques include concrete jacketing, carbon fibre reinforced polymer (CFRP) laminate, and near-surface mounted rebars (NSM). Concrete jacketing is one of the oldest methods that are used for improving damaged columns. Although this method provides high resistance and increases the column's bearing strength, stiffness, and ductility, it is increase the column's cross-sectional area and cause corrosion to the steel reinforcement, resulting in a limited bond with the concrete (**G. Lin and Teng, 2016**).

Strengthening by CFRP laminate is another commonly used approach with many benefits, including excellent mechanical properties, significant corrosion resistance, usability and substantial durability. This technique can be applied in several formats, including external wrapping, sheets, fabric or spraying. It is worth mentioning that CFRP sheets are commonly used to strengthen and sustain damaged columns, exceptionally rounded columns because it is simple to perform **(Haji et al. 2018)**.

The strengthening technique by wrapping the CFRP laminates requires preventing stress concentration in a specific position on the laminates, leading to their failure. For this, it is preferable to round the corners of rectangular and square columns to avoid the stress concentration in these positions, as shown in Fig.(1.2) **(Parvin and Brighton, 2014)**.
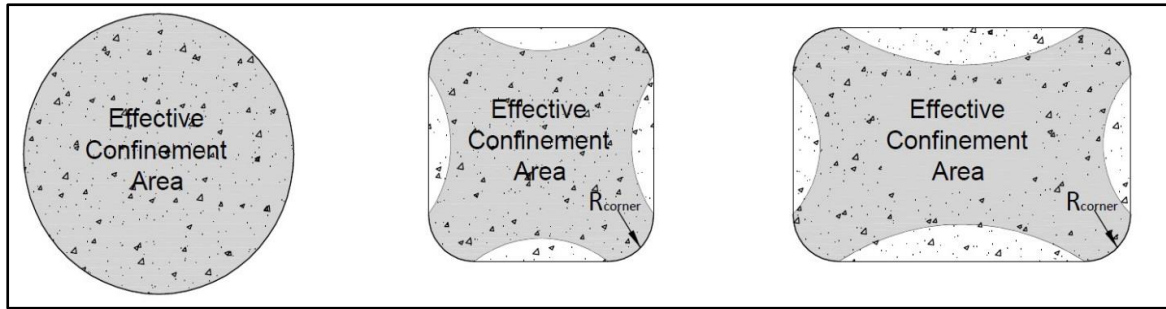
Fig. 1.2. Effect of confinement by CFRP (Parvin and Brighton, 2014)

In the same regard, the extra lateral moment in reinforced concrete columns, resulting from the eccentric compression loads, can dramatically reduce the axial load strength. Furthermore, most existing steel and concrete jacketing systems do not necessarily fulfil revised code provisions performance criteria due to the increase in seismic load, ageing, and damage; thus, it needs improvement. The vast amount of work and time necessary for implementation makes traditional enrichment activities such as steel and concrete jacketing less common **(Garzon-Roca et al., 2012; Chai et al., 1994)**. FRP and NSM strengthening have been widely used in the last three decades to improve the performance of RC columns axial compression, torsion and shear loads. There are two common types of strengthening: (1) FRP to external axial compression resistance and shear load containment and (2) NSM to bending resistance. The containment of RC columns leads to better compliance with eccentric compression loads with high strength. **(Hadi and Widiarsa, 2012; Lignola et al, 2007; Wu and Wei, 2010)**

1.4 High-Strength Concrete (HSC)

HSC columns have become increasingly used popularly in recent years, particularly in high-rise buildings **(Kottb et al., 2015)**. HSC is defined by the as concrete that has a strength of 41MPa. Subsequently, the concrete was classified as high strength with a compressive strength of more than 62 MPa. More recently, compressive strengths approaching 138 MPa have been used in cast-in-place buildings) **(ACI-363 R, 2019)**

Because of their greater strength and superior material performance, HSC columns have become more popular during the last two decades. However, advances in strength come at the expense of deformation. Indeed, HSC columns are brittle, putting their application in seismically active areas in jeopardy. Concrete deformation can be improved by confining it. Concrete that has appropriately been wrapping can create sufficient ductility **(Ozbakkaloglu and Saatcioglu 2006).**

Due to its superior durability and long lifespan, HSC is recommended in structures subjected to a harsh environment and column construction, medium and long span-lift bridges and heavily loaded reinforced concrete off-shores structures. HSC has been used in Kuala Lumpur, Malaysia; for example, Petronas Towers 1 and 2. HSC has also been designed in the columns and walls with compression strength up to 70 MPa.

In addition to its widespread use in recent years, HSC is better than normal concrete (NC) due to its superior mechanical and durability properties and low porosity. Superplasticizers, additional cementing materials, silica fume, furnace slag and natural pozzolan can provide the superior properties of HSC. Fortunately, most of these materials are industrial by-products, which can help reduce the amount of cement needed to produce concrete. **(Shannag, 2000)**.

1.5 Advantages of HSC

HSC has several benefits over NC, such as **(Kusumawardaningsih and Hadi, 2010; Yazici, 2012; Priestley and Hoshikuma, 2000)**

1- High compressive strength as it could be approximately (3-7) times higher than NC;

2. Standards of elasticity of HSC is nearly two times greater than NC, which means lower deformations value;

3. Higher durability;

4. The dimensions of sections with HSC are smaller compared to NC, which allow the reduction in the dead load and the increase in the spaces of structural elements;

5. HSC columns with a hollow section are often used in long bridges due to their light weight.

1.6 Disadvantages of HSC

There are some of the drawbacks of the HSC, such as **(Hadi, 2002; Buckle and Friedland, 1994)**

1. brittle than NC ;

2. The sudden collapse of the concrete, since the fracture occurs through the rough aggregate and not around it;

3. The higher compressive strength increases, the brittleness upon failure, and the deformation capacity of the sections decreases compared to NC, which is a significant disadvantage of using HSC;

4. It is not desirable to use it in seismically active areas due to the inflexibility of deformations of concrete structures and the lack of energy dissipation.

1.7 Research Aims

The following points represent a summary of the objectives of this research:

1. Investigate the structural behaviour of partially damaged high strength concrete columns strengthened with CFRP laminates experimentally and numerically using finite element analysis.

2. Studying the effect of strengthening technique by CFRP sheets for various schemes on columns and compare their results.

1.8 Thesis Layout

This thesis involves six chapters. The first chapter provides a general introduction about columns and their potential damages, as well as the strengthening methods in addition to the development and importance of high-strength concrete (HSC). The second chapter demonstrates a literature review related to this research, such as the use of several types of concrete, especially HSC, in producing columns as a structural member in addition to all techniques used to strengthen columns. The third chapter explains the studied models, the materials, the preparation of HSC, and the proposed strengthening techniques for the column. At the same time, the fourth chapter clarifies the experimental results and their discussions. The fifth chapter illustrates the numerical analysis of the studied models by finite element to build a verified model that reasonably predicts the new proposed case studies. Finally, the sixth chapter represents the conclusions of the research and recommendations for future work.

CHAPTER TWO
LITERATURE REVIEW

2.1 Introduction

Most buildings use columns and knowing how much capacity a building has depends on accurately evaluating the expected capability of each column. Any kind of structural building necessitates reinforced concrete columns. They must be constructed to support beams and slabs safely and also bear weight to the foundations. This chapter explains and summarises the research in which the structural behaviour of HSC columns has been studied and their outcomes compared to NC. In addition, column strengthening technologies were also presented to increase their strength, rigidity and ductility, such as CFRP and GFRP sheets, NSM rebar, or both.

2.2 High-Strength Concrete (HSC): Production and Benefits

The development of high strength concrete (HSC) was gradual over many years. The definition of HSC has been changed due to its continuous development. In the 1950s, concrete with compressive strength larger than 34 MPa was considered as HSC. Later, in the 1960s and 1970s, concrete with a compressive strength of 62 MPa was produced and considered HSC. Recently, the concrete with compressive strength reaching 138 MPa has been used in cast-in-place structures. The applications of HSC have been increasingly growing due to the development of materials and additives. The use of HSC in civil structures leads to selecting smaller sections, longer spans, and lower dead load (ACI-363R, 2019).

HSC has increased usage in the construction industry because it offers superior strength and performance compared to NC. When using HSC, stronger concrete can be created. Indeed, using hollow structural members can maximise strength capacity and stiffness ratios while minimising weight, reducing the structure's overall budget. Furthermore, HSC structural members show brittle behaviour in failure, which impairs their ability to withstand deformation. Nevertheless, adequate transverse reinforcement or FRP design can eliminate this deformation, as explained in Fig. (2.1) **(Kusumawardaningsih and Hadi (2010))**.

Fig 2. 1. Typical failure of in wrapped columns. (Kusumawardaningsih and Hadi (2010))

2.3 Studies on the Structural Performance of HSC Columns

In this part, an investigation has been implemented on previous research that discusses the structural behaviour of columns made with HSC. Most studies dealt with the proportions of materials and the description of HSC.

In 1994, **Cusson et al.** examined the behaviour of large-scale reinforced concrete columns limited by rectangular links under concentric loading. The fundamental changes studied in this research program that influence the outcome included concrete compressive strength, tie spacing, longitudinal reinforcement, transverse reinforcement, and concrete cover cracking. For HSC columns, the concrete cover has been separated unexpectedly, causing a loss in the axial force before the onset of lateral confinement. After the fully spalling of concrete, gains in maximum strength, stiffness, and ductility index were reported for the concrete core of the restricted columns. Figure (2.2) illustrates the overall dimensions of the test specimens and instrumentation.
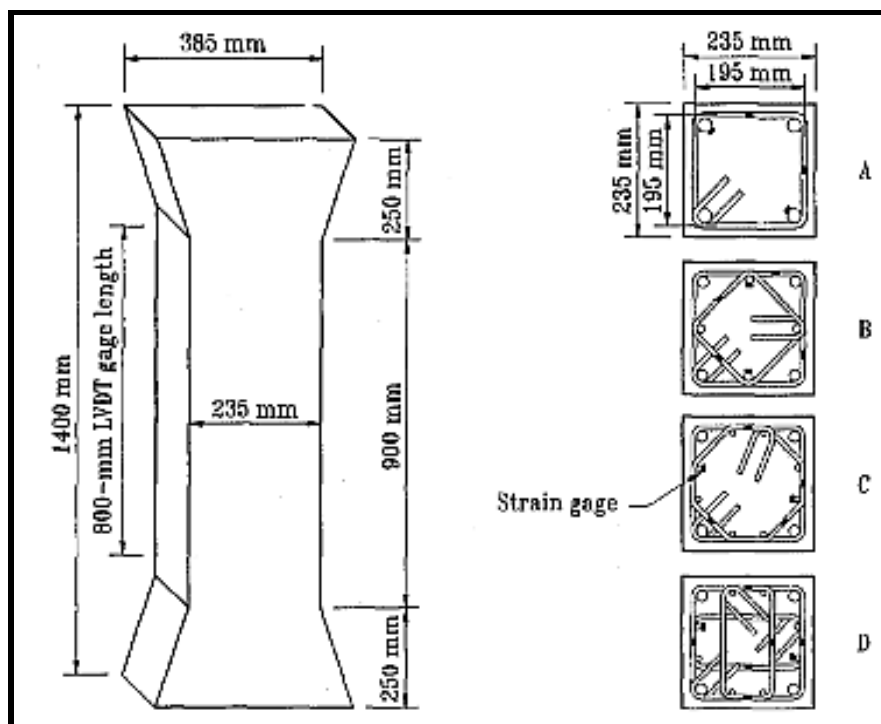
Fig 2. 2. Dimensions of Test Specimens and Instrumentation (Cusson et al., 1994)

Claeson and Gylltoff (1998) conducted an experimental examination of the behaviour of slender RC columns. They tested twelve short square columns of various lengths under eccentric monotonic loading, with compressive strengths of either 50 MPa or 120 MPa. Half of the columns were made using NC, while the other half were cast with HSC. The effect of main variables such as slenderness of the columns, stirrup spacing, concrete strength, and eccentricity of the applied axial load was studied. The strength of the model differed according to the ratios of longitudinal reinforcement to the transverse reinforcement. The results showed that lowering stirrup spacing did not contribute to the loading capacity and the brittle behaviour of HSC columns. Also, the strength of HSC specimens decreased faster than that of NC columns when the deflection increased. In addition, HSC columns had more remarkable bearing ability than NC columns.

Sharma et al. (2005) examined the behaviour of HSC short columns with spiral and square ties under concentric compression. The test variables included longitudinal and transverse reinforcements, characteristics of steel components, the cross-section of the specimen, concrete compressive strength. The results showed higher reinforcement is required in HSC columns than NC to achieve the necessary. For HSC columns, the loss of axial capacity is caused by the unexpected breakage of the concrete cover. Figure (2.3) provides the details of column specimens, reinforcement arrangement and location of the strain gauges.
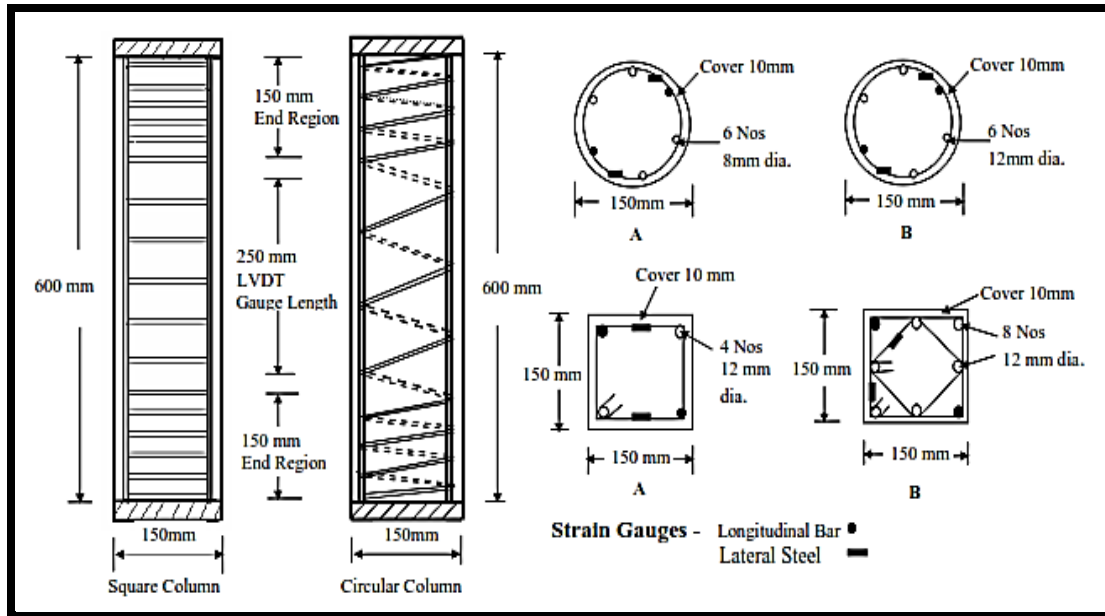
Fig 2. 3. Details of column specimens, reinforcement arrangement and location of strain gauges (Sharma et al. (2005))

In 2011, **Portolés et al.** aimed to determine the effect of using HSC over NC by comparing three performance indices: ductility, stiffness and concrete contribution ratio. They studied thirty-seven thin circular tubular columns from NC and HSC loaded at an eccentric axial load. Several parameters were studied, such as various concrete strengths (35, 50 and 70MPa), the eccentricity to column slenderness per cent, the diameter to thickness per cent and the length to column slenderness ratio. At 50 MPa compressive strength, the experimental loads for each test were compared to the design loads for this investigation. The results show for the limited cases analyzed that the use of high strength concrete for slender composite columns is interesting since this achieves ductile behavior despite the increase in load-carrying capacity is not greatly enhanced.

In 2019, **Ghanim Jumah** tested nine high-strength circular columns of 600 mm in length and 150 mm outer diameter under axial compressive loads to check their strength, three of which were solid as reference. The remaining six columns had internal holes of 50 mm and 75 mm in diameter. The effect of the hole size and longitudinal steel reinforcement's area were studied. The steel area

used was 0, 301 and 471 mm^2, and the two-hole measures were 50 and 75 mm, as shown in Fig. (2.4). Results indicated that increasing the longitudinal reinforcement ratio from 0% (plain) to 2.67% (steel reinforcement area of 471 mm^2) causes an increase in the ultimate strength by 33.6%. In contrast, the ultimate strength for the hollow columns with 75 mm internal holes increased by 33.2 %. Besides, Increase the hole diameter from 50 to 75 mm led to a reduction in the capacity of the column by 33% for columns with 301 mm^2 steel area and to 32 %, for columns with 417 mm^2.
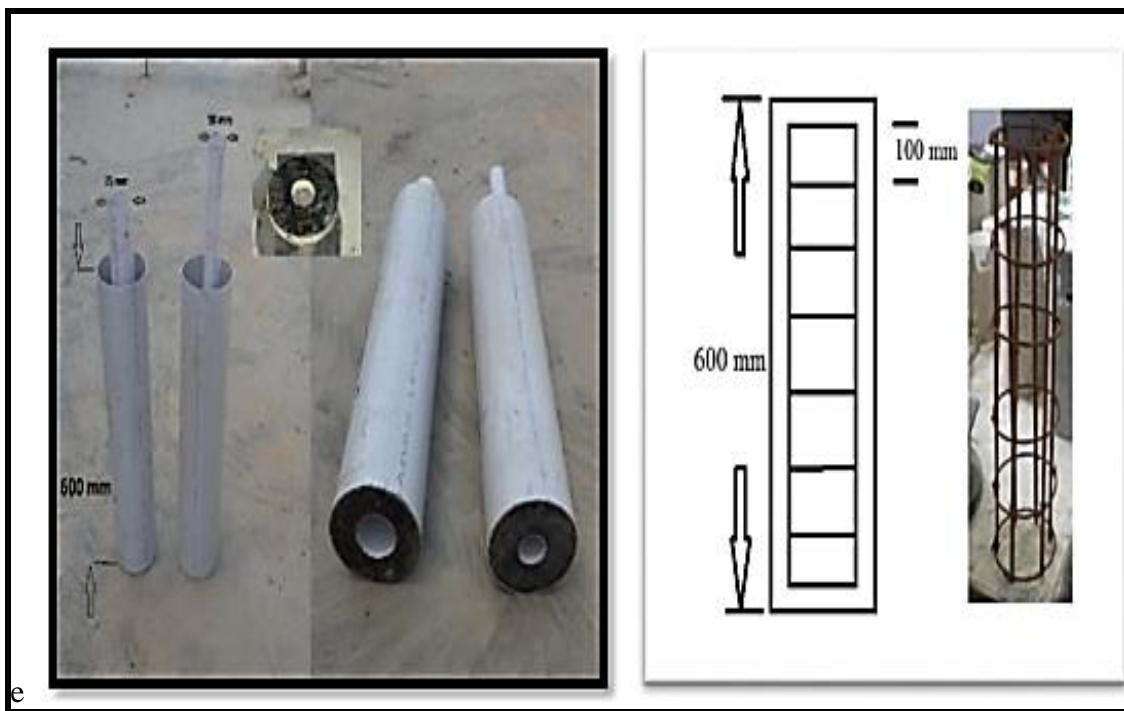
Fig. 2. 4. Set-up and configuration of tested columns (Jumah, 2019)

Taheri et al. (2020) studied eight one-third scale concrete columns designed based on the latest seismic provisions. The columns were loaded to allow vertical and lateral loading to reach 35% of their capacities. Damage states were developed considering the samples attributed to the HSC basis curve, as explained in figure (2.5). Additionally, for the reinforced HSC columns used in unique moment frame systems, a range of deflection ratios and damage index restrictions were developed and employed. Finally, the deflection ratio was compared to various observed damages, such as concrete cover spalling, initial crack, concrete core cracking and longitudinal bar buckling. The findings showed, relative to other levels, that strengthened HSC columns performed better in terms of immediate occupancy and damage level management compared to unstrengthened specimens.
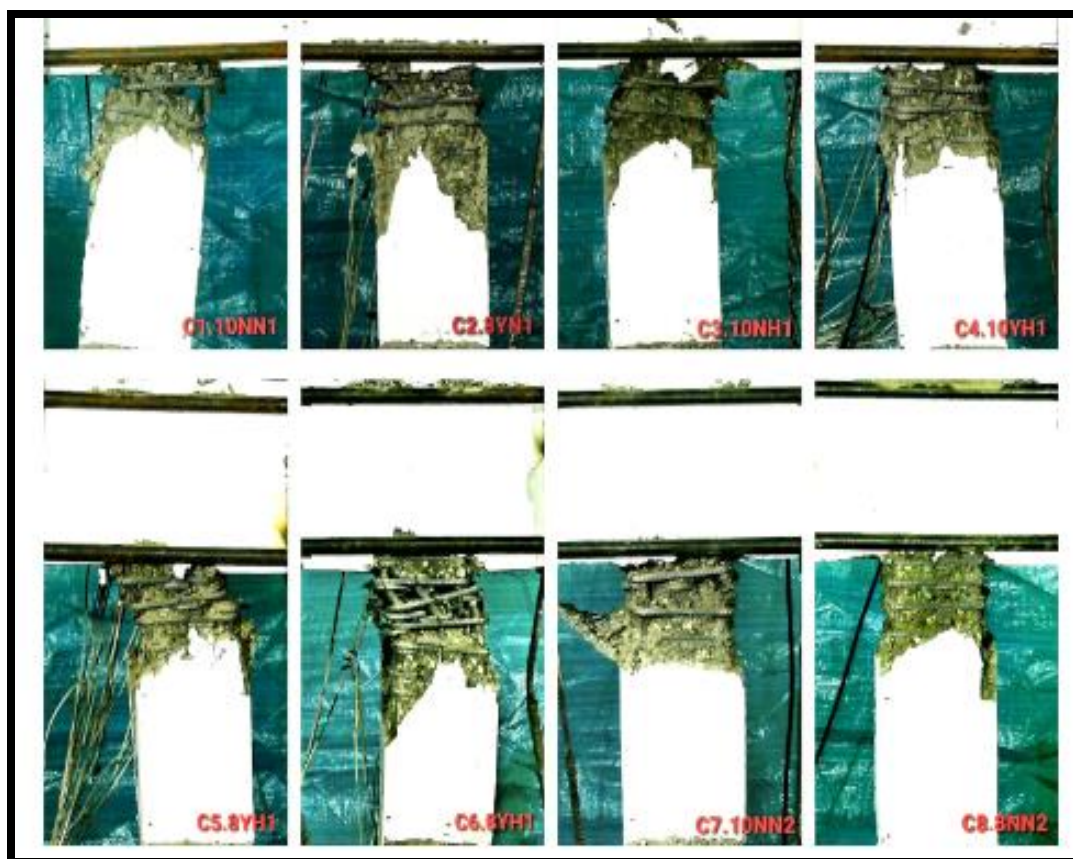
Fig 2. 5. The final damage photos in the central part of specimens (Taheri et al. (2020))

2.4 FRP Strengthening Techniques for Columns

Over the past years, several techniques were used to strengthen the structural behaviour of columns, such as external wrapping by CFRP laminate, GFRP and NSM with FRP system or NSM with steel reinforcement.

In 2006, **Hadi** used CFRP to strengthen concrete columns and other structural elements under eccentric load, and the results were generally acceptable. Plenty of studies have been done on centrally loaded columns, wherein strengthened columns by CFRP under eccentric loading were less common. In the current research, the author presented the results of testing six concrete columns of NC under the influence of an eccentric load. Columns were enveloped with a various number of CFRP layers. The results showed that covering the columns with an appropriate number of CFRP layers will result in better ductility and greater strength than a column strengthened with steel bars.

Furthermore, **Maaddawy (2009)** presented in his paper the outcomes of the experimental testing and analytical program to upgrade eccentrically loaded reinforced concrete columns for the effective evaluation of FRP schemes. A total of 12 reinforced concrete specimens were tested. The column had an overall length of 1200 mm, and the corbel cross-section of each end was (250×250) mm with a length of 350 mm. The dimensions of the tested specimens are illustrated in Fig. (2. 6). In the test area, the sample was (125×125) mm with a 1.9 per cent vertical steel rate. The studied variables were: the confinement condition, full FRP wrap, partial FRP wrap, and deflection ratios (e/h) of 0.3, 0.43, 0.57, and 0.86. Research results showed that as e/h deviation increases, the maximum load of the strengthened specimens decreases. Strengthening columns fully by FRP wrapping increased the maximum load by about 37 % at a ratio e/h of 0.3, against only 3 % at a ratio e/h of 0.86. Also, the strength of partially wrapped specimens was lower by

only 5% than that of fully wrapped specimens. The results of the analytical program showed good convergence with the experimental test.
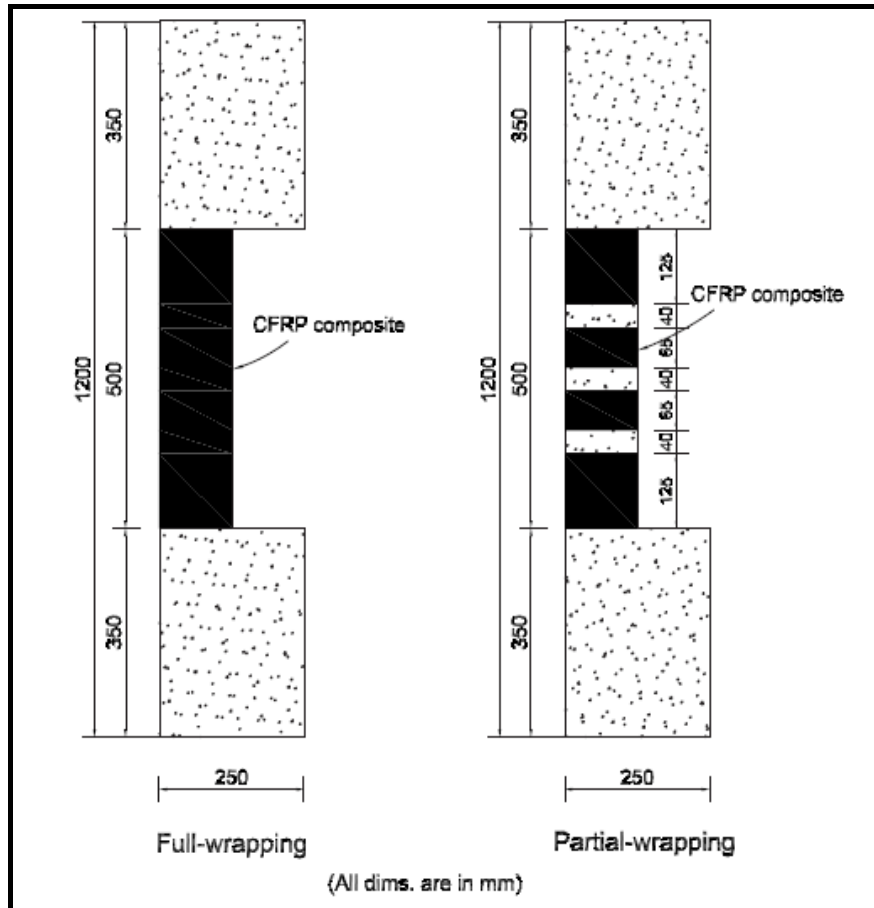
Fig 2.6. CFRP Wrapping Schemes of Column Specimens (Maaddawy, (2009))

Sadeghian et al. (2010) investigated in their experimental studies the structural behaviour of RC columns strengthened with combinations of multiple CFRP layers under various axial load and bending moments. Seven columns with a rectangular cross-section (200×300) mm were prepared and tested until failure under eccentric loading. The average high was 2700 mm for specimens with two corbel heads. Several parameters were studied: the number of CFRP layers (2, 3, and 5 layers), Various CFRP directions (0°, 45°, and 90°), and various eccentricities(e): 200 and 300 mm. The effects of the above parameters on the

load-displacement, the moment-curvature behaviour and the variation of longitudinal and transverse strains on different faces of the columns were studied. Compared with the unstrengthened columns, the results showed a substantial increase in the efficiency of the strengthened columns.

In 2011, **El-maaddawy and El-dieb** studied the structural behaviour of columns strengthened with a hybrid technique that involves assembling between NSM - GFRP rebar with an external wrapping of CFRP laminate. The authors constructed and tested nine 150 mm square cross-section columns under biaxial eccentric loads with various strengthening ways. Test parameters included load eccentricity, concrete compressive strength and the number of CFRP layers employed in conjunction with GFRP–NSM steel rebars. At a lower eccentricity, the gain in load capacity due to the strengthening by NSM-GFRP was more significant. Also, for columns with a low level of CFRP confinement, the increase in the load capacity attributed to the NSM-GFRP reinforcement was higher at a higher eccentricity. The load strength improvement was noticeable in the columns with NC. In contrast, combining GFRP –NSM steel rebars with two layers of CFRP wrapping increased the strength columns.

Torabian (2012) studied short circular NC columns strengthened by CFRP techniques under different eccentricity loads. The author prepared 35 samples with 150 mm and 500 mm in diameter and height, respectively. These columns were categorised into five groups in which each group was under load with an eccentricity of (0, 30, 60, 90, and ∞) mm. Every single group consisted of seven columns, where one of them works as a reference for each group. Other columns were classified as followed: column strengthened with longitudinal layers of CFRP along the perimeter of the cylinder, column reinforced with longitudinal layers of CFRP with eight strips of NSM-CFRP strips, column strengthened with longitudinal layers of CFRP along to the half of the perimeter with four strips of NSM-CFRP strips in the same position, another one

strengthened with a horizontal wrapping of CFRP layers with a width of 110 mm, column assemble between longitudinal layers of CFRP, the last column combined between longitudinal layers of CFRP and NSM-CFRP strips. The results showed that the effectiveness of the reinforced columns by longitudinal layers of CFRP along the perimeter of the cylinder increases as the eccentricity decreases. Using the longitudinal layers with NSM –CFRP strips technique increased the ultimate strength ability of the samples loaded with various eccentricities (0,30,60,90, and ∞). The increases in comparison with the reference column were 8.3, 12.2, 25.8, 36, and 53.3%, respectively. The horizontal layers of CFRP were not helpful when used with longitudinal layers of CFRP or with NSM-CFRP strips.

In 2012 **Sarafraz** strengthened columns with NSM bars and CFRP wrapping techniques to improve the performance of the columns. The columns were exposed to different loads, including compression and bending moments. For this purpose, seven concrete columns were cast in which some of them were strengthened with NSM bars while others were strengthened additionally with an external CFRP wrapping. From the test results of the columns, the researcher concluded that the NSM-CFRP bars technique increases the capability of columns to bending loads. Indeed, increasing the number of NSM bars was found to have a contribution to the bearing resistance. Also, it has been stated that using an additional layer of CFRP can increase the ductility and energy dissipation of the columns. Furthermore, the strengthened columns with NSM-CFRP bars were more robust than the non- strengthened columns, as it prevents buckling of the primary reinforcement and reduces the deterioration of the columns.

In 2012, **Hadi and Widiarsa** conducted an experimental test on concrete specimens strengthened by CFRP strips under eccentric loading. Sixteen samples were prepared and subjected to tests to study the effect of CFRP layers

number, the value of eccentricity, and the presence of vertical CFRP straps. The columns were 200×200×800 mm in dimension and featured round edges with a diameter of 68 mm, as shown in **Fig** (2.7). Twelve specimens were tested as columns under axial compression load, and four specimens were tested as beams under flexural load. The Denison 5000 kN compression testing machine was used to test all the specimens until failure. The outcomes demonstrated that wrapping columns by CFRP improved the load-carrying capacity and ductility under eccentric loading. Furthermore, the application of vertical CFRP strips significantly improved the performance for the columns with large eccentricity.

Fig 2. 7. Typical failure of unwrapped columns (Hadi and Widiarsa (2012))

Waryosh and Rasheed (2012) explained the effect of strengthening concrete specimens with CFRP strips under eccentricity load (axial force and bending moment in combination). The samples tested consisted of 11 columns that had a square cross-section with a dimension of 120 mm. The length of the columns with a 2-headed corbel was 1230 mm. Test parameters were the type of concrete material(Normal and Self-compacting), number of layer (CFRP)and the load eccentricity. All specimens were prepared and loaded eccentrically up to failure. The load-deflection, bending moment parameters' influence and the variability of vertical strain on various specimens' faces were explored. The study found that the strengthened columns showed better performance in comparison with the unstrengthened columns.

In 2012, **Issa et al.** explained the structural behaviour of reinforced concrete columns of GFRP and steel when subjected to eccentrically axial loads. Six columns of 150*150 mm cross section were tested. Four of them were strengthened with GFRP, while the other two were used steel as a reinforcement. The concrete compressive strength of the columns strengthened with GFRP was either 24.72 MPa or 38.34 MPa, whereas it was 24.73 MPa for the columns reinforced with steel. In addition, there was either 50 mm or 25 mm of eccentricity and 80 mm or 130 mm of tie spacing. For columns strengthened with GFRP and with large tie spacing, more longitudinal deformation was reported. Indeed, results showed that tie spacing had no notable impact on the ductility index and the maximum lateral deflection. For columns with an initial eccentricity of 50 mm, the maximum compression strength was around 60 per cent of the concrete compressive strength for columns with initial eccentricity of 50 mm. GFRP bars registered more considerable strength than steel bars. Further, the results pointed that the strains were more significant as the tie spacing become wide. The increase in the concrete strength was associated with a decrease in the GFRP bars strength.

Hassan et al. (2013) examined the structural behaviour of reinforced concrete columns when exposed to biaxial bending that is strengthened by CFRP sheets. The study involves research into 8 RC columns with dimensions 150×150×500 mm, checked in various load environments. Variables included in the software test involved the longitudinal reinforcement effect (Ø12mm or Ø6mm). The test findings are addressed in load-longitudinal and transverse displacement behaviour, maximum strength, and failure shape modes. The study showed that the specimens strengthened with CFRP sheets needed higher load to failure, and the CFRP strengthening permits a complete change in the failure mode of the columns. As well, The effect of longitudinal reinforcement in the case of biaxial bending is more pronounced for strengthened columns than for unconfined columns and The effect of strengthening decreased when the eccentricity are increased. Thus , with increasing eccentricity , there will be a need for longitudinally directed fibers.

In 2015, **Alwash and Jasim** studied the behaviour of concrete columns strengthened by CFRP bars and exposed to an axial eccentric load. Ten concrete columns supported the building. Every column had the same dimensions and sizes. The study constructed columns with a square cross-section of 140×140 mm and a total length of 820 mm. The distance between corbels was 400mm for fixed eccentricity columns. The dimensions, the cross-section and the reinforcement details of the columns are illustrated in Fig. (2.8). Three columns were made as control columns, one without longitudinal steel reinforcement and two with longitudinal steel reinforcement, while the others were longitudinally reinforced with CFRP bars. Axial load–moment and load-deflection response analyses were employed to quantify the behaviour of these columns. The study concluded that the CFRP bars contributed to about 14.51 per cent of column capacity under axial load. For columns reinforced with CFRP bars, the ultimate load decreased by 3.78% under axial load compared to the column reinforced

21

with steel bars, while the ultimate load increased by 38.21% under load eccentricity (e/h) values 0.857. Thus, it can be inferred that strengthening by CFRP can substantially impact the ultimate load capacity of the columns with high eccentricity.
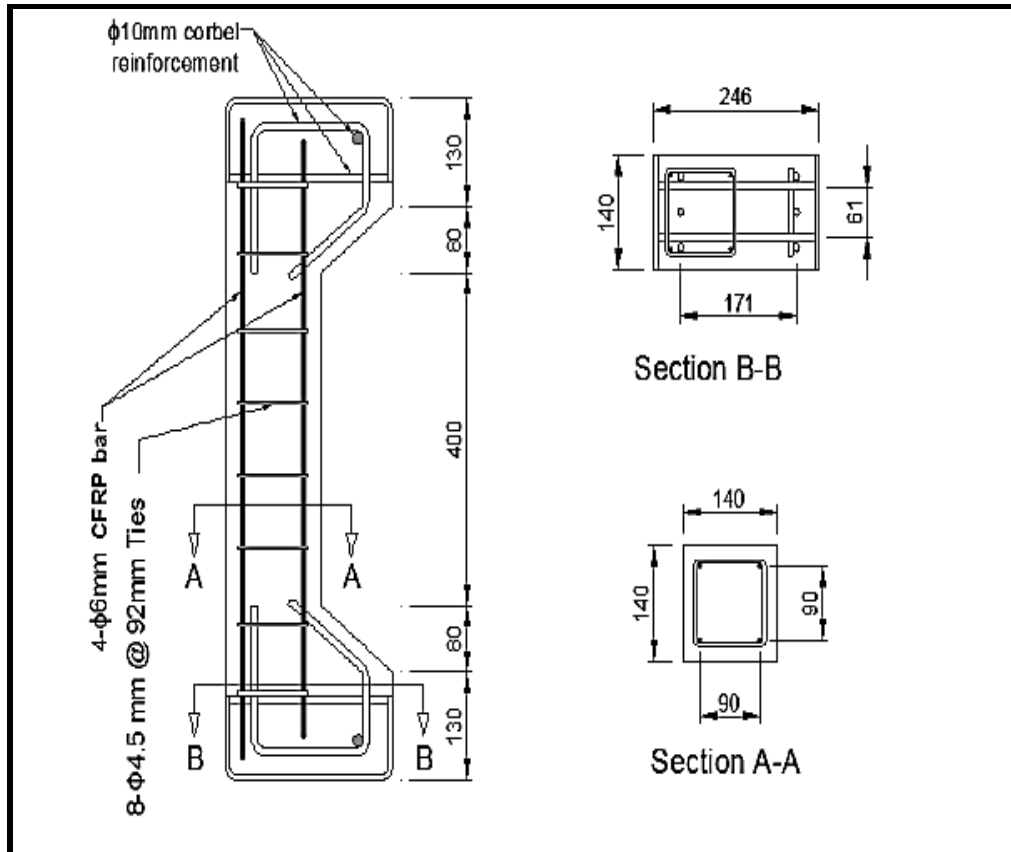
Fig 2.8 . CFRP reinforced column detail. (Alwash and Jasim (2015))

In 2017, **Pour et al**. examined through an experimental study the behaviour of high strength concrete (HSC) columns with a circular cross-section under eccentric compression loading strengthened with CFRP sheets. Axial load was applied to samples with different eccentric loads ranging from 0 to 50 mm. The results indicated that the load-deflection influences the axial stress and stress behaviour of HSC confined by CFRP. In contrast, an increase in the load eccentricity can increase the ultimate axial stress.

Hadhood et al. (2017) conducted experimental research on circular, high-strength concrete columns strengthened with glass fiber reinforced polymer bars and spirals under concentric and eccentric loads. Ten specimens were subjected to monotonous loads with various deviations. Longitudinal strengthening ratio and deflection to diameter ratio were the test variables. Results showed that the Compression failure in the concrete controlled the ultimate capacity of specimens tested under small eccentric loading. A flexural-tension failure initiated in specimens tested under high eccentric loading, however, resulted from excessive axial and lateral deformations and cracks on the tension side until a secondary compression failure occurred owing to the strain limitations in the concrete. The study result also pointed out that strengthening HSC samples with GFRP can effectively improve the strength of the damaged concrete. Figure (2.9) shows the specimens that are eccentrically loaded.
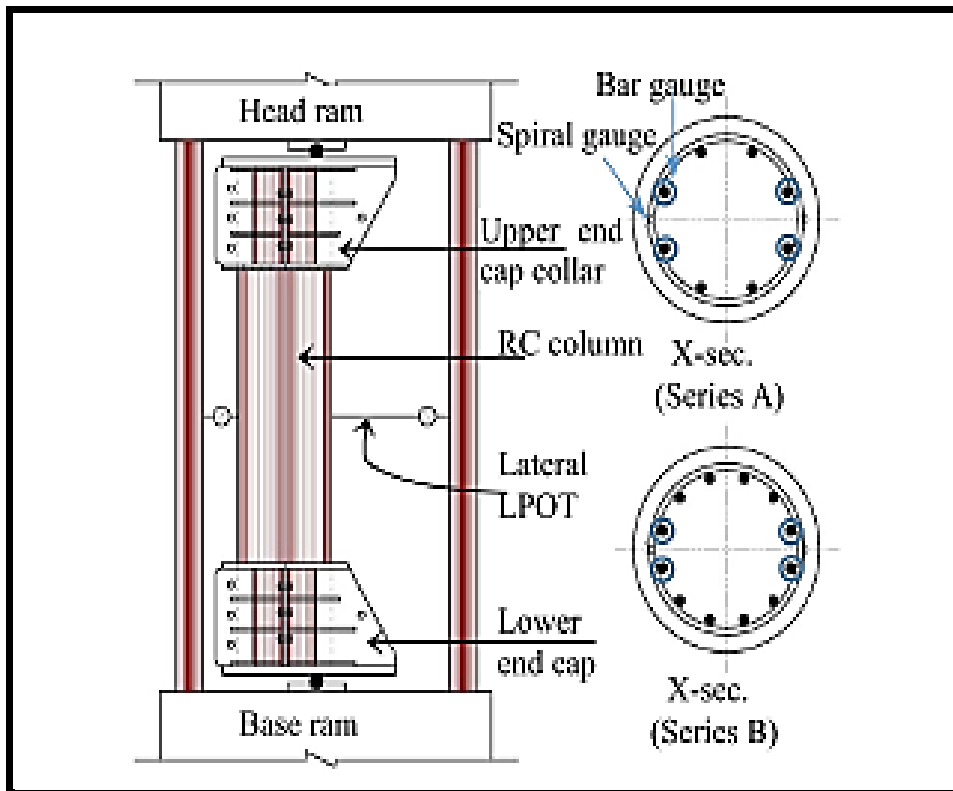
Fig 2.9 . specimens testing for eccentrically loaded. (Hadhood et al. (2017))

In 2018, **Chellapandian** et al. studied the effect of strengthening columns under axial and non-axial loads. First, six NC columns were prepared with precise dimensions and carried under the influence of non-axial loads (e=145 mm). Then, one column was loaded to the failure or collapse stage and considered as a reference column. The other five columns were loaded with a load value less than the designed ultimate load by 20% under the same eccentric load (high ratio of eccentric compression e/d=0.63). After removing the damaged concrete cover and enhanced all columns with a quick-cement grout, one column was used with this strategy of strengthening. Then, two columns were enhanced with NSM CFRP strips, and the other two columns were enhanced by a hybrid FRP technique, which was a combination between NSM CFRP strips and external wrapping of CFRP laminate, as shown in Fig (2.10). Finally, all columns were compared with columns identical specifications but under axial loads (e=0). The examination results showed that the enhancement by cement grout was the worst technique under different loads. However, the enhancement by NSM with CFRP strips showed its effectiveness in increasing the strength and stiffness of the columns under non-axial loads with the inability of this technique to restore the original strength of the column under axial loads. On the other hand, the hybrid technique was the best and most efficient way to improve the column's properties as it was efficient under axial and bending loads. Furthermore, the external layer of CFRP prevented the failure of CFRP strips and the NSM technique and thus increased the load capacity of the column. The failure of the hybrid technique was the rupture of the external CFRP layer in the compression side.

(i) Repair using NSM Technique

(ii) Grinding of Corners and Epoxy application

(iii) First Layer of FRP Wrapping

(iv) Finished Hybrid Repair specimen

Fig 2. 10. Details of strengthening of hybrid FRP technique (Chellapandian et al.)

Alotaibi and Galal (2018) used CFRP jackets to strengthen RC columns under eccentric loading for strength and ductility enhancement. The details of measuring 28 half-scale fully grouted reinforced concrete masonry columns under various concentric, eccentric loading conditions and variations in CFRP jacketing are shown in Fig. (2.11). The capacity of CFRP jackets to enhance structural efficiency was assessed. To assess the strengthening in moment and strength, axial force- diagrams of bending moment interactions of confined strengthened concrete masonry specimens are measured against unconfined masonry specimens. The results indicated that increasing the thickness of the CFRP jacket can improve the performance of masonry columns concerning axial strain and strength. However, when expanding the eccentricity level, there was a significant reduction in strength gain under stress gradient conditions. Also, confined masonry specimens' axial force-bending moment interaction diagrams showed an increase in the load and the moment capacity compared to unconfined masonry specimens.

Figure 4 Test setup and instrumentation for masonry columns.
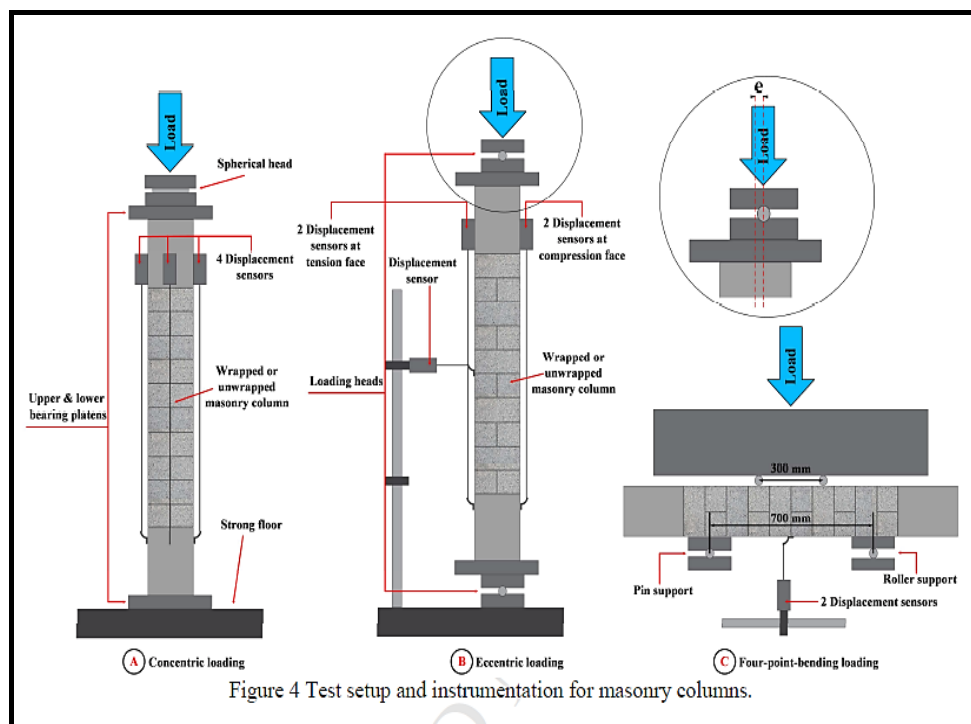
Fig 2.11. Specimens testing and instrumentation (Alotaibi and Galal (2018))

In 2018, **Yang et al.** tested a set of 16 rectangular HSC columns, in which 14 of them were strengthened with CFRP strips along with the columns. They were tested under an eccentric load with a deflection range of 50 to 100 mm. The authors studied diverse variables using different schemes and quantities of CFRP strips. The test findings showed that the ductility and ultimate load of the columns increased significantly by CFRP wrapping around the columns at deflection 50 mm. Moreover, the fully horizontal wrapping by CFRP showed a distinct performance from other improved samples when the deflection increased to 100 mm. Also, the column capacity was significantly improved in longitudinal carbon fibre reinforced polymer wrapped specimens, thus increasing ductility and strength. Section dimension and reinforcement details of samples are shown in Fig. 2.12.
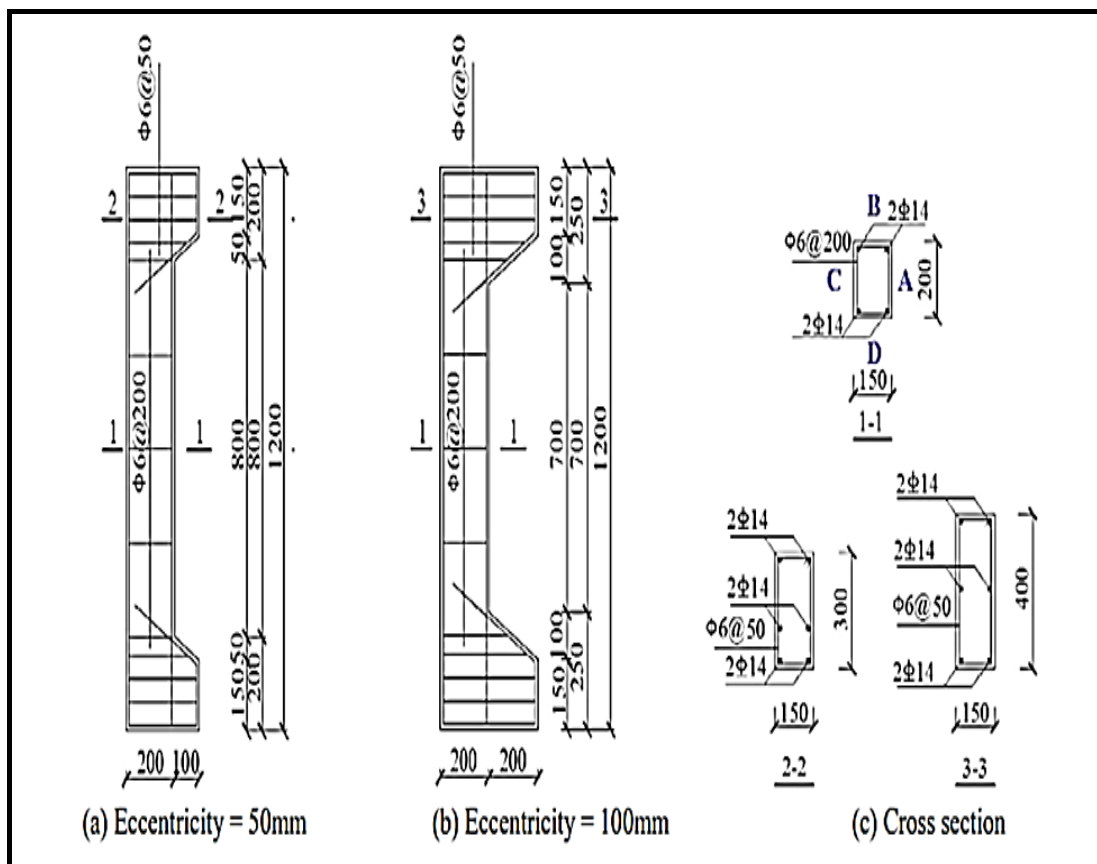
Fig. 2. 12. Section dimension and reinforcement details of specimens (Yang et al. (2018))

Al-Nimry et al. (2019) studied the strengthening of medium-scale circular columns by CFRP wrapping under concentric and eccentric loads. Five sets of columns were prepared in which the first four were tested under loads with different deflections of (0, 25, 50, 65) mm, while the fifth set was tested under infinite loads. Three column subcategories were tested under each of the five loading eccentricities: unwrapped; wrapped with one ply of hoop FRP sheets; and wrapped with two FRP plies with fibers oriented at 0 and 90° to the longitudinal column axis thereby providing externally‑bonded longitudinal reinforcement and hoop confinement, respectively. Results illustrated that warping by CFRP can increase the capacity and ductility of the column even for high deflection, but its effectiveness decreased with increasing the deflection. Besides, the results showed that strengthening by CFRP collar was more effective under bending moments than axial loading, as the resistance of the columns increased when deflection increased. On the other hand, strengthening by using a two-layer of CFRP increased the resistance of the column's capacity under non-axial loads by up to 115%.

In 2019, **Othman and Mohammad** researched 18 rectangular reinforced concrete columns under various eccentric loads through an experimental program. Of the eighteen specimens, fifteen columns were reinforced with longitudinal iron rods made of CFRP bars and links. Three were strengthened with normal iron rods and anchors as control samples. This study included the following variables: the steel replaced by carbon fibre reinforced polymer rods, longitudinal strengthening ratios, tie spacing and load deflection. Test results showed that the column strengthened with CFRP bars behaved similarly to that columns strengthened with conventional steel bars in terms of load-stress, load-mid height deviation curves, and fracture patterns, with a bit of variation in the ultimate load and flexural ability. Furthermore, the increment in CFRP longitudinal reinforcement ratios from 1.4% to 2.0% and 3.6% reasonably

increased the maximum carrying capacity for different eccentricities used. Finally, the steel reinforcement bars were not favoured in some concrete constructions as they cause corrosion compared to CFRP rods that better replace steel bars.

In 2019, **Obeidat** used the ABAQUS program to reinforce partially encapsulated CFRP columns and studied their structural behaviour, including failure pattern and load capacity, by performing a nonlinear finite element model. The author prepared samples with dimensions (160×250×960) mm to compare it with a practically tested model by (**Farghal, 2016**), as shown in Fig. (2.13)) in addition to studying other factors, including investigating the impact of reducing the distance between CFRP sheets and modifying the number of CFRP layers. The finite element results were in good agreement with the experimental tests. In addition, it was found that expanding the layer thickness of CFRP strips and lowering the distance between CFRP laminates could increase the columns' ultimate load capacity and joints contributed to developing the columns capacity.
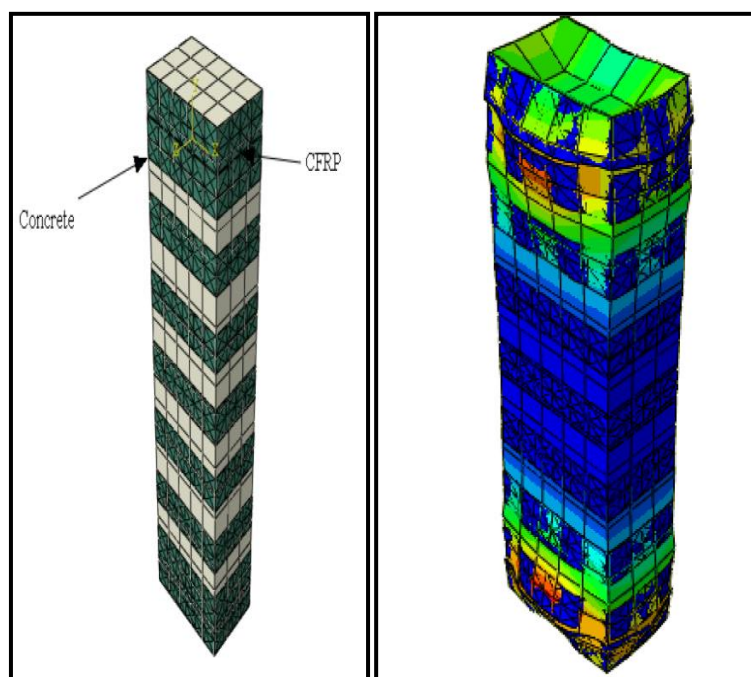
Fig. 2. 13. Description of the finite element model and failure mode (Obaidat (2019))

Talaeitaba et al. (2020) studied improving the properties of circular columns using various techniques under specific loads. The authors constructed 20 circular NC columns with a 150 mm diameter and a 500 mm height. The columns were divided into five groups in which each group comprising four columns: reference column, a column strengthened by NSM rebar using 6 Ø8, a column strengthened with CFRP laminate and NSM rebar as a hybrid technique, and the last column loaded up to 80% of the peak load, then it repaired and enhanced with hybrid technique. The first four groups were loaded with axial loads with (0, 30, 60, and 90) mm eccentricity. In comparison, the last group was loaded under flexural loads with four points. After testing the specimens and analysing the data, the strengthening by CFRP laminate and NSM rebar showed high effectiveness, in particular, the third group (e=60 mm) and gave an increase in ductility, strength, and bending moments by (504 %, 98 %, 89 %), respectively in comparison with the reference column. Indeed, CFRP laminate has a significant influence, mainly when applied with NSM rebar, as it prevents the buckling of steel rebar and increased confinement. The increment percentage resulted from adding a CFRP laminate to the NSM rebar was 37-98%. The behaviour of the columns varied according to the technique used for strengthening, as it was brittle when using the NSM technique, while it was more ductile when using the hybrid approach.

In 2020, **Jiang and Wu** performed an experimental program by checking samples from 78 square columns containing CFRP (32 samples without confinement, 32 samples with single CFRP layer wrapping, and 14 samples with double CFRP layer) under eccentric loading. It was observed that the failure of all the confined samples by CFRP was the rupture of CFRP, which is occurred suddenly, and the sound of tearing the CFRP strips could be heard during the failure. The findings also showed that samples strengthened with

CFRP offered higher maximum load strength than the unstrengthened columns. For CFRP-confined square concrete specimens, the strength enhancement due to CFRP confinement increases with increasing load eccentricity. However, the increasing load eccentricity decreases the confinement efficiency for CFRP-confined square concrete samples.

Chotickai et al. (2021) explained the structural performance of RC columns damaged strengthened by CFRP sheets under eccentric load. Samples with dimensions (125 ×125×1375) mm were treated for 28 days with a compressive strength of 17.7 MPa, as shown in Fig (2.14). This was investigated by testing twelve RC columns of different quantity ratios of CFRP to study their performances after the rehabilitation. The experimental results showed that the effectiveness of the strengthening system was strongly dependent on the quantity of CFRP. If the amount of CFRP is relatively high, the ductility and strength of the column are greatly improved.
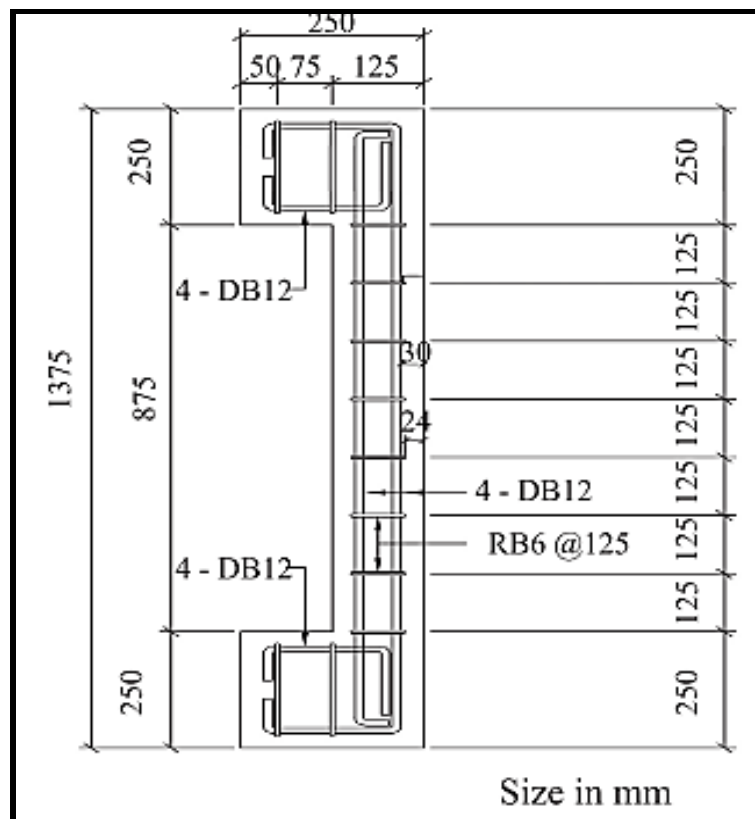
Fig. 2. 14. Configuration of specimens. (Chotickai et al., 2021))

2.5 Summary

The following points can be summarised through the research of studies regarding HSC:

1. When failing, HSC breaks down more quickly than NC; thus, proper strengthening should be used for transverse reinforcement or FRP to minimize brittleness;

2. NC block weighs and costs more due to its larger size, thus hollow structural members from HSC are used to reduce the cost and size and gain high strength;

3. The collapse of HSC cover can occur suddenly and at low levels compared to NC, since the fracture occurs through the rough aggregate and not around it;

4. HSC has numerous advantages, but its strength varies depending on what materials are used near the zone of manufacture

Several reinforcement strategies for damaged columns were also discussed in the study, such as full or partial wrapping of CFRP laminate and the combination of NSM technology and CFRP laminate wrapping. However, the following points can be summarised as the main findings:

1. The column modes of failure are different depending on the strengthening method, as it is more brittle when using the NSM technique and more ductile when using wrapping or hybrid approaches;

2. Columns wrapped by number of CFRP sheets will have better ductility, higher strength, and absorbency than a steel-bar strengthened column;

3. CFRP wrapping was successful under concentric and eccentric loads. Full CFRP wrapping was better than partial wrapping as it reduces the appearance of cracks, especially the early ones, as the applied tensile

stresses are lower. Indeed, horizontal CFRP was better than vertical CFRP;

4- The hybrid strengthening process, which incorporates NSM technology and CFRP laminate, has been beneficial in terms of the structural behaviour of columns under axial and non-axial loads;

5- The strength of the column is improved by decreasing the distances between the CFRP laminate. In addition, there is a sufficient number of additional CFRP wrapping layers in which there is no impact on extra layers above that number;

6- The columns potential strength can be improved by increasing the concrete compressive strength.

According to what have mentioned above, it can be concluded that no studies were found that reviewed the structural behaviour of high strength damaged concrete short columns under eccentric loads with a deflection of 50 mm and an initial load of 25% and 50% of the ultimate design load then strengthened with CFRP sheets and reloaded until failure.

CHAPTER THREE
EXPERIMENTAL WORK

3.1 Introduction

In this chapter, all samples were described with all materials used in the production of the HSC and their properties. The formwork process and equipment used were also illustrated. In addition, the compressive and tensile strengths of the concrete mix were also determined in this chapter. At the end of the hardening phase, the initial loading of the prepared columns at 25% and 50% of their designed ultimate loads were also conducted. Further, the strengthening process for each sample with CFRP strips was also described and discussed in details.

3.2 Specimens description

The experimental work consists of casting nine short columns using HSC, with one selected as a control column and tested to failure. The other eight columns were divided into two groups in which each group has four columns. The first group was loaded with an initial load of 25% of ultimate design loads, where the first cracks appear. At the same time, the second group was loaded to 50% of ultimate design loads. All eight pre-loaded samples cracks were repaired with fast cement mortar and reinforced with CFRP strips using various strengthening schemes, as shown in Fig (3. 2). All strengthening details by CFRP for the first and second groups are tabulated in Table 3.1. All specimens were prepared with identical dimensions of a square cross-section (100 × 100) mm and a total length of 800 mm. The distance between the corbels was 500 mm, and each corbel head has a height of 150 mm, as shown in Fig. 3.1. The columns were designed following the **(ACI committe 318, 2019)**, and the initial reinforcements and ties for all samples under eccentric loading (axial load

and bending moment) by an eccentricity of 50 mm from the center (e/h = 0.5). (for more details, see Appendix A). The primary steel reinforcement consists of 4 Ø 8 mm rebar, one at each corner, while the stirrups was Ø 6 mm starting at a 40 millimeters distance from the edge of the column and ending 100 mm in the centre, as shown in Fig (3. 1).
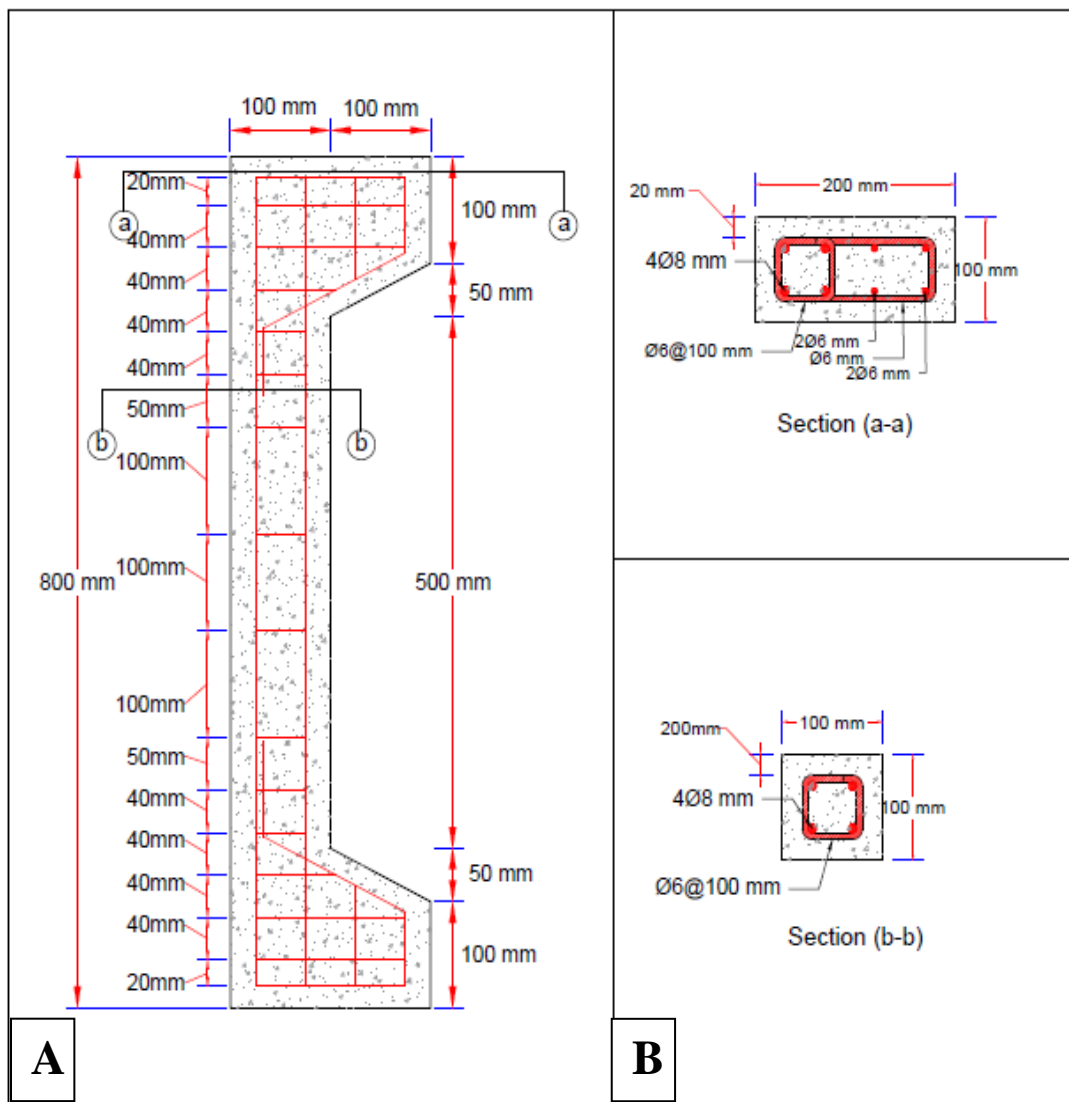
Fig. 3. 1. Details of steel reinforcement for the columns (A) Side view (B) Cross-section

Table 3. 1. Various strengthening techniques for the tested columns

Group No.	Specimen load / Ultimate load ratio	Column designation	Strengthening techniques
Reference	100%	CC	No strengthening
Group 1	25% (Quarter)*	CQFFL	Full longitudinal wrapping with CFRP for all column faces
		CQRF	Full longitudinal wrapping with CFRP for rear face only
		CQFFW	Full horizontal wrapping with CFRP for clear column height
		CQ25FW	Horizontal wrapping with CFRP for 250 mm length at column mid-height
Group 2	50% (Half)**	CHFFL	Full longitudinal wrapping with CFRP for all column faces
		CHRF	Full longitudinal wrapping with CFRP for rear face only
		CHFFW	Full horizontal wrapping with CFRP for clear column height
		CH25FW	Horizontal wrapping with CFRP for 250 mm length at column mid-height

* The specimens were loaded with an initial load of 25% of the final design load. Then it was strengthened and reloaded until failure.

** The specimens were loaded with an initial load of 50% of the final design load. Then it was strengthened and reloaded until failure.
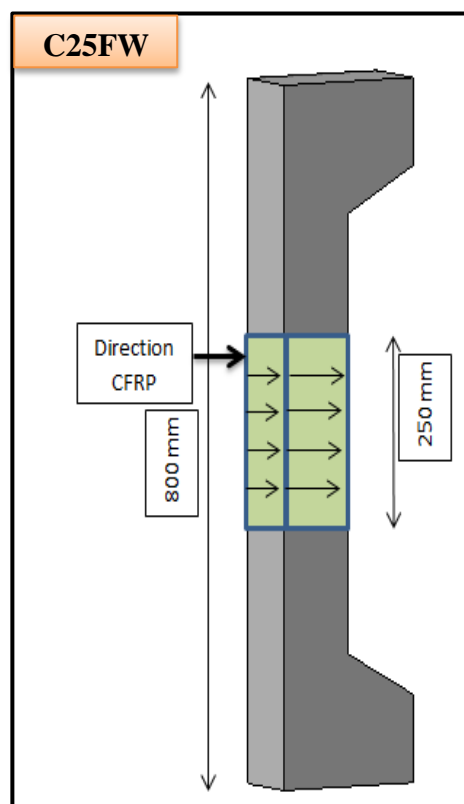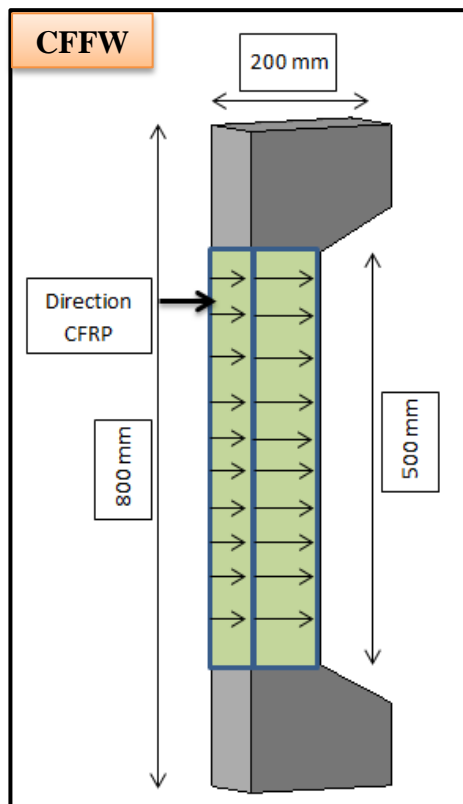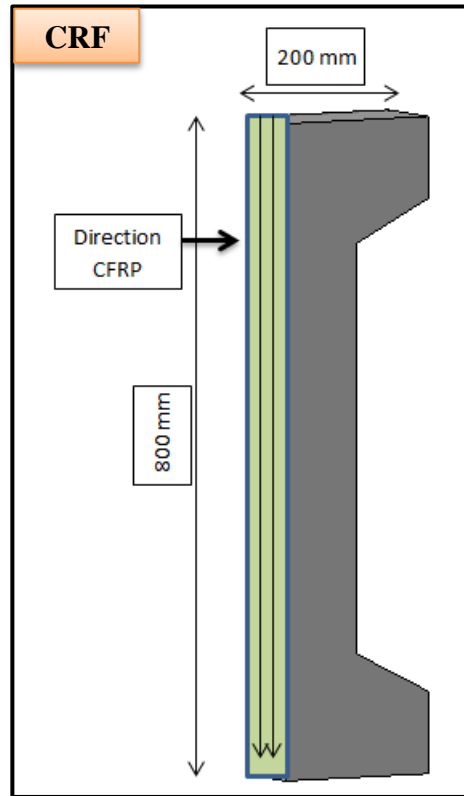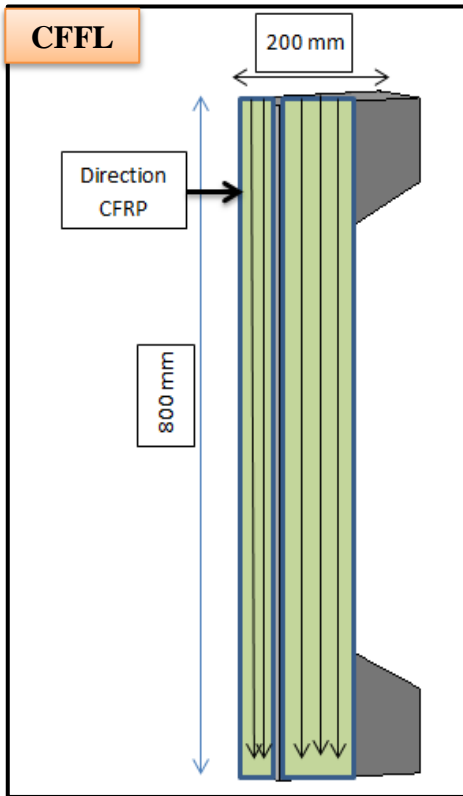
Fig. 3. 2 Description of strengthening with CFRP for specimens

3.3 Materials

3.3.1 high-strength concrete (HSC)

Materials used in manufacturing the HSC were ordinary Portland cement, coarse aggregate with a maximum size of 12.5 mm, fine aggregate with a maximum size of 4.75 mm, silica fume known as Sika® Fume S 92 D, produced by Sika Corporation **(Sika® Fume S 92 D, 2015)**, and superplasticiser known as Sika 5930 **(Sika ViscoCrete® -5930, 2015)**. In this study, the HSC mix was taken by designing several experimental mixes to obtain 28 days compressive strength equal to nearly 70 MPa following the ACI (211-15**) (ACI- Committee 211 R- 2015)**, Table (3.2) provides the quantities of the components required to have one cubic meter of HSC.

Table 3. 2. Quantities of HSC ingredients

Ingredients	Weight kg/m^3
Cement	470
Coarse aggregate	1040
Fine aggregate	670
Silica fume	52
Superplasticizer	10
Water	135
W/C	0.26

3.3.1.1 Ingredients Used

- **Cement**: Ordinary Portland cement (Type 1) manufactured in Iraq-Kerbala, which is commercially known as Al-Jasir, conforming to the **Iraqi standard specification No. 5/1984** was used. Appendix B contains information on the physical and chemical properties of the cement used in the mix.

- **Fine aggregate**: Natural sand is used in producing the HSC mix with a maximum size of 4.75 mm, which is brought from Najaf factories. The tests were implemented in the laboratory of the University of Kufa, which was compiled with the **Iraqi Specifications No. 45**, as described in Appendix B.

- **Coarse aggregate**: A black crushed gravel with a maximum size of 12.5 mm was used. It was washed with water before being air-dried. The sieve analysis for the coarse aggregate used in producing the HSC mix that was conform with the **Iraqi Specifications No. 45** is given in Appendix B.

- **Water**: Tap water was used in producing the HSC and the curing process for all cubes, cylinders, and columns. It was clean and free from unwanted materials like organic salts, acids, and Alkalis.

- **Silica fume**: Silica powder was used in producing HSC mixes. The form used in this study is known as Sika Fume S 92 D (See Appendix B for more details).

  - **Superplasticizer**: The superplasticiser helps with HSC output by reducing the required amount of water. The used form in this study is known as a viscocrete-5930, which is developed by Sika. This kind has many benefits, such as reducing water and growing strength, particularly at early ages. Appendix B

includes the properties and characteristics of the superplasticiser **(ASTM C494, 2013).**

3.3.1.2 Mechanical properties of HSC

1- Compressive strength

A digital compressive machine electronic was used to perform the compression strength test with an ability of 2000 kN **(BS 1881-116, 1983)**, as shown in Plate (3.1) using a 150 mm cube on the side. The cubes were examined on the same day as the columns and the results are given in Table (3.3).

Plate 3. 1. The compression strength test machine

2- Splitting tensile strength

According to ASTM C 496 **(ASTM C496/C496M, 2011)**, the tensile strength was measured using cylinders with dimensions (100×200) mm. An ultimate force was applied to evaluate this test at the end of the curing time after 28 days, as shown in Plate (3.2). To evaluate the tensile strength of HSC, three samples were used to measure the mean value using Eq. (3.1).

$$f_{st} = \frac{2P}{\pi \, dL} \quad \text{………………………………………………….. (3.1)}$$

Where; f_{st}: Splitting tensile strength (MPa); **P**: Maximum load applied (N); d: Diameter of the cylinder (mm); **L**: Length of the cylinder (mm).

Plate 3. 2. Splitting tensile strength test machine

Table 3. 3. Mechanical properties of HSC

Groups	Column symbol	average compressive strength (28-day) (MPa)	average tensile strength 28-day (MPa)
Refrence	CC	70.51	5.12
Group 1	CQRF		
	CQFFW	70.51	5.12
	CQFFL		
	CQ25FL		
Group 2	CHRF	69.32	5.01
	CHFFW		
	CHFFL		
	CH25FL		

3.3.2 Steel reinforcement

Ø 8 mm steel reinforcement was used as a primary reinforcement, while Ø 6 mm was used as stirrups. Three specimens of each type of reinforcement were used, which must be 370 mm long, to measure the strength and elongation of each type of reinforcement according to **(ASTM A615, 2016)**. The test has been carried out at the University of Kufa using a tensile testing machine, as shown in Plate (3.3). The tensile strengths of each type of reinforcement are given in Table (3.4).

Plate 3. 3. Tensile testing machine for steel reinforcement

Table 3. 4. properties of steel reinforcement

Assumed diameter(mm)	Actual diameter(mm)	(f_{sy}) yield strength (MPa)	(f_{su}) Ultimate strength (MPa)	Elongation Ratio %
8	7.78	380	570	24.41
6	5.85	360	495	10.33

3.3.3 Carbon fibre reinforced polymer (CFRP)

Carbon fibre reinforced polymer (Sika Wrap®-300) was used in strengthening the partially loaded columns. The properties of CFRP (Sika Wrap®-300) are given in Appendix **B**.

3.3.4 Epoxy

Epoxy type Sikadur-330 was used as an adhesive material between the CFRP sheets and HSC surfaces. The properties of epoxy Sikadur-330 are given in Appendix B.

3.4 Wooden mould

Nine moulds were produced with length, width, and height of ($100 \times 100 \times 800$) mm, correspondingly. The mould consists of a bottom piece with dimensions (200×800) mm, two small side pieces with dimensions (200×100) mm and two longitudinal side pieces (100×800) mm, in which the first was fixed and the second was inclined to the corbel, as shown in the Plate (3.4). These parts were attached with screws to shape the entire mould. Prior casting, the mould was lubricated and the steel bars were placed inside the mould and a 15 mm spacers were placed on each side of the bars to obtain the necessary cover. Then, the mould was fixed by pins from the top edge.

Plate 3. 4. Details of wooden mould for the column

3.5 Mixing procedure

Nine HSC short columns of a square-cross section were prepared and cast, following the preparation process, including material preparation, wood mould, and steel reinforcement. Next, The ingredients of the mix have been mixed in an electric mixer. The process of mixing includes the following steps:

Step 1. All materials used in producing the HSC mix were prepared and stored in a dry place before mixing;

Step 2. The coarse aggregate, fine aggregate, silica fume, and cement were added to the mixer, in addition to half amount of the water and superplasticiser, and they were left to mix for 2 minutes;

Step 3. The remaining amount of water and superplasticiser was added to the mixer, and they were left in the mixer for another 3 minutes;

Step 4. The concrete was cast in the wood mould in layers with stacking using rod steel, and the trowel was used to level off the surface of the concrete. To avoid water evaporation from the mould surfaces, the samples were wrapped with nylon sheets;

Step 5. All the specimens, cubes, and cylinders were left for 24 hours in the laboratory before removing the concrete from the moulds. After that, all samples were left in a water tank for curing, as shown in the Plates (3.5), (3. 6). The columns, cubes and cylinders were removed from the tank after 28 days and then tested after drying with dry piece of cloth.
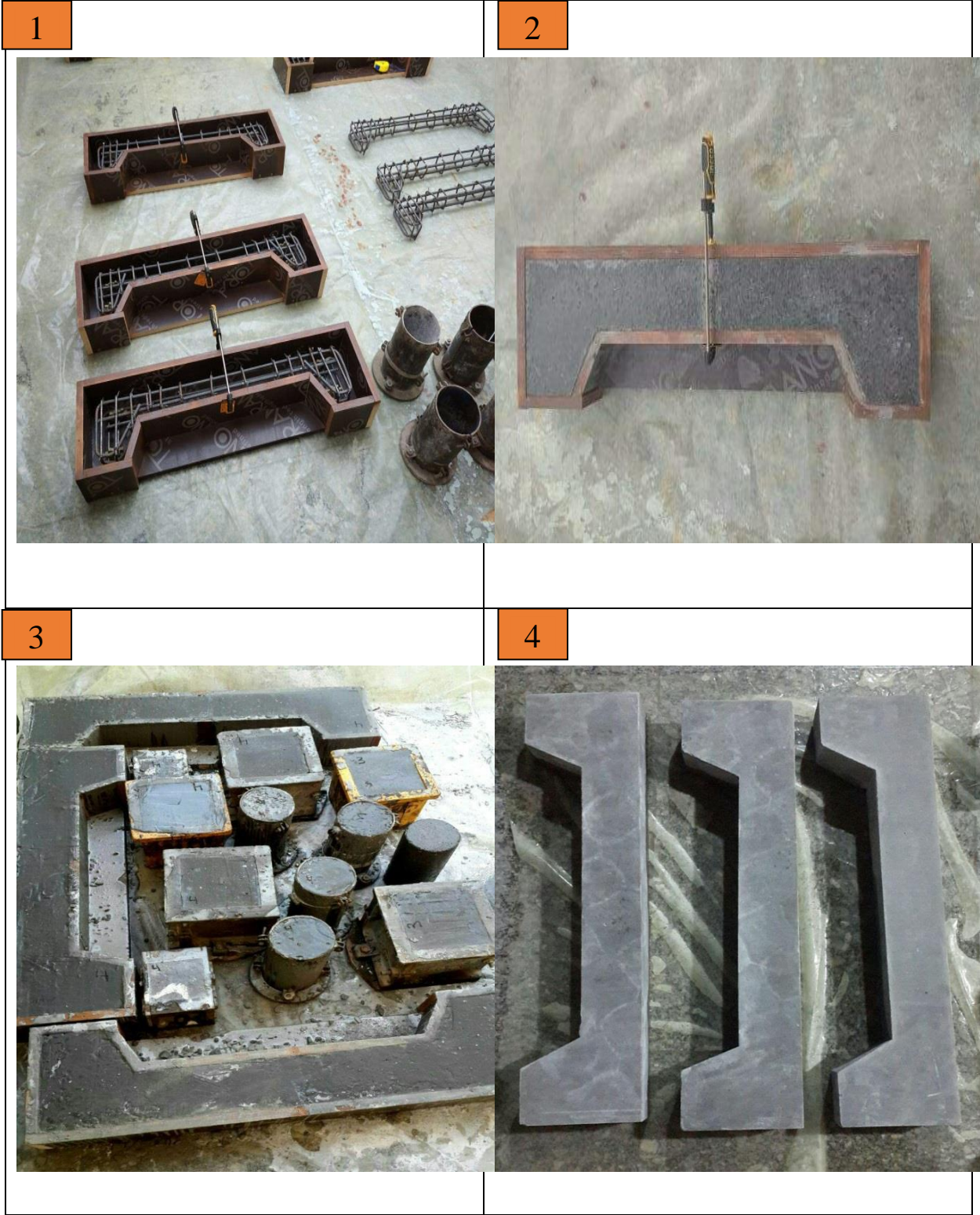
Plate 3. 5. The casting of the concrete

Plate 3. 6. Curing process for HSC

3.6 Testing procedure for the partially loaded columns

After 28 days, the specimens were painted white to clarify the cracks that appeared during the loading stage. Then, they were installed on an electrical testing machine with an ultimate capacity of 2000 KN. The test device exists in the laboratory of Civil Engineering at the University of Kufa. One of the nine columns was considered a reference column, where the load was applied until failure. At the same time, the other eight columns were divided into two groups, according to the initial loading ratio of 25% and 50% of their ultimate design loads, in which each group had four columns. All eight pre-loaded samples were repaired with CFRP sheets with various strengthening schemes. These samples were installed on the test machine using caps made of high-strength steel designed by **Hadi (2006)**, having dimensions of 225×125 mm and a thickness of 20 mm from the upper and lower ends of the column. The eccentric load was gradually applied to the steel cap diameter a 25 mm wedge plate placed in the 50 mm groove using a 2000 KN load cell until the first cracks appeared for these columns, which account for about 25% and 50% of the CC ultimate load, as shown in the plate. (3. 8). The method used LVDTs with a stabilization

47

capacity of 20 mm to measure the horizontal and vertical load-deflections where LVDTs (1) was placed at the outer side mid-height of the column to measure the horizontal load-deflections. In contrast, LVDTs (2) was placed at the outer side mid of the corbel head to measure the vertical load-deflections of the specimens. The LVDTs and these load cells were attached to a computer, as illustrated in the Plate (3.7).

(a) testing machine
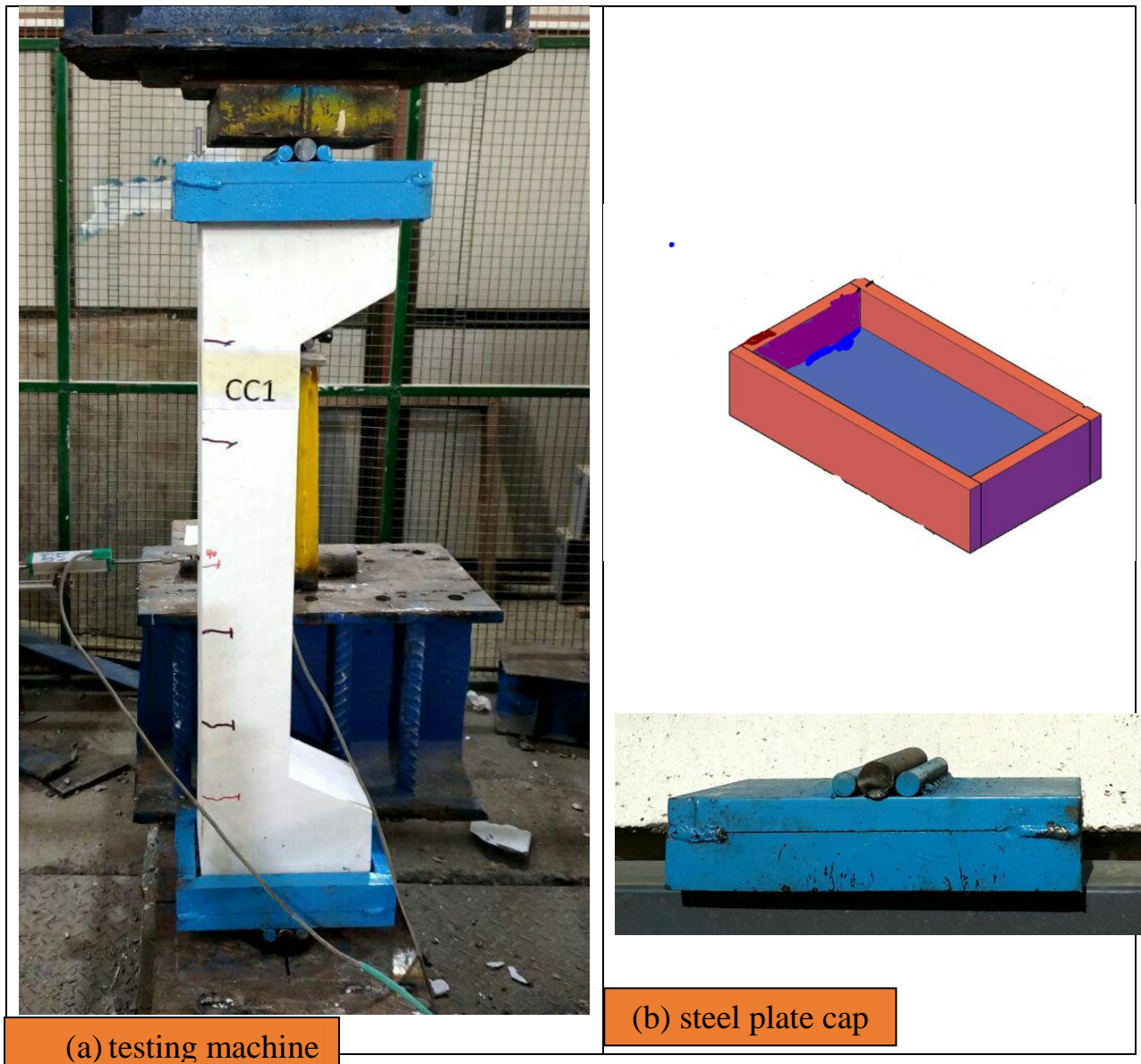
(b) steel plate cap

Plate. 3. 7. Installation of the columns on the testing machine (a) testing machine, (b) steel plate cap
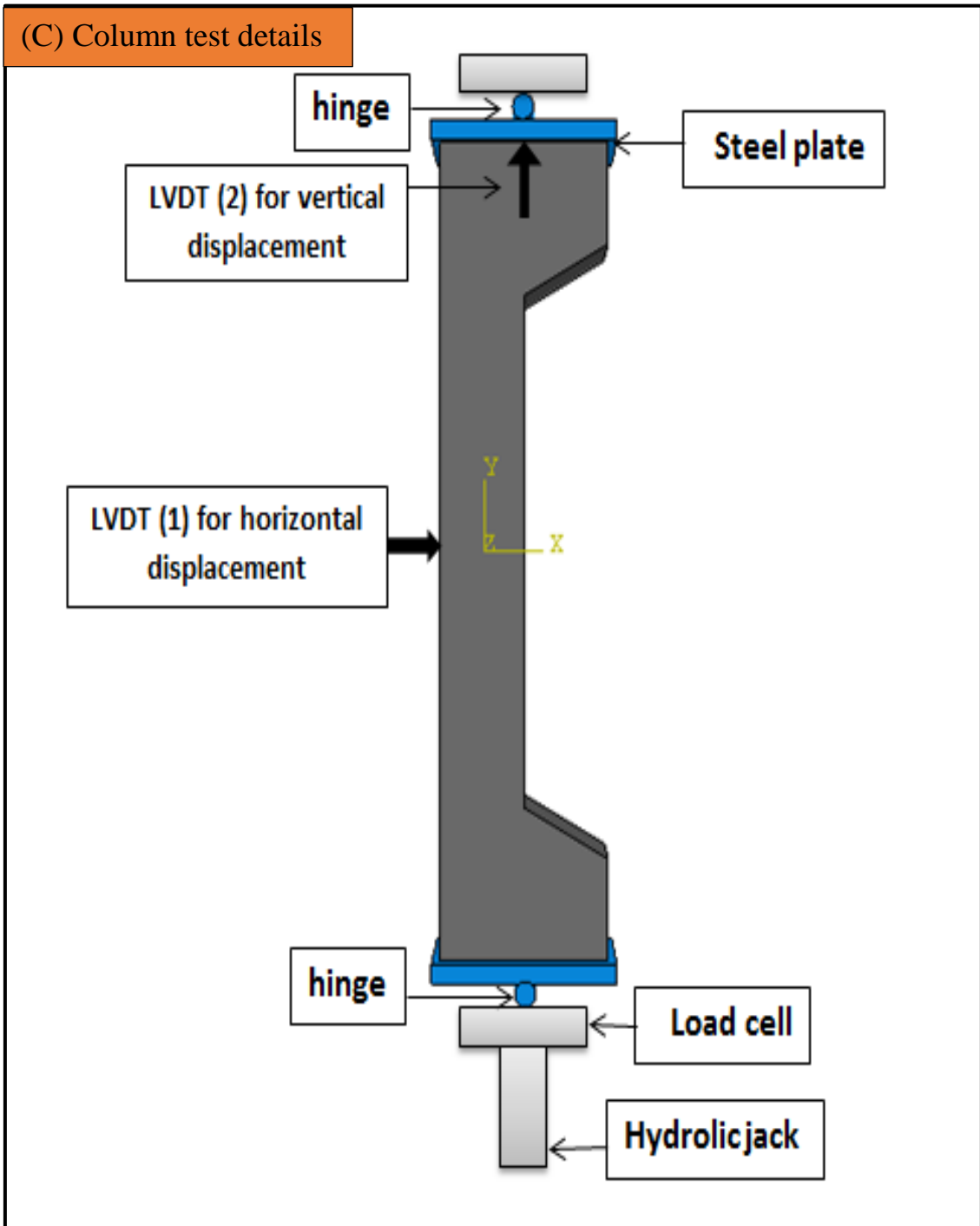
Fig. 3. 3. Column test details

plate. 3. 8. Columns after partially loaded stage

3.7 Strengthening by wrapping CFRP sheets

After 28 days from sample pouring (the curing time), all samples were subjected to an eccentric load with a distance of 50 mm from the center (e/h = 0.5). Two groups were subjected to an initial load of 25% and 50% of their ultimate design loads. After that, the samples were repaired by removing the damaged parts using fast cement mortar, followed by the strengthening of CFRP strips. Next, an electric hand grinder was used to remove and clean the obstacle parts such as paint, cement, dirt, and any obstructions separating the epoxy from the concrete's surface. Then, to avoid stress concentration in CFRP slices, the columns' edges were rounded. After that, the Sika Warp ®-300 fabric strips were cut to the desired lengths with scissors. Then, the strips were applied to the resin epoxy Sikadur-330 before the adhesive was pressed between the CFRP and the concrete. An extra adhesive material(epoxy Sikadur-330) layer can be used with a brush to create a superior bond between the CFRP and the concrete. Finally, the strengthened samples were left for seven days to dry, as shown in Plate (3.9). CFRP proposed different strengthening schemes on four samples for each group, where the first group was classified as CQFFL, CQRF, CQFFW, CQ25FW with similar details to the second group that was classified as CHFFL, CHRF, CHFFW, CH25FW, as detailed previously in Table (3. 1).
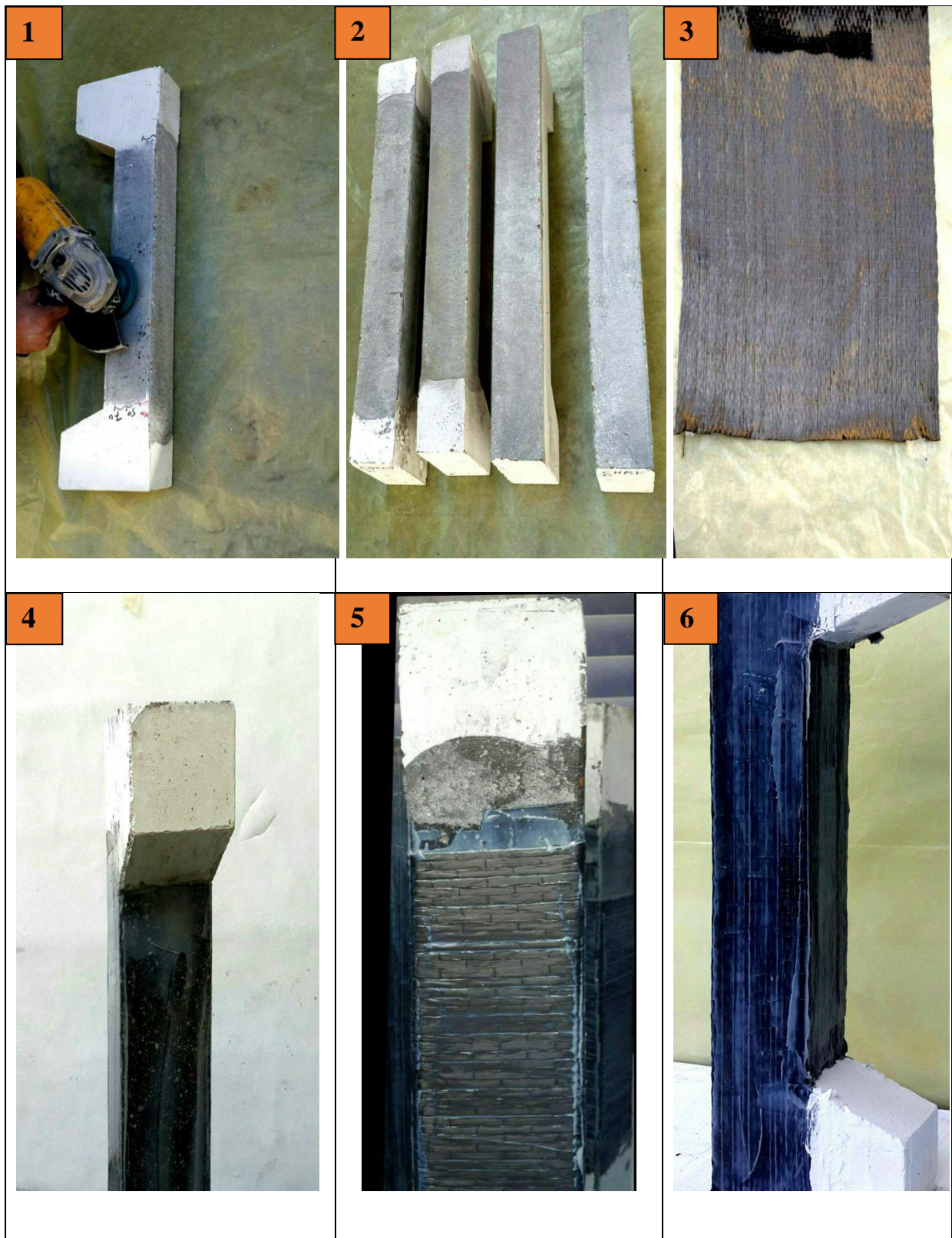
Plate 3. 9. The installation process of the CFRP strengthening

CHAPTER FOUR
EXPERIMENTAL RESULTS AND DISCUSSION

4.1 Introduction

The results and discussion of nine tested HSC square-cross section short columns explained in chapter three are presented in this chapter. All specimens were under eccentric loading (axial load and bending moment) by an eccentricity of 50 mm from the centre (e/h = 0.5), in which the control column (CC) was loaded up to failure. In contrast, the other eight columns were divided into two groups in which each group has four columns. The first group was loaded with an initial load of 25% of the ultimate design load, where the first cracks appear. At the same time, the second group was loaded with an initial load of 50% of the ultimate design load. All semi-damaged specimens were strengthened as a result of the initial loading according to schemes with CFRP strips. All specimens were tested to verify the strengthening effect of CFRP strengthening technique on its structural behaviour compared to the control sample (column without strengthening). The test results of the columns are discussed in terms of strength, stiffness, ductility index and horizontal and vertical load-deflection curves.

4.2 Experimental results

This part deals with the structural behaviour of damaged and undamaged HSC columns using CFRP strips strengthening technique.

4.2.1 Control column (CC)

After installing the column on the testing machine and set up the LVDTs in their positions in both the transverse and longitudinal directions, the load was applied gradually on the control column (undamaged column) until the first

transverse cracks appeared in the tension area at the middle of the column at a load of 37 kN, which represents approximately 0.25 of the ultimate design load. Increasing the applied load led to the expanding and spreading of cracks till failure at an ultimate load of 145 kN due to crushing of concrete (due of yielding steel reinforcement and failure of concrete). The value of the horizontal load-deflection curve noted that ductility index and stiffness were 1.69 and 45.93kN/mm, respectively. While the ductility index and the stiffness were 1.42 and 66.34 kN/mm, respectively, regarding the vertical load-deflection. Plate (4.1) showed the failure of the control column, while Fig. (4.1) presented the horizontal and vertical-load deflection curves.
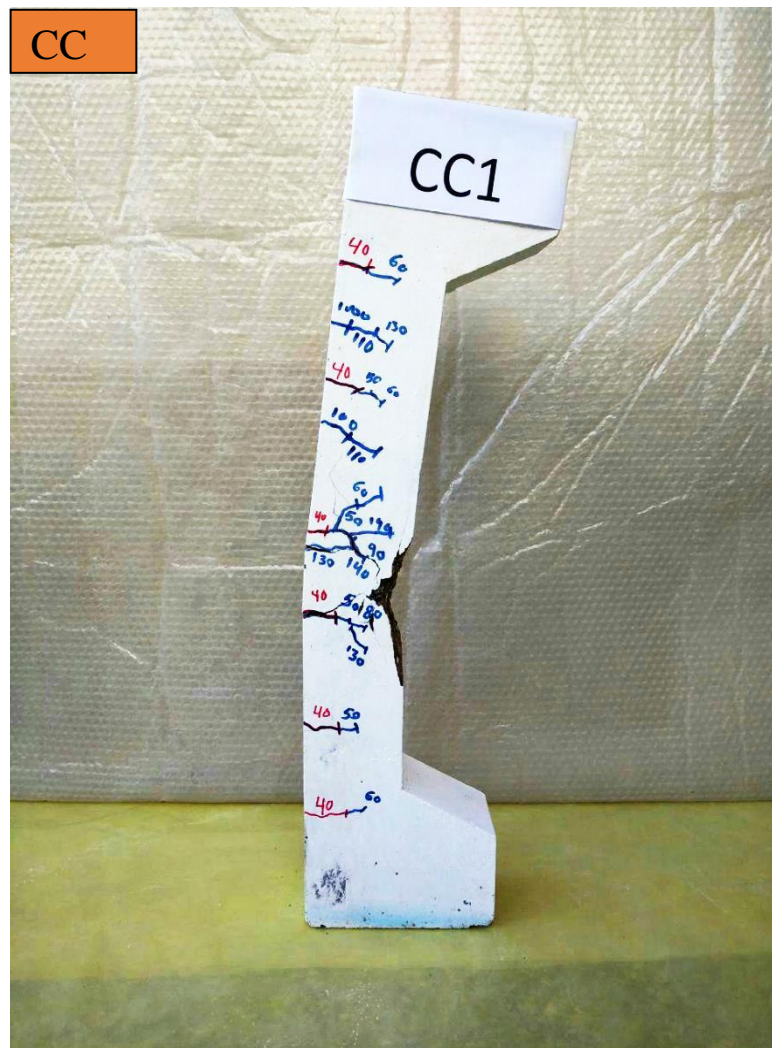
Plate 4.1. Failure for CC
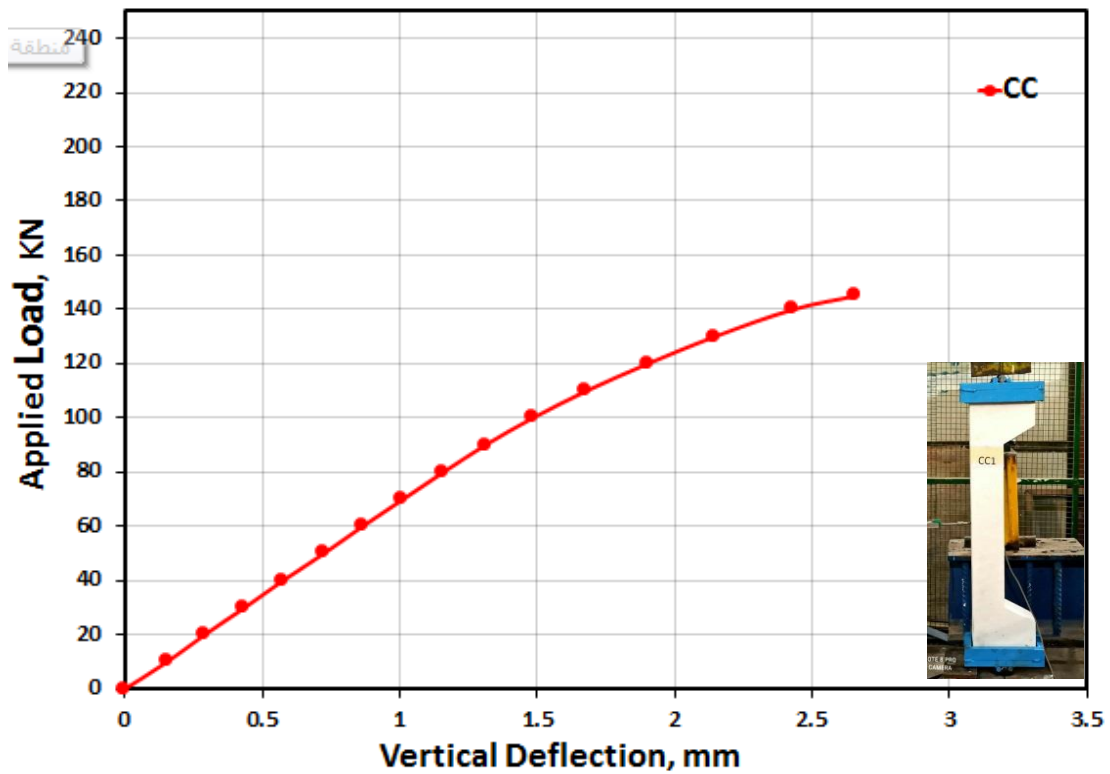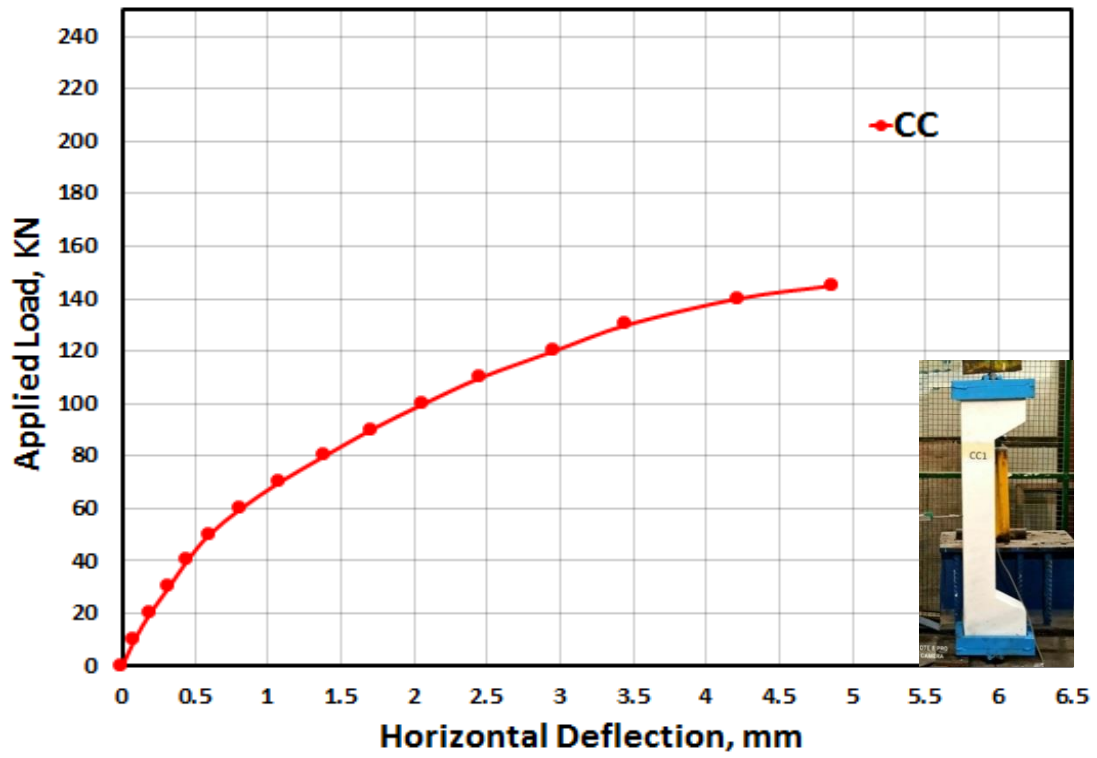
Fig. 4. 1. The horizontal and vertical load-deflection curve for CC

4.2.2 Columns Strengthened with CFRP Technique (Group 1)

4.2.2.1 Column Strengthened with Full CFRP Longitudinal Wrapping

      (All column faces (CQFFL))

This specimen was enhanced by an external CFRP sheets wrapping technique, including full longitudinal wrapping with CFRP for all column faces after been subjected to an initial load strength of 25% of the maximum design load. The load was applied gradually to the specimen, and no cracks were observed at the first step of the loading used process. However, with the progress of the loading process, the column failed at an applied force of 240 kN due to rupture of CFRP sheets, as shown in Plate (4.2). It is worth mentioning that the load capacity for this specimen increased effectively, which might result from the significant the effect of containment of concrete in the tension and compressive, which leads to an increase in the strength of the tension and compressive. Therefore, the structural behaviour of this specimen has been improved due to the increment in the ultimate load compared to CC. Based on data of the horizontal load-deflection curve, it has also been noted that the structural behaviour of this specimen improved due to the increase in the ductility index and the stiffness, as they recorded 1.78 and 53.17 kN/mm, respectively. In the same regard, the values of the ductility index and stiffness were 1.53 and 73.68 kN/mm, respectively, regarding vertical load-deflection. Figure (4.2) presented the load-horizontal and vertical deflection curves for CQFFL.

Plate 4. 2. Failure for specimens CQFFL
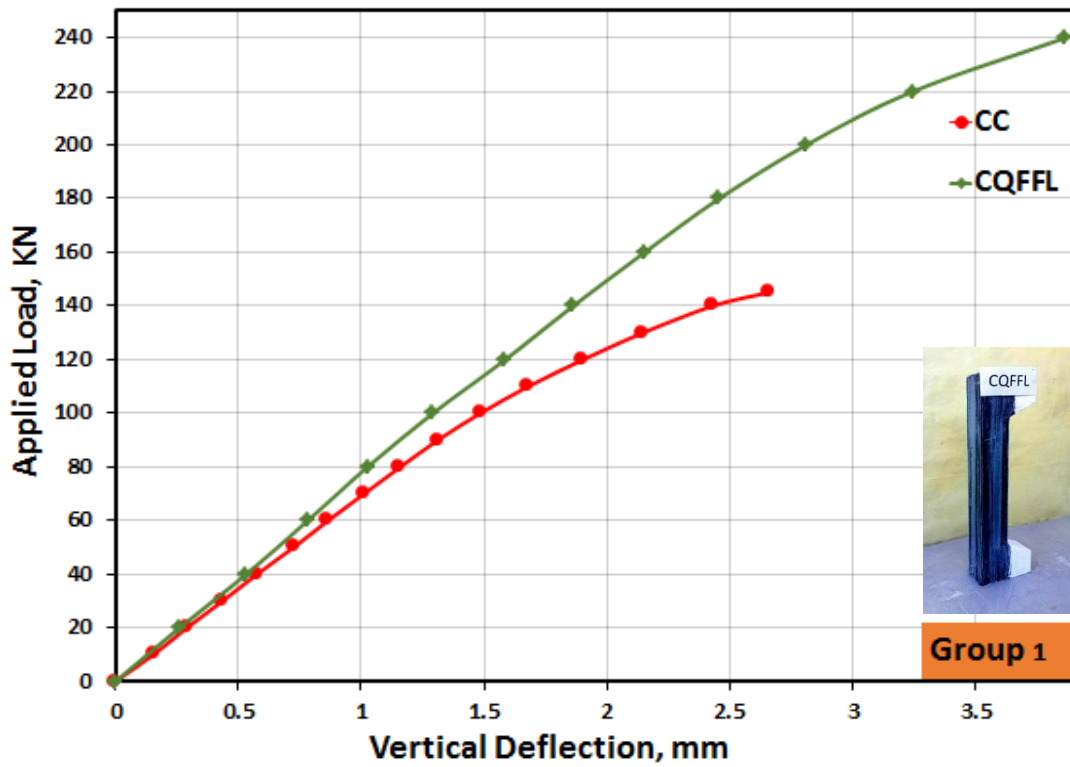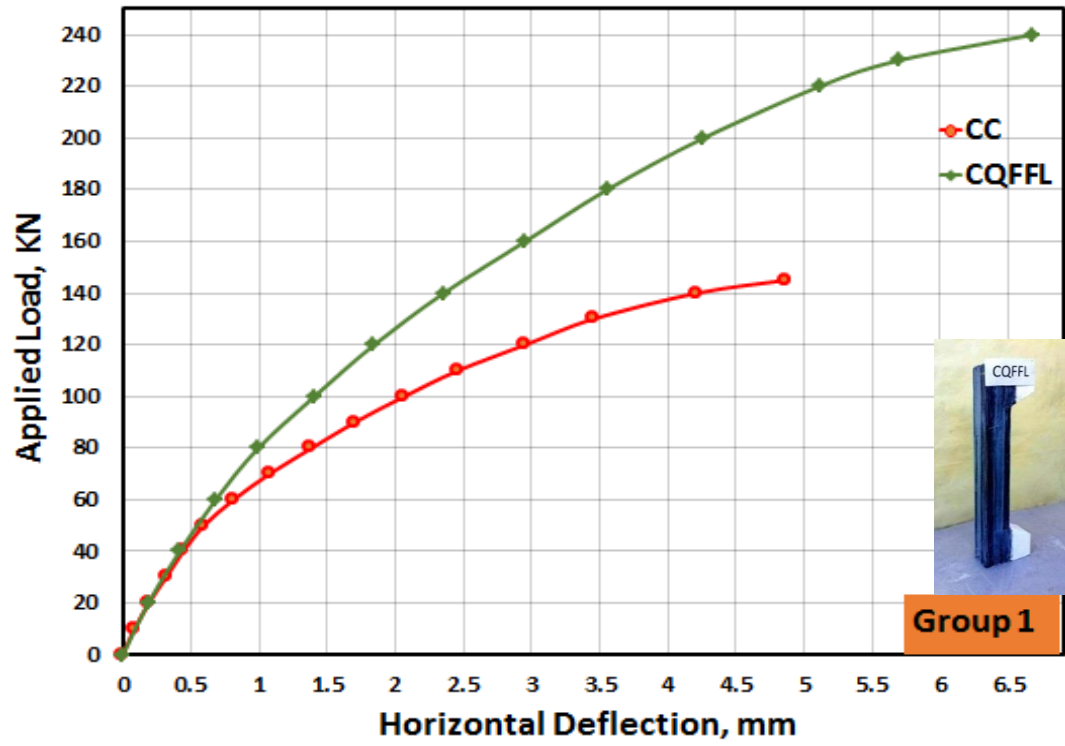
Fig. 4. 2 Horizontal and vertical load-deflection curves for CQFFL and CC

4.2.2.2 Columns Strengthened with Full CFRP Longitudinal Wrapping (tension face only (CQRF))

This specimen was strengthened by an external wrapping of CFRP sheets, including full longitudinal wrapping for the tension face only after been subjected to an initial load strength of 25% of the maximum design load. The load was applied gradually on the column, where no cracks were observed at the initial stage of the loading process due to CFRP sheets preventing cracks. With the progress of the loading process, the column failed at an applied load of 210 kN due to the crushing of concrete in which compression failure for concrete at the upper end of the column below the corbelled head was occurred, as shown in Plate (4.3). The increase in the column capacity was due to the effect of containment of concrete in the tension area in back, Which increases the strength of the tension. The structural behaviour for this specimen has been improved due to the increment that happened in the ultimate load. Through the value of the horizontal loads-deflection curve, it has also been noted that the structural behaviour of this specimen improved due to the increase in the ductility index and the stiffness, which became 1.76 and 52.87 kN/mm, respectively, in comparison with CC. However, the values of the ductility index and stiffness were 1.5 and 71.70 kN/mm, respectively, regarding vertical load-deflection. The horizontal and vertical load-deflection curves for CQRF are presented in Fig. (4.3).

Plate 4. 3. Failure for specimens CQRF
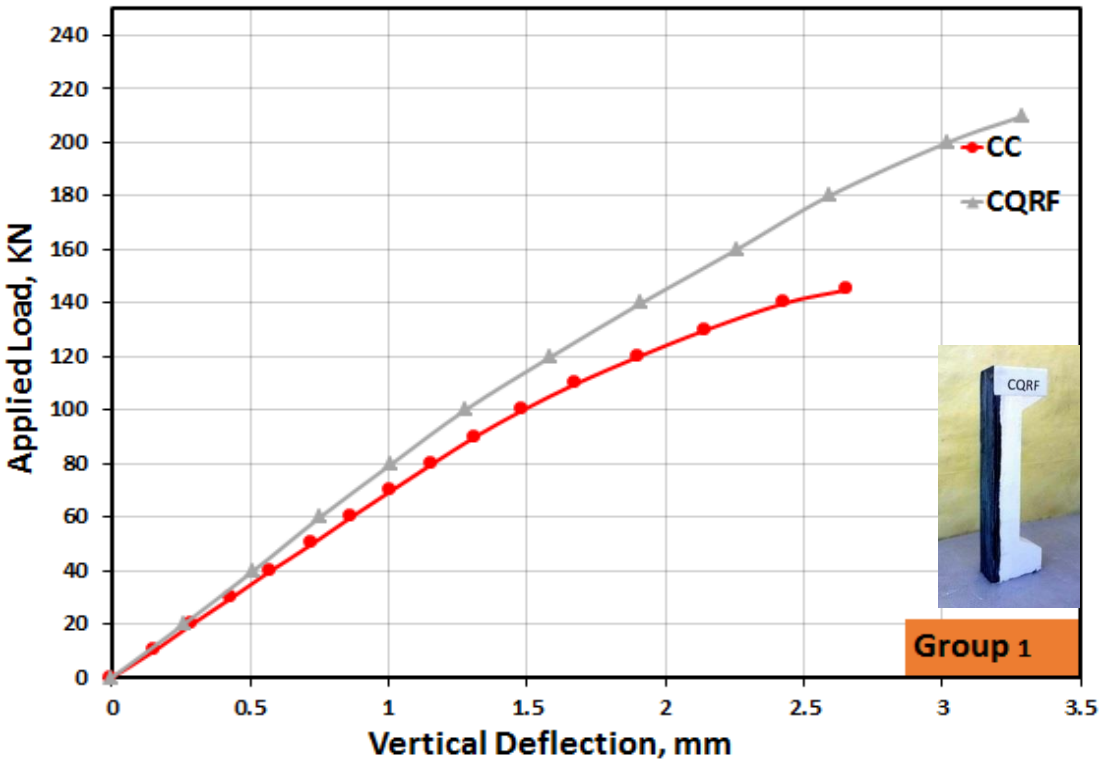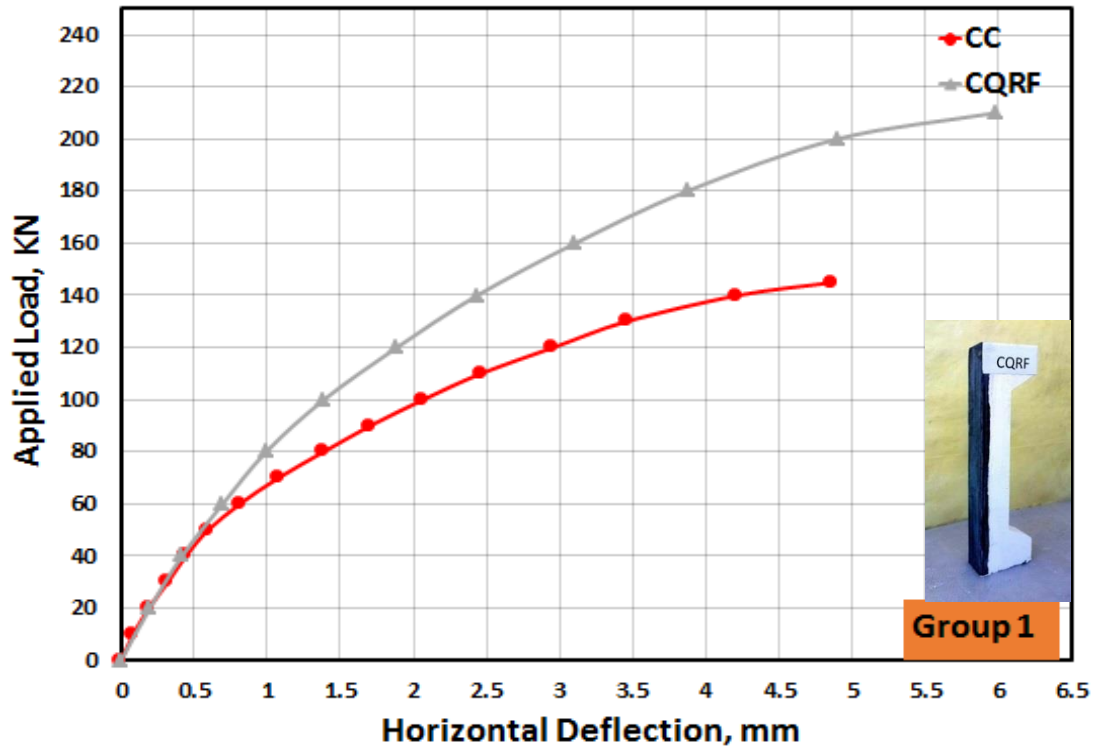
Fig. 4. 3 Horizontal and vertical load-deflection curves for CQRF and CC

4.2.2.3 Column Strengthened with Full CFRP Horizontal Wrapping (Clear column height (CQFFW))

This specimen was enhanced by an external CFRP sheets wrapping technique, including full horizontal CFRP wrapping for the clear column height after been subjected to an initial load of 25% of the ultimate design load. The column failed at a load of 180 kN with the progress of loading due to rupture of CFRP sheets, as shown in Plate (4.4). It is worth mentioning that the load capacity for this specimen increased due to the which confinement effect of CFRP sheets that covers areas of the concrete in the tensile and compressive, Where its effect was clear, especially in the compression, more than the tensile, so the increase in the ultimate load was small compared to the longitudinal strengthening. The structural behaviour for this specimen has been improved due to the increment that happened in the ultimate load compared to CC. Based on data of the horizontal deflections curve; it has also been noted that the structural behaviour of this specimen improved due to the increase in the ductility index and stiffness as they recorded values of 1.75 and 47.37 kN/mm, respectively. At the same time, the values of the ductility index and stiffness were 1.49 and 70.78 kN/mm, respectively when regarded the vertical deflections. Figure (4.4) illustrates the horizontal and vertical load-deflection curves for CQFFW.

Plate 4. 4. Failure for specimens CQFFW.
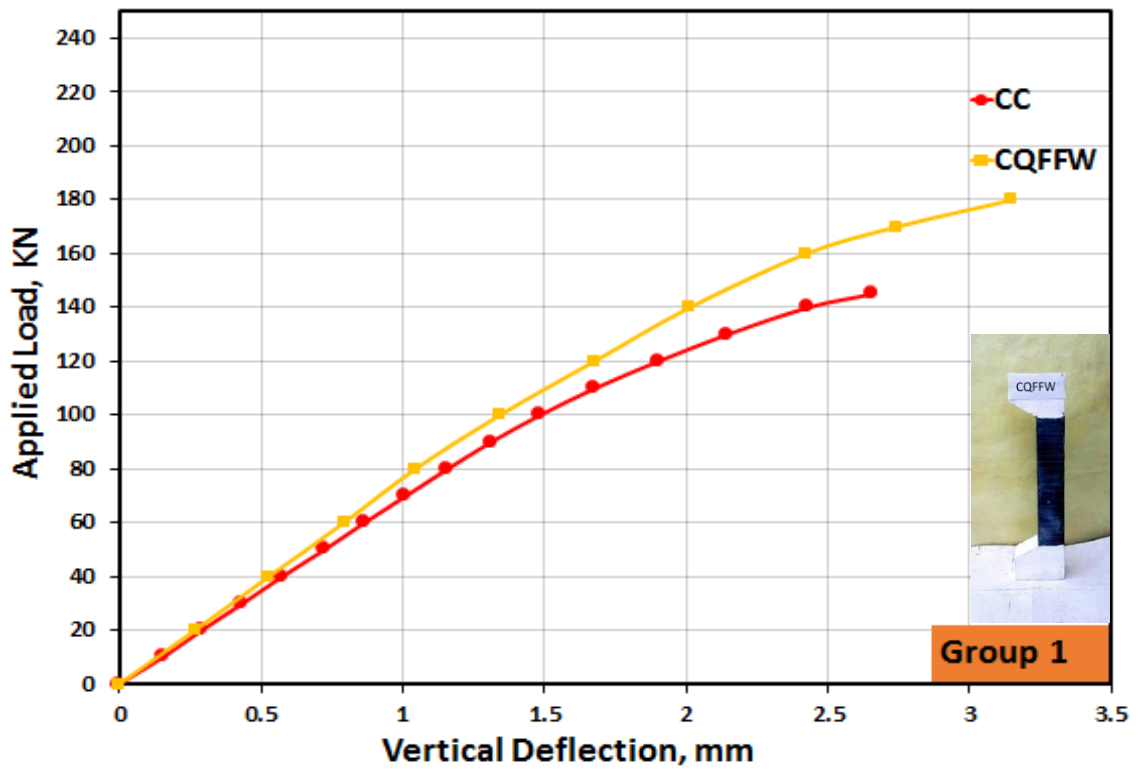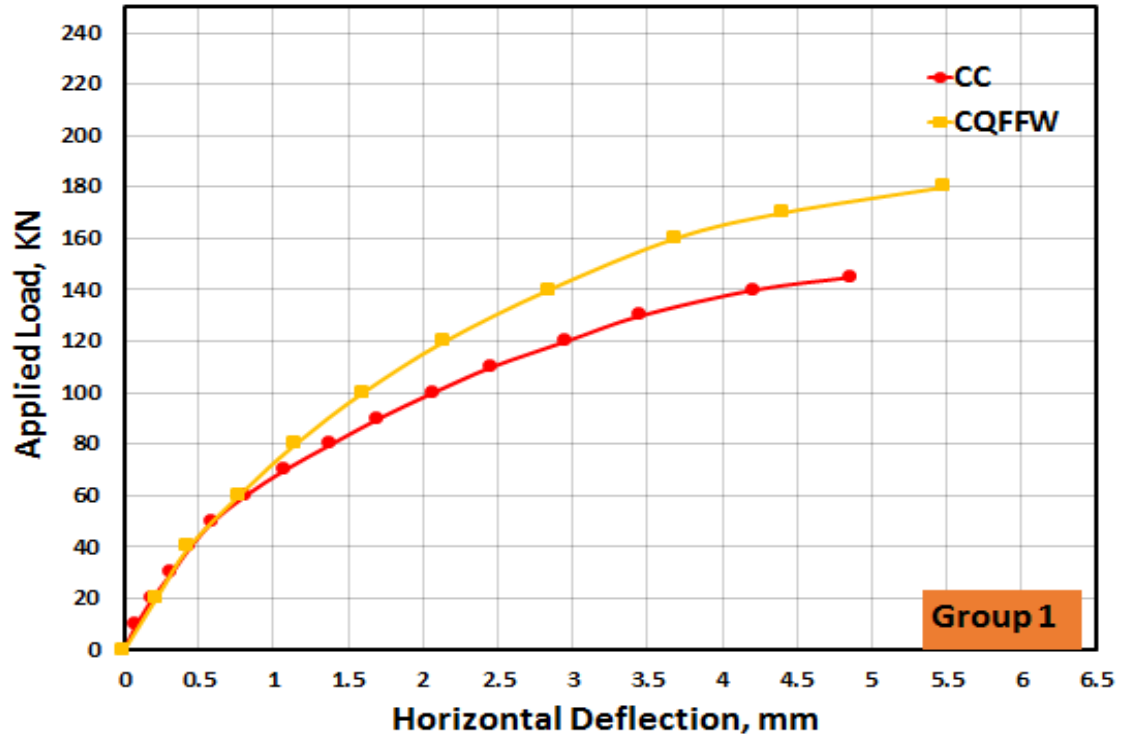
Fig. 4. 4. Horizontal and vertical load-deflection curves for CQFFW and CC

64

4.2.2.4 Column Strengthened with Horizontal CFRP Wrapping (250 mm length at column mid-height (CQ25FW))

This specimen was enhanced by an external CFRP wrapping technique, which includes horizontal wrapping with CFRP for 250 mm length at the mid-height of the column after been subjected to an initial load of 25% of the ultimate design load. This specimen failed at a load of 175 kN due to the crushing of concrete due to compression at the upper end of the column below the corbelled head due to the which confinement effect of CFRP sheets that covers small areas of the concrete in the tensile and compressive at in the middle of the column height. Thus, the increase was less for the column fully covered by the compressive area by horizontal, as shown in Plate (4.5). Therefore, the structural behaviour for this specimen has been improved due to the increment that happened in the ultimate load compared to CC. Furthermore, through the value of the horizontal load-deflections curve, it has also been noted that the structural behaviour of this specimen improved due to the increase in the ductility index and the stiffness, which were 1.70, and 46.22 kN/mm, respectively. While, the values of the ductility index and stiffness were 1.45 and 68.05 kN/mm, respectively, regarding vertical load-deflections. Figure (4.5) illustrates the horizontal and vertical load-deflection curves for CQ25FW.

Plate 4. 5. Failure for specimens CQ25FW

Fig. 4. 5. Horizontal and vertical load-deflection curves for CQ25FW and CC

4.2.3 Columns Strengthened with CFRP Technique (Group 2)

4.2.3.1 Column Strengthened with Full CFRP Longitudinal Wrapping (All column faces (CHFFL))

This specimen was enhanced by an external CFRP sheets wrapping technique, including full longitudinal wrapping with CFRP for all column faces after been subjected to an initial load strength of 50% of the maximum design load. The load was applied gradually to the specimen, where the first transverse cracks appeared in the tension area at the middle of the column. However, with the progress of the loading process, the column failed at a load applied of 210 kN due to rupture of CFRP sheets, as shown in Plate (4.6). It is worth mentioning that the load capacity for this specimen increased effectively, which might result from the significant the effect of containment of concrete in the tension and compressive area, which leads to an increase in the strength of the tension and compressive. Therefore, the structural behaviour for this specimen has been improved due to the increment that happened in the ultimate load compared to CC. Based on data of the horizontal load-deflections curve, it has also been noted that the structural behaviour of this specimen improved due to the increase in the ductility index and stiffness, which were 1.78, and 52.3 kN/mm 1, respectively. In the same regard, the values of the ductility index and stiffness were 1.52 and 74.62 kN/mm, respectively, when considered the vertical load-deflections. Figure (4.6) presented the horizontal and vertical load-deflection curves for CHFFL.
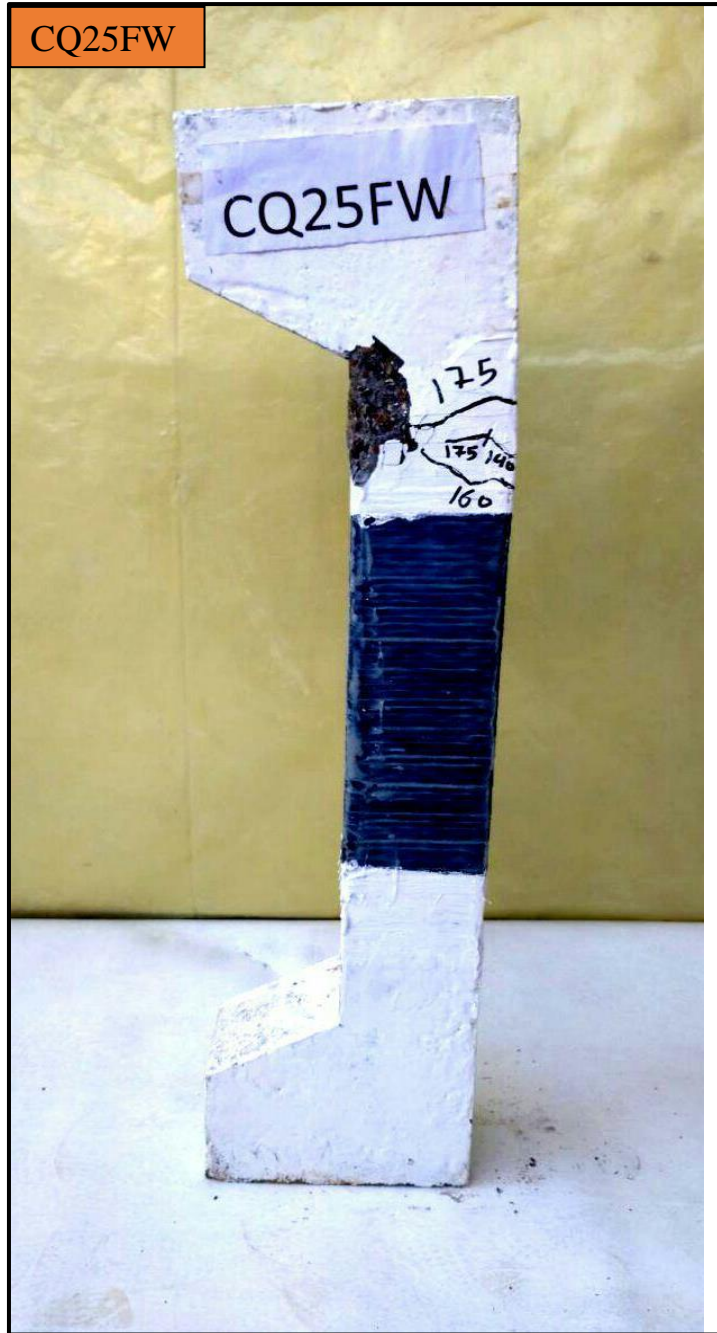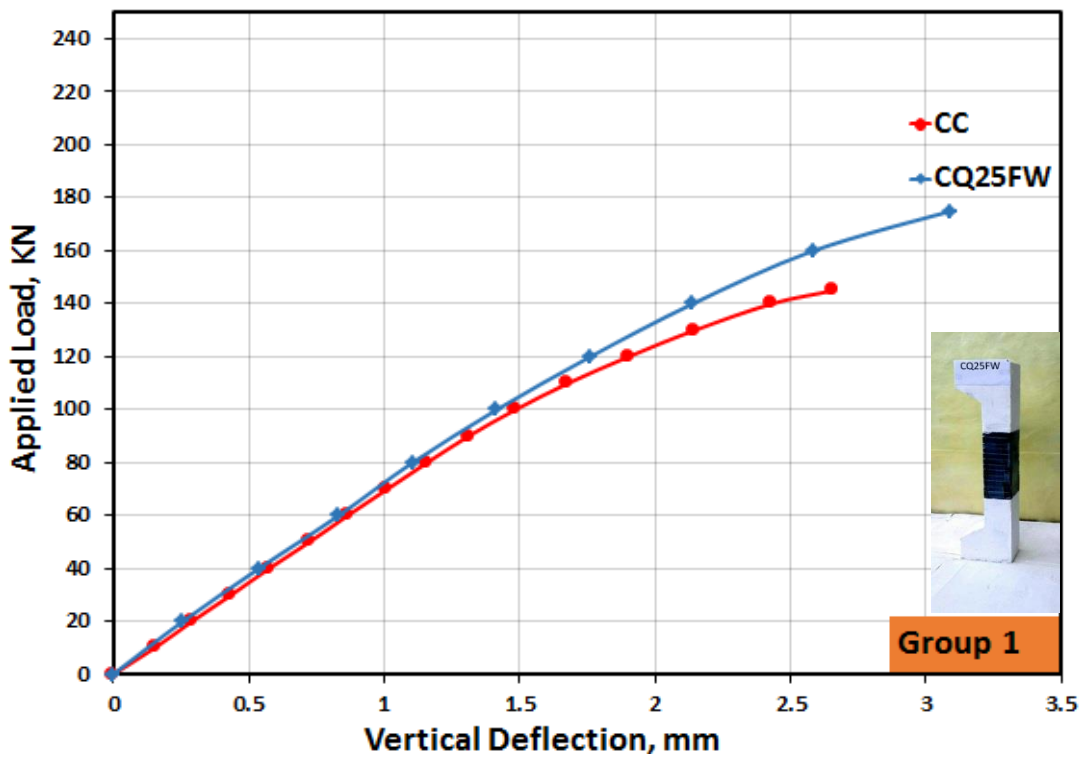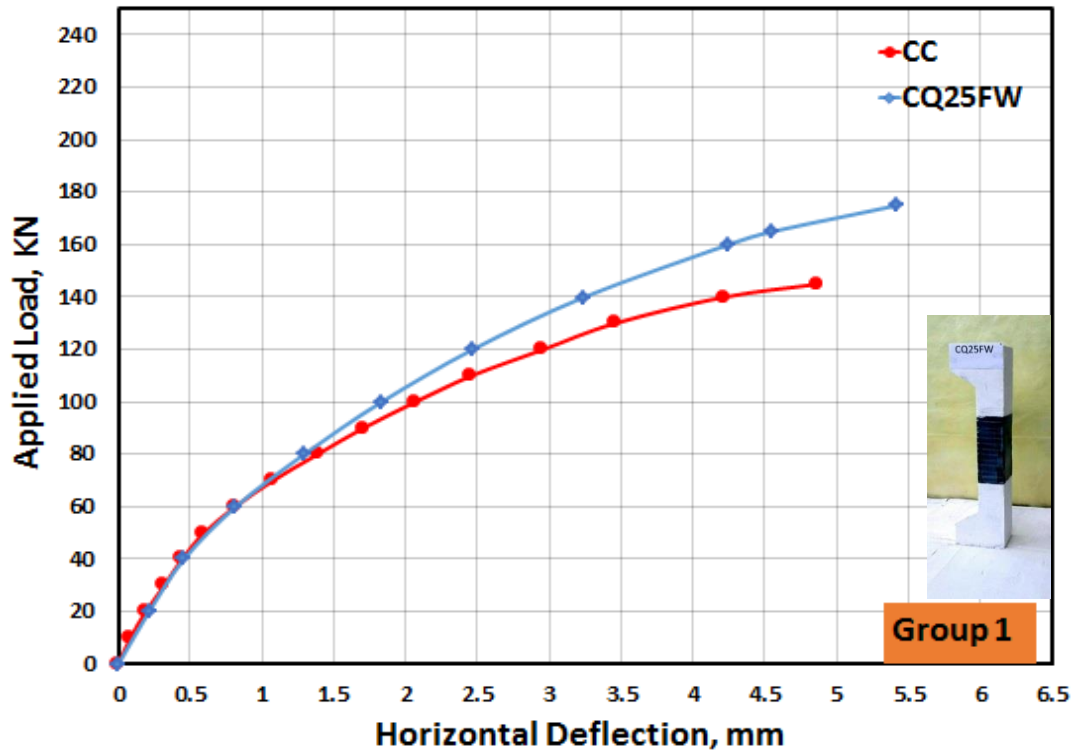
Plate 4. 6. Failure for specimens CHFFL.
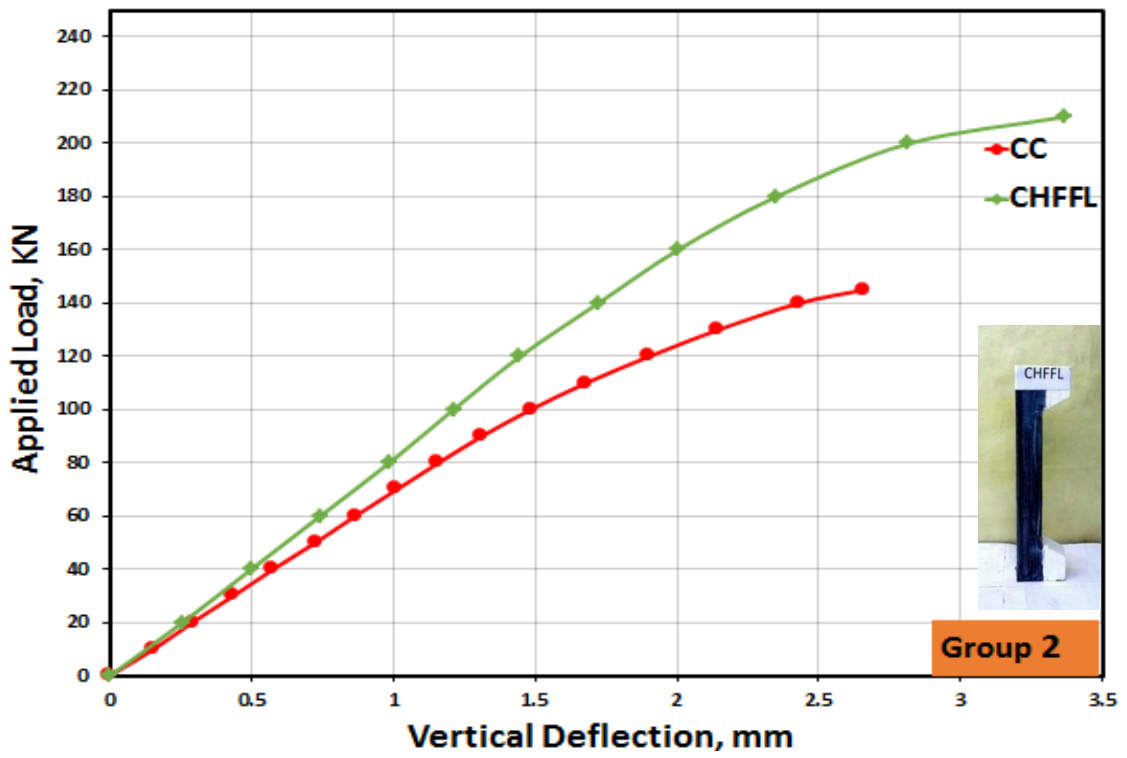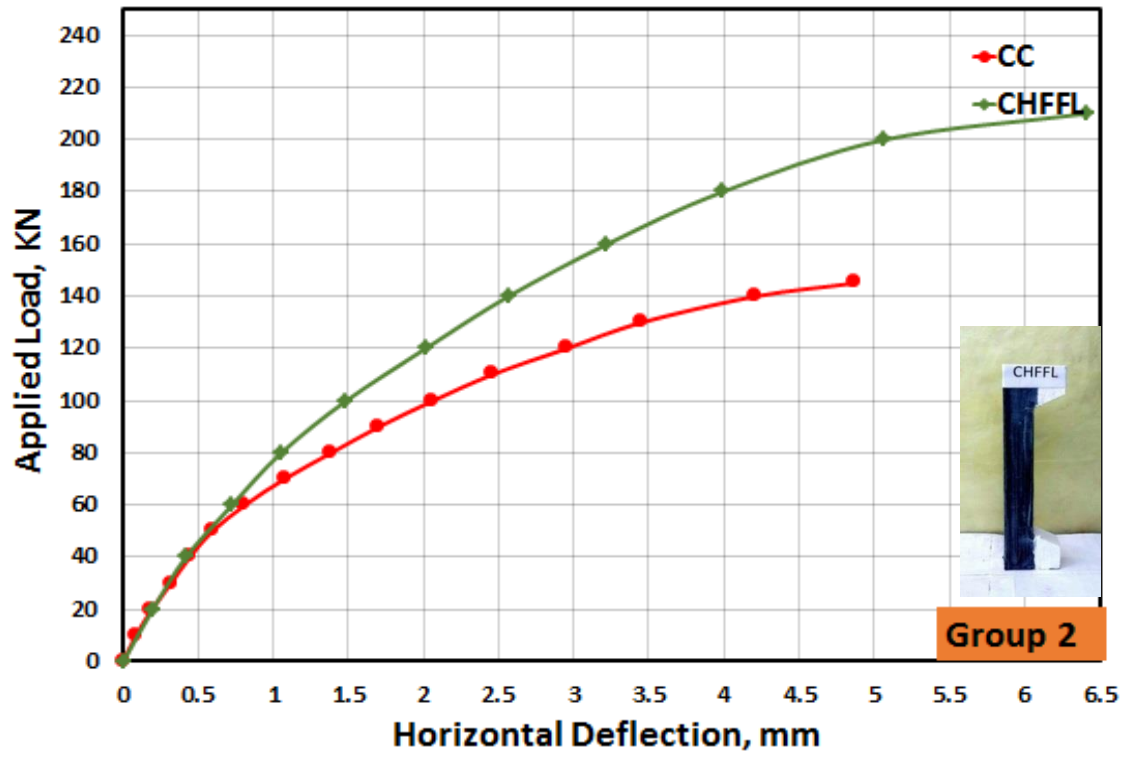
Fig. 4. 6 Horizontal and vertical load-deflection curves for CHFFL and CC

70

4.2.3.2 Columns Strengthened with Full CFRP Longitudinal Wrapping (Tension face only (CHRF))

This specimen was enhanced by an external wrapping of CFRP sheets, including full longitudinal wrapping for the tension face only after been subjected to an initial load applied of 50% of the maximum design load. The load was applied gradually on the column, where no cracks were observed at the initial stage of the loading process due to CFRP sheets preventing cracks. With the progress of the loading process, the column failed at a load applied of 200 kN due to the crushing of concrete in which compression failure for concrete at the upper end of the column below the corbelled head has occurred, as shown in Plate (4.7). The increase in the column capacity was due to the effect of containment of concrete in the tension area from the back, Which increases the strength of the tension. Therefore, the structural behaviour for this specimen has been improved due to the increment that happened in the ultimate load. Through the value of the horizontal load-deflections curve, it has also been noted that the structural behaviour of this specimen improved due to the increase in the ductility index and stiffness, as they recorded values equal to 1.72, and 50.18 kN/mm, respectively, in comparison with CC. In contrast, the values of the ductility index and stiffness were 1.49 and 72.91 kN/mm, respectively, when considering the vertical load-deflections. The horizontal and vertical load-deflection curves for CHRF were presented in Fig. (4.7).

Plate 4. 7. Failure for specimens CHRF.
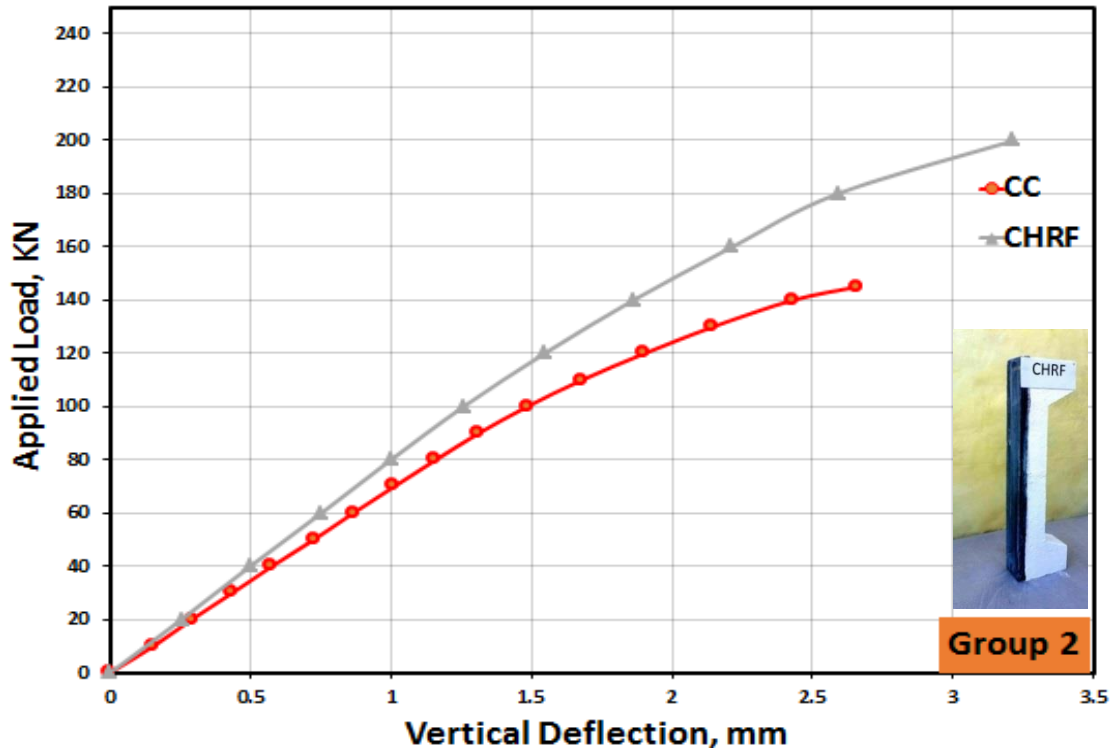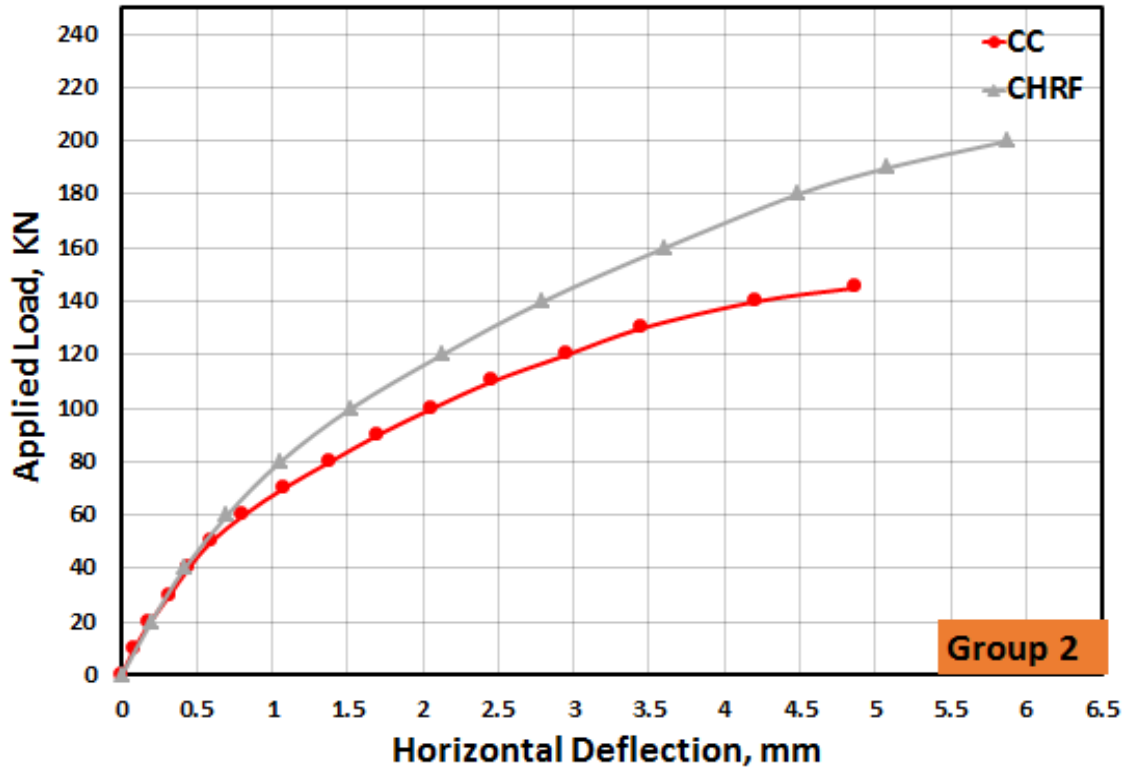
Fig. 4. 7. Horizontal and vertical load-deflection curves for CHRF and CC

4.2.3.3 Column Strengthened with Full CFRP Horizontal Wrapping (Clear column height (CHFFW))

This specimen was enhanced by an external CFRP sheets wrapping technique, including full horizontal CFRP wrapping for the clear column height after being subjected to an initial 50% of the ultimate design load. The column failed at a load of 165 kN, due to the rupture of CFRP sheets, as shown in Plate (4.8). It is worth mentioning that the load capacity for this specimen increased due to the which confinement effect of CFRP sheets that covers areas of the concrete in the tensile and compressive, Where its effect was clear, especially in the compression area, more than the tensile. Therefore, the structural behaviour recorded for this specimen has been improved due to the increment that happened in the ultimate load compared to CC. Furthermore, based on data of the horizontal load-deflections curve, it has also been noted that the structural behaviour of this specimen improved due to the increase in the ductility index and stiffness, as they recorded values of 1.72, and 50.88 kN/mm, respectively. At the same time, the values of the ductility index and stiffness were 1.48 and 69.57 kN/mm, respectively, when considering the vertical load-deflections. Figure (4.8) illustrates the horizontal and vertical load-deflection curves for CHFFW.
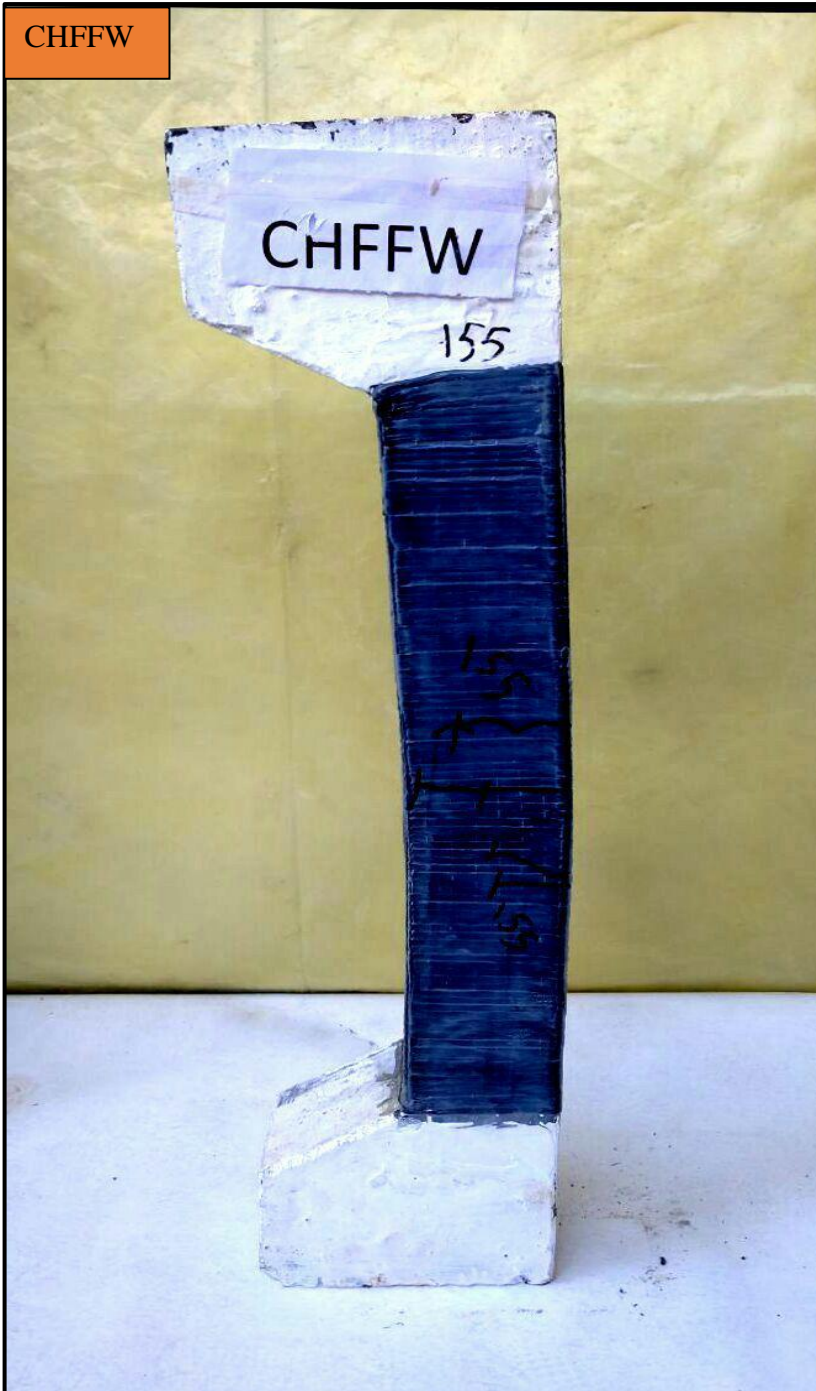
Plate 4. 8. Failure for specimens CHFFW
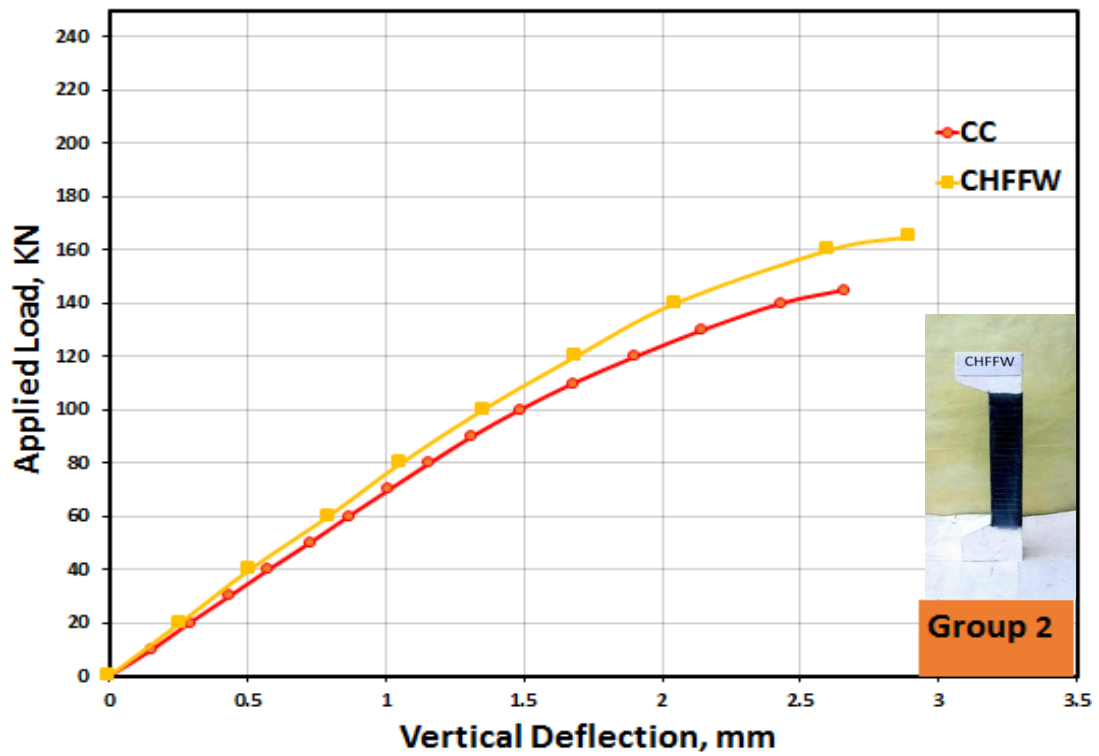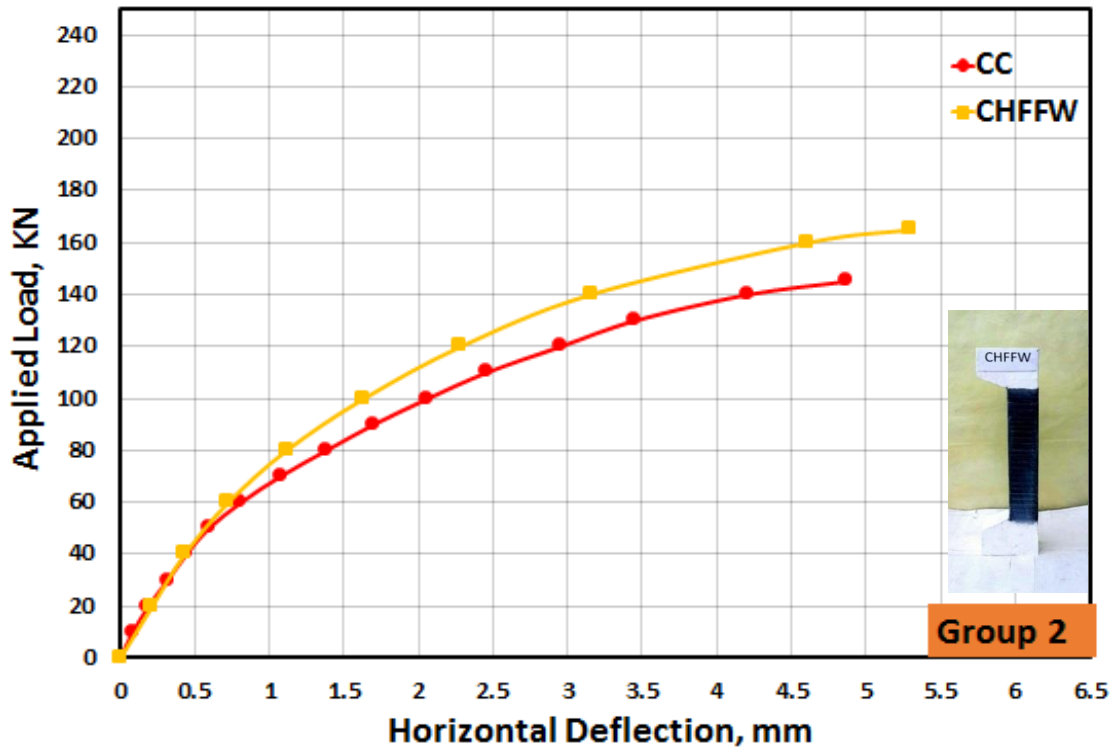
Fig. 4. 8. Horizontal and vertical load-deflection curves for CHFFW and CC

76

4.2.3.4 Column Strengthened with Horizontal CFRP Wrapping (250 mm length at column mid-height (CH25FW))

This specimen was enhanced by an external CFRP sheets wrapping technique, which includes horizontal wrapping with CFRP for 250 mm length at mid-height of the column after been subjected to an initial load of 50% of the ultimate design load. This column failed at a load of 160 kN due to the crushing of concrete due to compression at the upper end of the column below the corbelled head due to the which confinement effect of CFRP sheets that covers small areas of the concrete in the tensile and compressive at in the middle of the column height. Thus, the increase was less for the column fully covered by the compressive area by horizontal, as shown in Plate (4.9). Therefore, this specimen's structural behaviour has improved due to the increment in the ultimate load. Furthermore, through the value of the horizontal load-deflections curve, it has also been noted that the structural behaviour of this specimen improved due to the increase in the ductility index and stiffness, which were 1.71, and 48.91 kN/mm, respectively, in comparison with CC. At the same time, the values of the ductility index and stiffness were 1.47, and 69.13 kN/mm, respectively, regarding vertical load-deflections. Figure (4.9) illustrates the horizontal and vertical load-deflection curves for CH25FW.

Plate 4. 9. Failure for specimens CH25FW
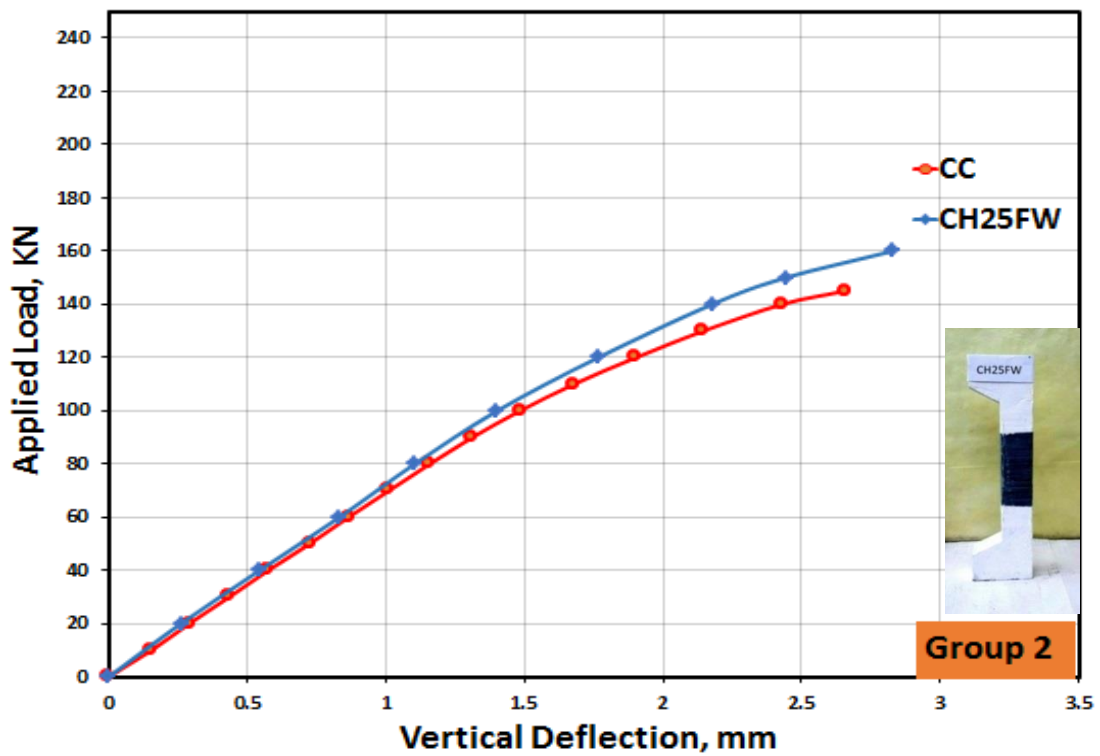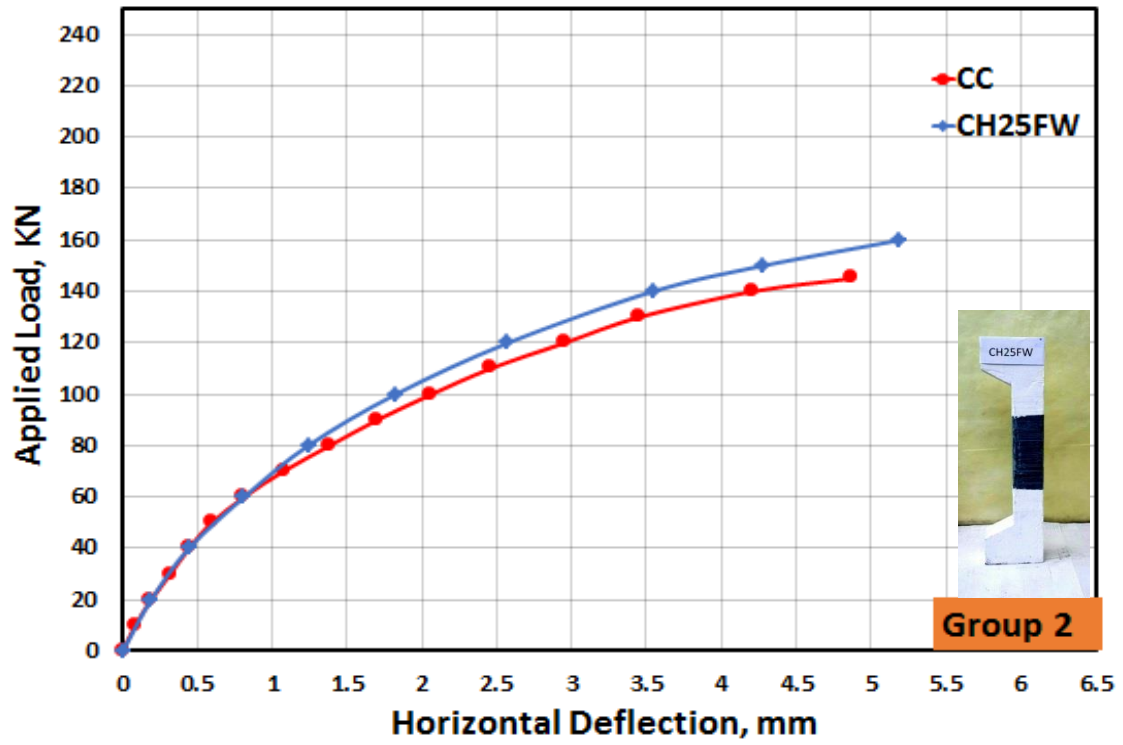
Fig. 4. 9. Horizontal and vertical load-deflection curves for CH25FW and CC

Figures (4.10),(4.11) comparing for columns strengthened with the CFRP sheets wrapping technique to the initial load ratio of 25% and 50% of the CC ultimate design load and CC.
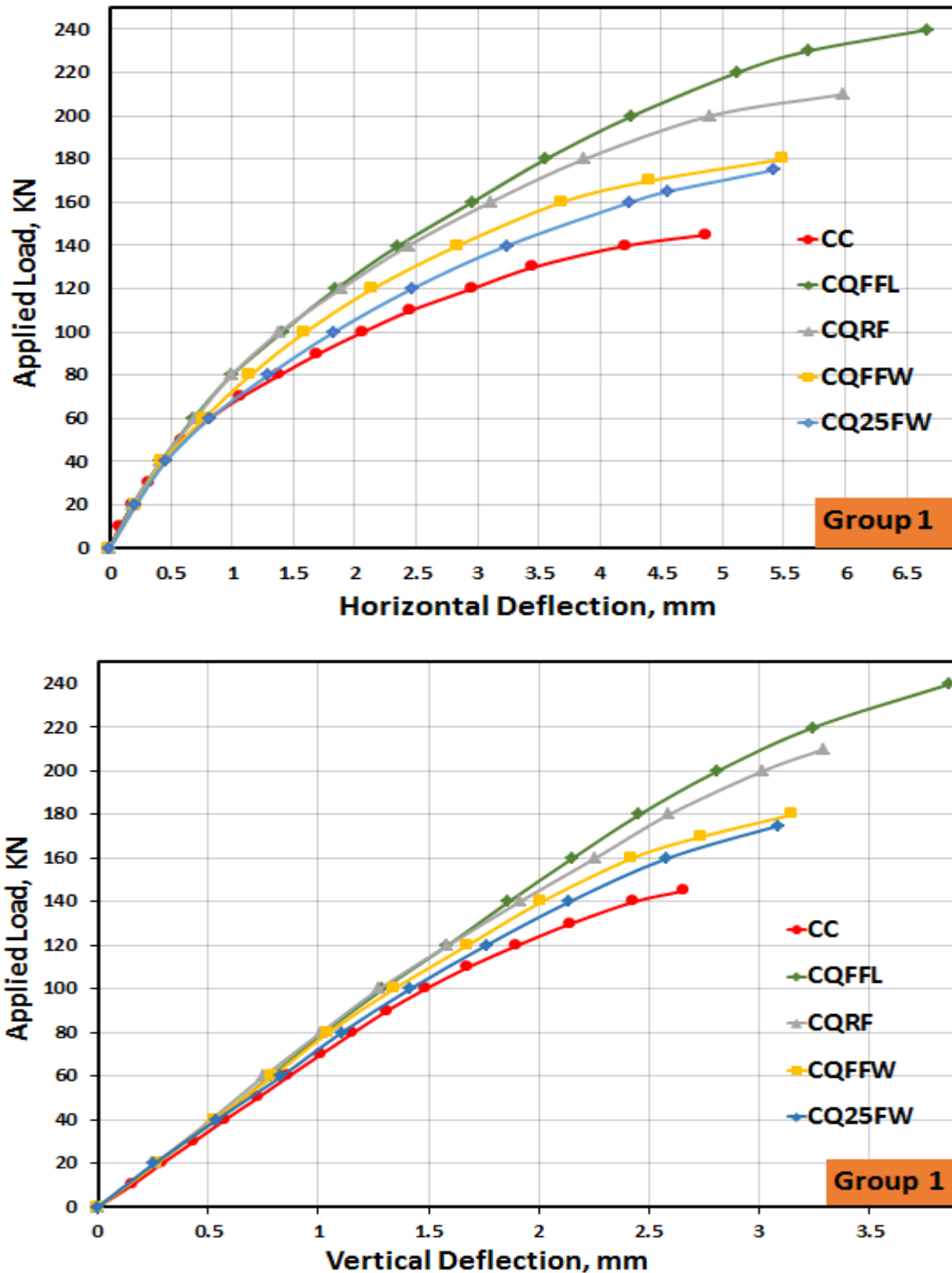
Fig. 4. 10. Horizontal and vertical load-deflection curves for the columns in Group 1 and CC
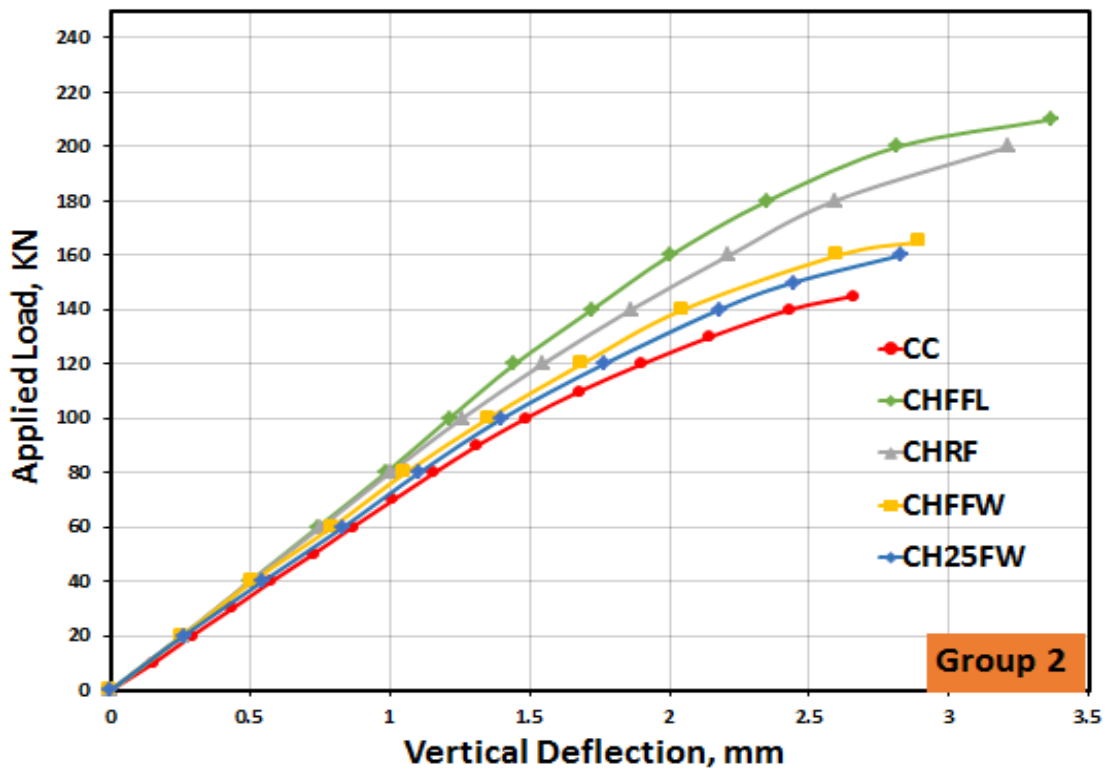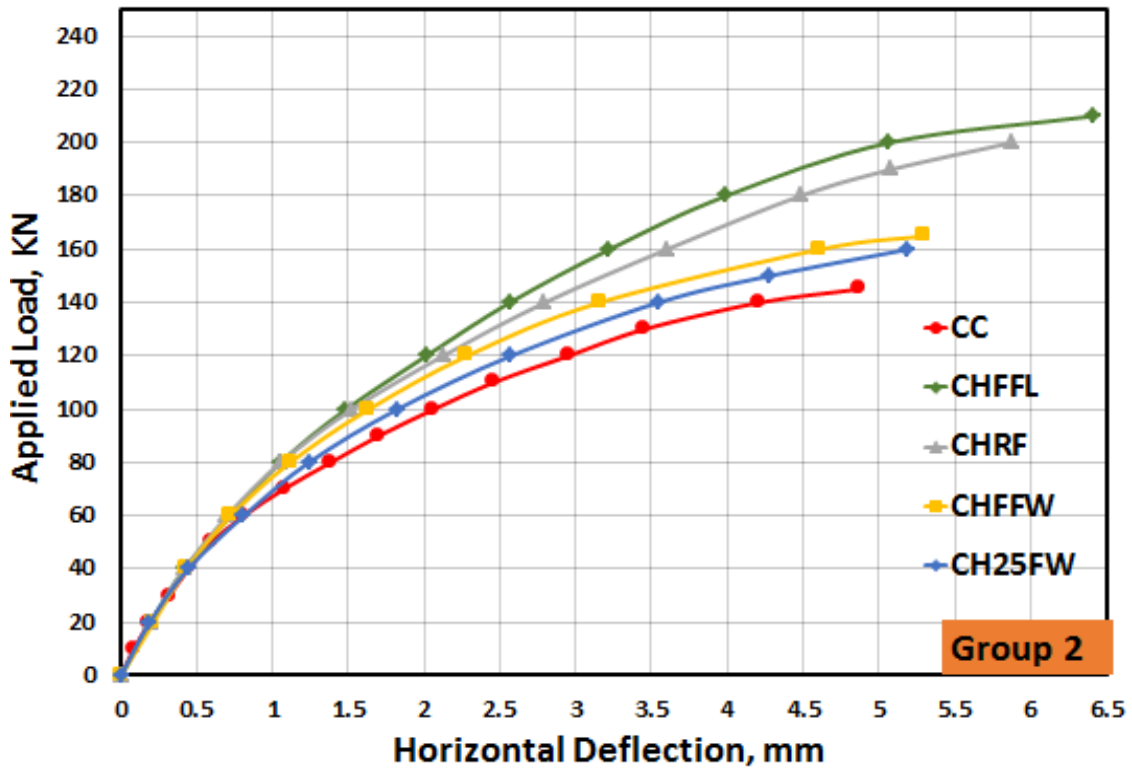
Fig. 4. 11. Horizontal and vertical load-deflection curves for the columns in Group 2 and C

Table 4. 1. The load capacity for the tested columns

Group number	Column designation	Ultimate strength (f_u) KN	Ultimate load ratio %	Failure nature
reference	CC	145	--------	Crushing of Concrete
`	CQFFL	240	65.55	Rupture of CFRP
Group 1	CQRF	210	44.82	Crushing of Concrete
	CQFFW	180	24.14	Rupture of CFRP
	CQ25FW	175	20.69	Crushing of Concrete
Group 2	CHFFL	210	44.83	Rupture of CFRP
	CHRF	200	37.93	Crushing of Concrete
	CHFFW	165	13.79	Rupture of CFRP
	CH25FW	160	10.34	Crushing of Concrete

Table 4. 2. The ductility index for the tested columns

No. Group	Column designation	Yielding strength (fy=0.8×fu)KN	Ultimate displacement horizontal(Δ) mm	Yielding displacement(Δy) mm at (fv)	Ductility index DI= Δ/ Δy	Ultimate displacement vertical (Δ) mm	Yielding displacement(Δy) at (fy)	Ductility index DI= Δ/ Δy
reference	CC	116	4.86	2.87	1.69	2.65	1.86	1.42
Group 1	CQFFL	192	6.67	3.75	1.78	3.86	2.53	1.53
	CQRF	168	5.98	3.40	1.76	3.29	2.19	1.50
	CQFFW	144	5.49	3.14	1.75	3.15	2.12	1.49
	CQ25FW	140	5.42	3.19	1.70	3.08	2.13	1.45
Group 2	CHFFL	168	6.41	3.59	1.78	3.36	2.21	1.52
	CHRF	160	5.87	3.42	1.72	3.21	2.16	1.49
	CHFFW	132	5.30	3.08	1.72	2.89	1.95	1.48
	CH25FW	128	5.19	3.03	1.71	2.82	1.91	1.47

Where is **Ductility Index** The ability to resist inelastic deformation without a reduction in ultimate load until failure, It is calculated from the equation:

Ductility Index = Δ /Δy

$\Delta y = \Delta (0.8 \ fu)$

Table 4. 3. The stiffness for the tested columns

	Column designation	service load FS= 0.7 fu	Ultimate displacement horizontal at service load (Δy) mm	Stiffens at service load KN/mm K= FS/Δy at(Δy) horizontal	Ultimate displacement vertical at service load (Δy) mm	Stiffens at service load KN/mm K= FS/Δy At (Δy) vertical
reference	CC	101.5	2.21	45.93	1.53	66.34
Group 1	CQFFL	168	3.16	53.17	2.28	73.68
	CQRF	147	2.78	52.87	2.05	71.70
	CQFFW	126	2.66	47.37	1.78	70.78
	CQ25FW	122.5	2.65	46.22	1.80	68.05
Group 2	CHFFL	147	2.81	52.31	1.97	74.62
	CHRF	140	2.79	50.18	1.92	72.91
	CHFFW	115.5	2.27	50.88	1.66	69.57
	CH25FW	112	2.29	48.91	1.62	69.13

Where is **Stiffness (K)** of a body is a measure of the resistance offered by an elastic body to deformation. , It is calculated from the equation:

K : 0.7fu /Δ (0.7fu)

4.3 Summary

The following points can be summarised from strengthening the pre-partially loaded HSC short columns with square- cross-section using various strengthening schemes by CFRP strips:

1. The first crack for the control column appears nearly at the quarter value of the ultimate design load of the column;

2. Strengthening specimens in the first group with total longitudinal CFRP for all sides of the column or the tension face only (i.e. CQFFL, CQRF) were very beneficial in terms of their strength capacities ratios in which they were 65.55% and 44.82%, respectively, compared to CC. Further, there were improvements in both the stiffness and ductility index as they recorded 53.17 kN/mm, 52.87 kN/mm, 1.78, and 1.76 according to the horizontal load-deflection data and 73.68, 71.70, 1.53, and 1.50 for the vertical load-deflection data, respectively, as shown in Tables (4.1), (4. 2), (4. 3);

3. For the first group, specimens strengthening with horizontal encapsulation (i.e. CQFFL, CQ25FW) resulted in a lower improvement in strength capacity ratios by only 24.14 and 20.69% when compared with CC. There were also increases in both the stiffness and ductility index values as they were 47.37 kN/mm , 46.22 kN/mm, 1.75, and 1.70 according to the horizontal load-deflection data and 70.78, 68.05, 1.49, and 1.45 for the vertical load-deflection data, respectively compared to CC, as shown in Tables (4.1), (4. 2), (4. 3);

4. For the second group of specimens, the strengthening for CHFFL and CHRF were beneficial in terms of increasing the strength capacity ratios as they were increased by 44.83% and 37.93 %, respectively in comparison with CC. Moreover, the values of the stiffness and ductility index were 52.31 kN/mm, 50.18 kN/mm, 1.78, and 1.72 according to the horizontal

load-deflection data and 74.62, 72.61, 1.52, and 1.49 for the vertical load-deflection data, respectively, as shown in Tables (4.1), (4. 2), (4. 3);

5. For the second group of specimens, the strengthening for CHFFW and CH25FW resulted in a lower improvement in strength ratios by only 13.79 and 10.34%, respectively, in comparison with CC. Indeed, the values of the stiffness and ductility index were 50.88 kN/mm, 84.91, kN/mm 1.72, and 1.71 according to the horizontal load-deflection data and 69.57, 69.13, 1.48, and 1.47 for the vertical load-deflection data, respectively compared to CC, as shown in Tables (4.1), (4. 2), and (4. 3);

6. It was noted that the strengthened of the samples with CFRP in the direction parallel to the vertical direction provides the highest final loading capacity when repairing damaged columns with the same material in the direction parallel to the horizontal direction due to the effect for containment of the concrete in the compressive and tension areas and this leads to strengthening the tensile and thus increasing the ultimate load , as shown in Tables (4.1), (4.2), (4. 3);

7. The values of the horizontal load-deflection curves gave the highest ductility index for the samples strengthened with CFRP compared to the vertical load-deflection curves. In contrast, the vertical load-deflection curves showed higher stiffness values from horizontal load-deflection.

8. The first group of samples that were initially loaded by 25% of the ultimate design load gave higher strength than the specimens of the second group that were initially loaded by 50%.

9. There was an increase in the stiffness and ductility index for all the strengthened specimens compared to the control column.

10. Crushing the concrete (compression failure of concrete) was the typical failure mode for CC, C25TF, C50TF, C25FH25, and C50FH25. In contrast, the rupture of CFRP sheets was the typical failure for C25FFL, C50FFL, C25FFH, and C50FFH.

CHAPTER FIVE
FINITE ELEMENT ANALYSIS

5.1 Introduction

This chapter aims to build a model based on the experimental results using non-linear finite elements to ensure the suitability of material properties, form elements, and convergence requirements for modelling and the response of undamaged and damaged HSC square-cross section short columns strengthened technique with CFRP by various schemes. In addition, other parameters were analysed in terms of their structural behaviour by the verified model that used the non-linear finite element method (ABAQUS).

5.2 Description of Finite Element Modeling

This section explains the assembling process for the tested columns, loading, and boundary condition used.

5.2.1 Modelling the used Material

The same geometry, material properties, loading and boundary conditions used in the experimental study were carried out in finite-element modelling to simulate the tested HSC columns. Modelling the control column (CC) involves four parts, including concrete, primary reinforcement, stirrups, and steel plates, as illustrated in Fig. (5.1). These parts are drawn separately to be collected later to form the control model. In the contraction step, all parts were bonded to each other such as the primary reinforcement and the stirrups embedded inside the concrete by embedded region constrain. On the other hand, the tie constraints were utilised to bond the steel plate with the concrete. Columns strengthened with the CFRP sheets technique comprised the exact geometry of CC. The same process was followed in CC to assemble and constraint all parts.

Moreover, tie constrain was used to connect the CFRP with the concrete for the specimens strengthened by wrapping CFRP sheets. Besides, the CFRP sheets have been treated as a linearly elastic material to later select the lamina option from the elastic behaviour and model as a shell element. Finally, the meshing of CFRP sheets was implemented using S4R, i.e., a 4-node thin shell with reduced integration, as shown in Fig. (5.2)
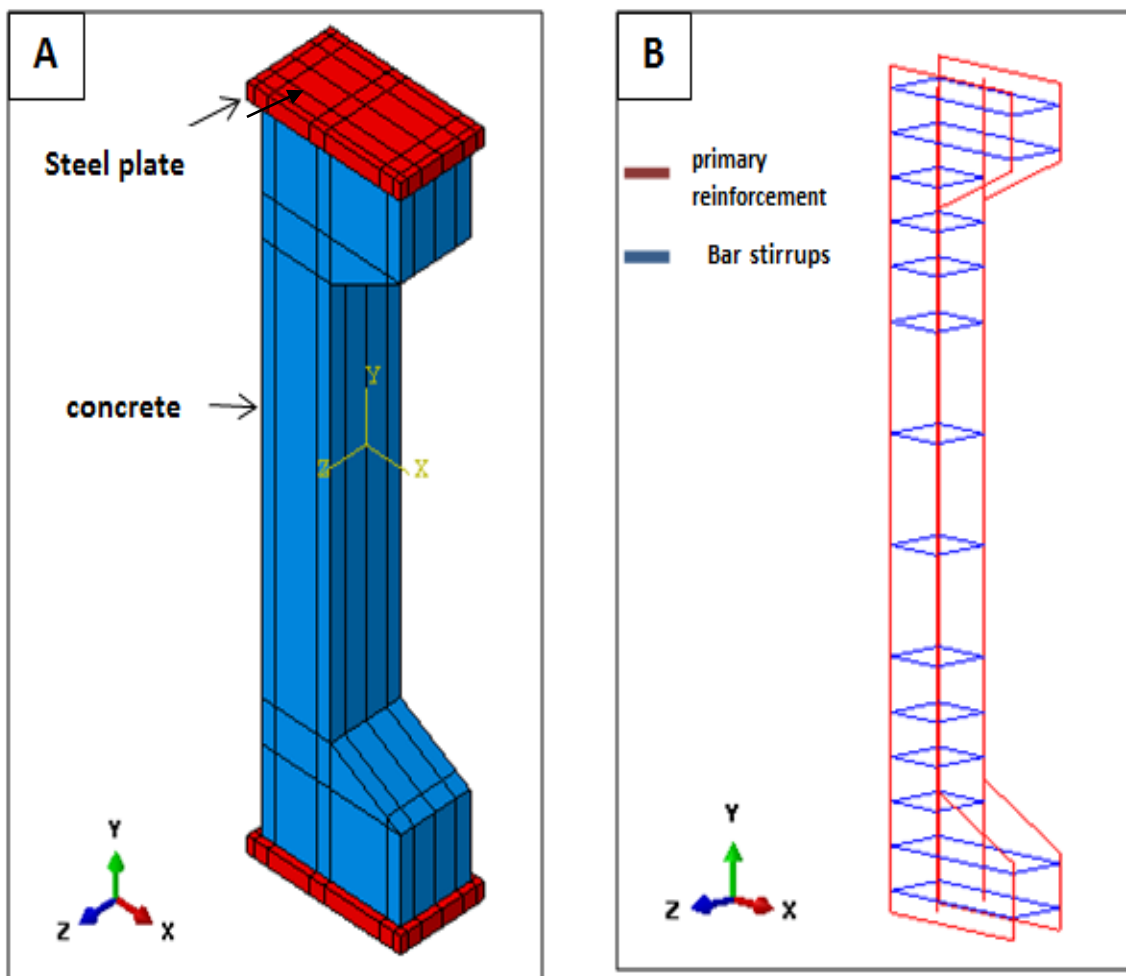

Fig. 5. 1. The assembled parts (A) and steel reinforcement (B) for the control model.

Figure (5.2) showed the details for modelling specimens strengthened by wrapping CFRP sheets. Further, Appendix **C** has presented concrete properties, the filling materials, and CFRP sheets.

5.2.1.1 High Strength Concrete

All specimens were prepared with identical dimensions of a square cross-section (100 × 100) mm and a total length of 800 mm. The length between the corbels was 500 mm, and each corbel head has a height of 150 mm, as shown in Figure 1. In the 3D finite element analysis, concrete is treated as a linear solid brick element. (Table 5.1 shows the general properties used in modelling HSC).

Table 5.1. General properties used in the model for the damaged concrete

Dilation angle (Degree)	Eccentricity (mm)	Fb0/fc0	k	Viscosity parameter	Young modules (N/mm)	Poisson Ratio
36	0.1	1.16	0.667	0	32500	0.2

5.2.1.2 Steel reinforcement

As illustrated in Fig. 5.2. steel reinforcement (8 mm) was employed as a primary reinforcement, while stirrups (6 mm) were employed as ties. Embedded region constraint was used to embed the steel reinforcement inside the concrete. the reinforcement steel was treated as a linear truss element. The Poisson's ratio and elasticity modulus were 0.3 and 200MPa, respectively.

5.2.1.3 Steel plates

At the two ends of the model (top and bottom), two steel plates with dimensions of (220×120×20) mm in length, breadth, and height were used. The Poisson's ratio and elastic modulus for the plates were and 0.3 and 200 GPa, respectively. Fig. 5.2. shows how tie constraints were used to attach the plates to the concrete surfaces.

5.2.1.4 Carbon Fiber Reinforcement Polymer Sheets

Specimens strengthened by wrapping CFRP sheets, tie constrain was used to connect the CFRP with the concrete. Besides, the CFRP sheets have been treated as a linearly elastic material to select later the option of the lamina from the elastic behaviour and model as a shell element. All CFRP properties are clarified in Table 5.2.

Table 5.2. Properties of CFRP sheets

Material	Dry Fiber Modulus of Elasticity in Tension(MPa)	Dry Fiber Tensile Strength (MPa)	Laminate Nominal Thickness (mm)
CFRP	230 000	3400	0.169

| Linear solid Brick Element | Linear Truss Element | Shell Element |
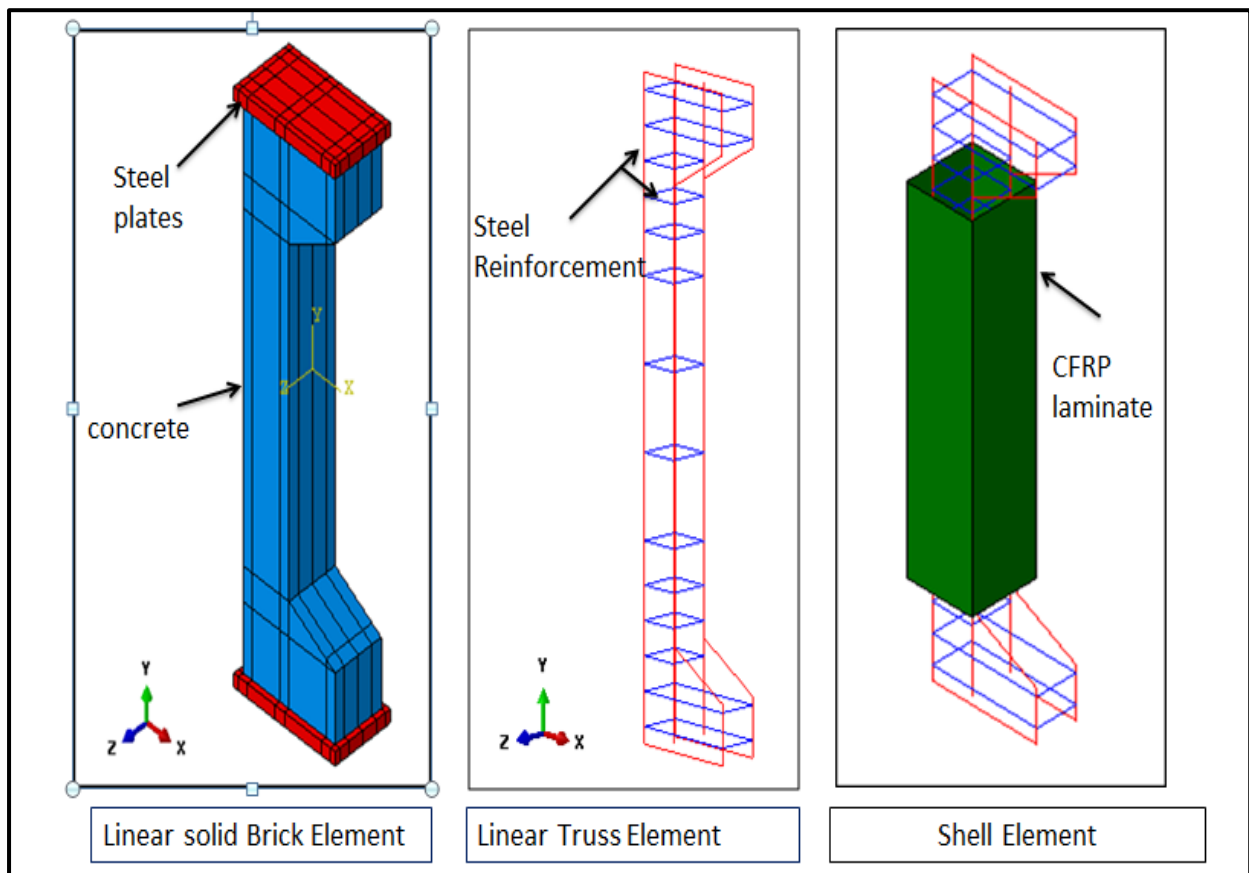
Fig. 5. 2. Details for element type

5.2.2 Loading stage and boundary condition

Loads were applied on steel plates of each specimen using in a similar way to the experimental work. The loads have been applied on a steel plate with dimensions of 220×120×20 mm under eccentric by an eccentricity of 50 mm from the center, which is located at the down of the column to transform the loads to it. All reinforced concrete columns models were constrained using boundary conditions displacement to get the most appropriate solution. Besides, all samples were constrained along the line in the top plate of the column with the same 50 mm deviation from the centre, ((Uz = Uy = Ux = 0), as shown in Fig. (5.3)
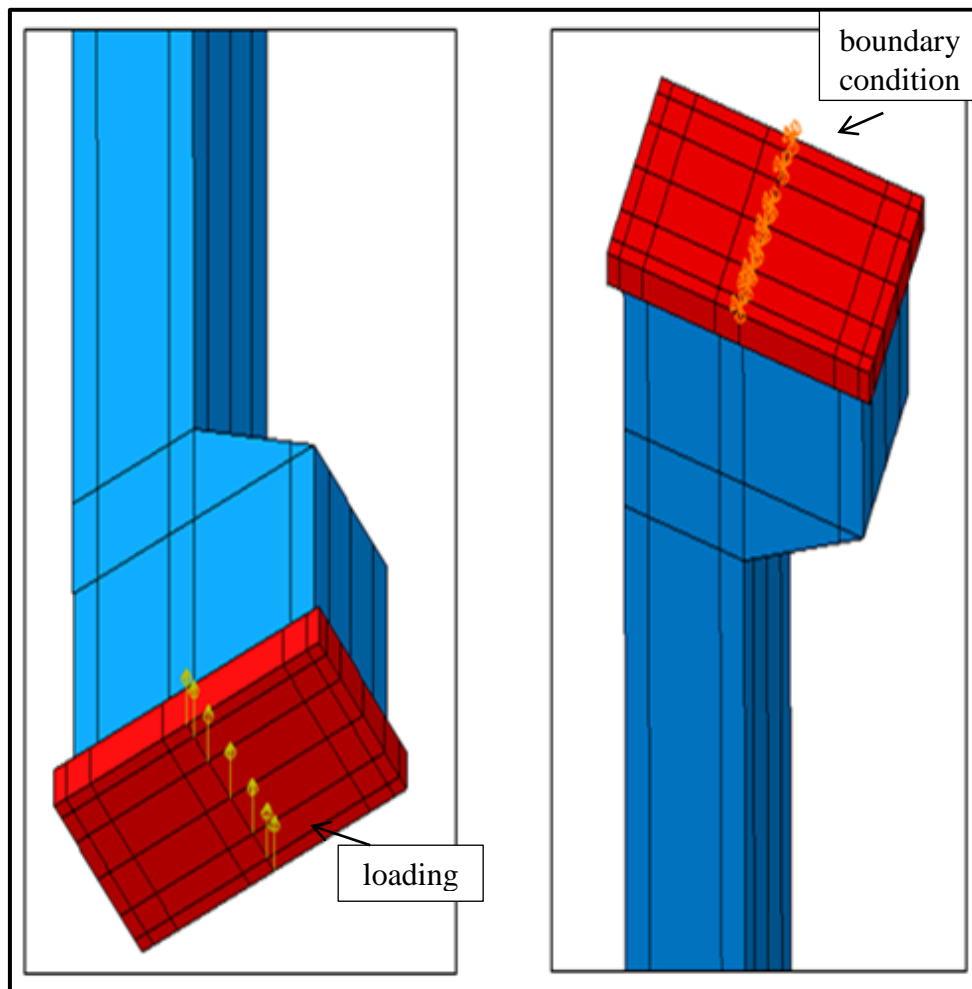
Fig. 5. 3. Loading and boundary conditions for the models

5.3 Convergence study

Element size selection is an essential step in finite element analysis. The density that gives the desired precision was chosen after making suitable analyses for different element sizes. Dividing specimens into a sufficient number of components leads to strong convergence, which becomes evident that there is a slight impact on the result. The convergence study was carried out by selecting various element sizes (25, 22.5, 20, 17.5, 15, and 12.5 mm), as shown in Fig. (5.5). From the element size results, the closest exact values of ultimate load and horizontal and vertical deviation of experimental results for CC were with 20 mm element size (see Table (5.3)). Thus, for all of the tested columns, an element size of 20 mm was chosen. Figure (5.4) illustrated the experimental and theoretical horizontal and vertical load-deflection curves with various mesh sizes.
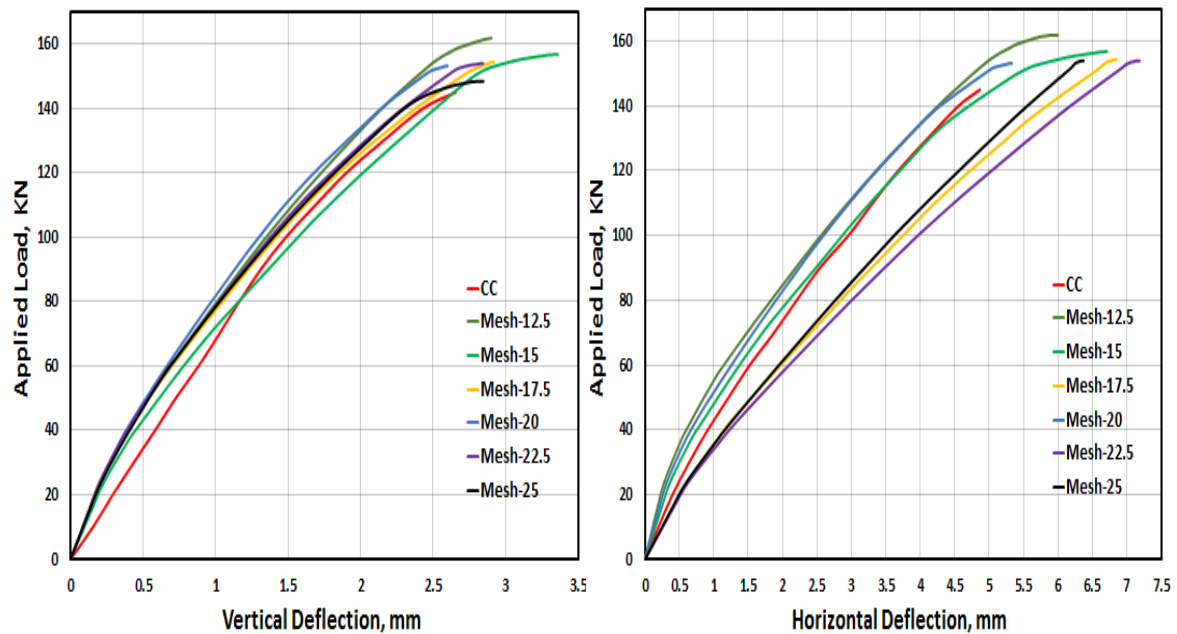
Fig. 5. 4. The impact of the element size on horizontal and vertical load-deflection curves

Table 5. 3. The impact of mesh size on the ultimate capacity and horizontal and vertical load-deflection values

Mesh size mm		Ultimate load KN	Horizontal deflection mm	Vertical deflection mm
12.5	Exp	145	4.86	2.65
	FEA	161.85	6.001	2.902
15	Exp	145	4.86	2.65
	FEA	156.75	6.712	3.359
17.5	Exp	145	4.86	2.65
	FEA	154.33	6.849	2.920
20	Exp	145	4.86	2.65
	FEA	153.78	5.332	2.589
22.5	Exp	145	4.86	2.65
	FEA	153.92	7.182	2.844
25	Exp	145	4.86	2.65
	FEA	154.92	6.373	2.965

| Case NO.1: Mesh 12.5mm | Case NO.1: Mesh 15 mm | Case NO.1: Mesh 17.5 mm |
| Case NO.1: Mesh 20 mm | Case NO.1: Mesh 22.5 mm | Case NO.1:Mesh 25 mm |

Fig. 5. 5. Finite element mesh density

5.4 Stress-Strain Relationship

The model of the stress-strain relationship given in **Ayub et al. (2014)** for the high strength concrete in the compression behaviour was used in 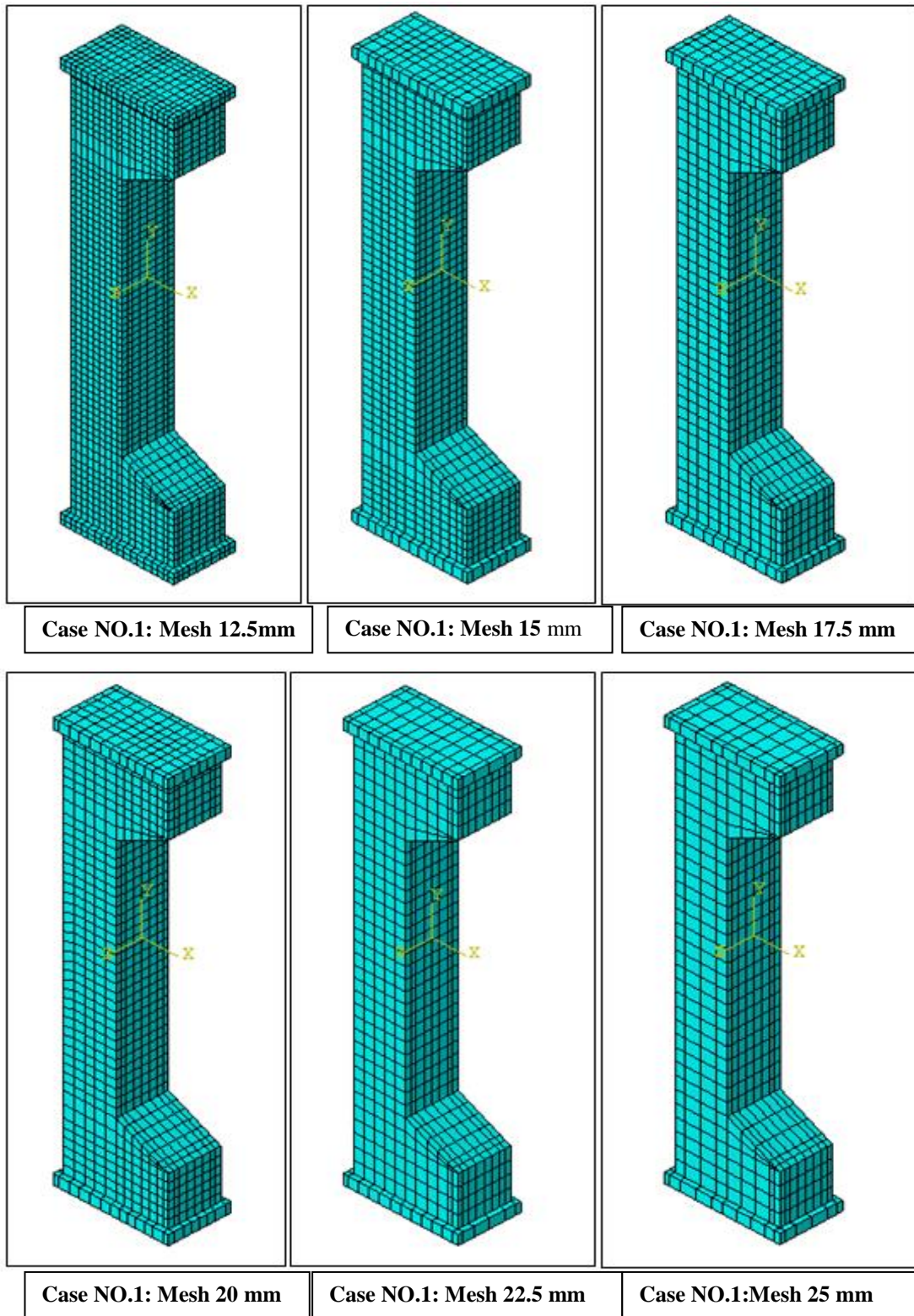this research. Table 5.4, and Figure 5.6. provide the data and the stress-strain relationship model used in this research, respectively.

Table 5.4 The stress-strain relationship used in this research

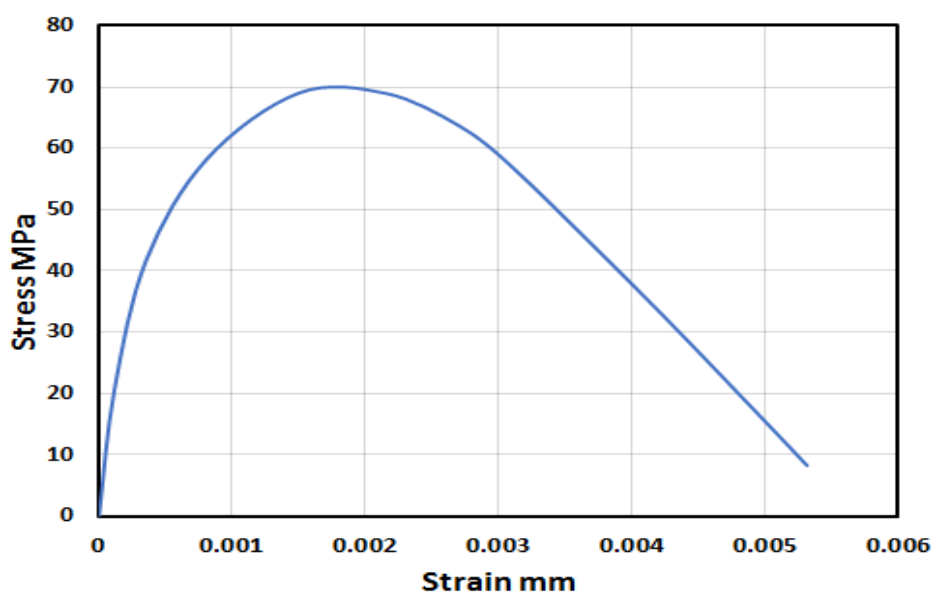| Number	Yield stress (MPa)	Plastic strain (mm)
1	0	0
2	20.48	0.0001141
3	41.65	0.0003521
4	58.25	0.0008094
5	69.02	0.001501
6	68.95	0.002154
7	63.55	0.002695
8	57.25	0.003085
9	35.54	0.004105
10	15.55	0.004995
11	8.25	0.005314

Figure 5.6 Model of stress-strain relationship (Ayub et al. (2014))

95

5.5 Load application sequence

The partially loaded columns comprise three phases of loading in which the first phase presents the loading of the column to a specific ratio of the ultimate load. At the same time, the second phase involved removing the load from the column, which is implemented by the restart analysis. On the other hand, the last phase included loading the column until failure after implementing the strengthening techniques for each specimen. The second phase stresses are inserted into the third phase from the initial step for the last one. On the other hand, the control column (undamaged column) included one phase, which presents the loading of the column until failure.

5.6 Comparative study between FEM and experimental results

In this part, a comparative study was implemented among the experimental and finite element results regarding the ultimate capacity and the horizontal and vertical load-displacement for all tested columns.

5.6.1 Load-displacement behaviour

Figures (5.7) to (5.15) illustrated a comparison between the experimental and FEM load-horizontal and vertical deflection curves. The horizontal deflections were measured at the mid of the column at the lateral while the vertical deflections were measured at the top edge for steel plate for all tested columns in a similar way in the experimental tests. The comparison showed the validity of the numerical analysis by ABAQUS with the experimental results discussed in chapter four.

Fig. 5. 7. Numerical and experimental horizontal and vertical load-deflection curves for CC

Fig. 5. 8. Numerical and experimental horizontal and vertical load-deflection curves for CQFFL

Fig. 5. 9. Numerical and experimental horizontal and vertical load-deflection curves for CQRF
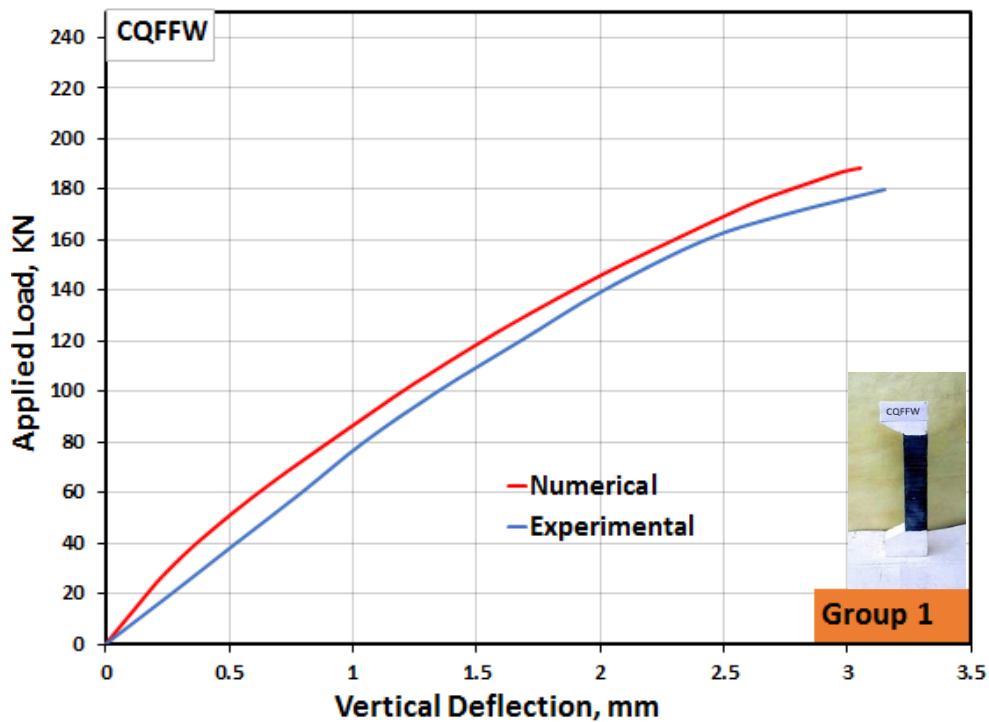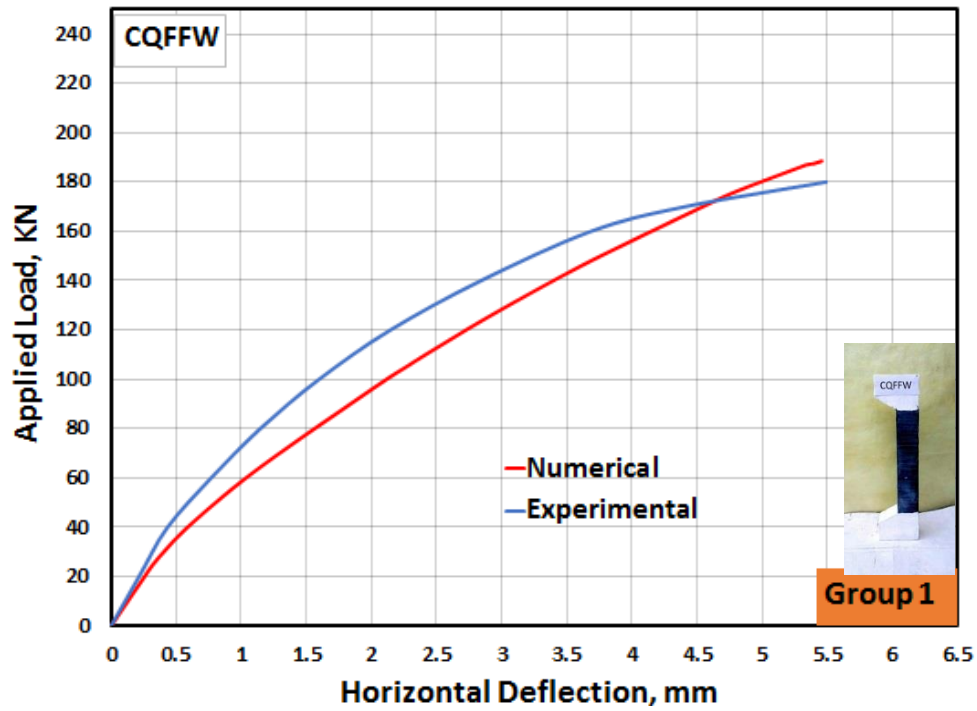
Fig. 5. 10. Numerical and experimental horizontal and vertical load-deflection curves for CQFFW

100
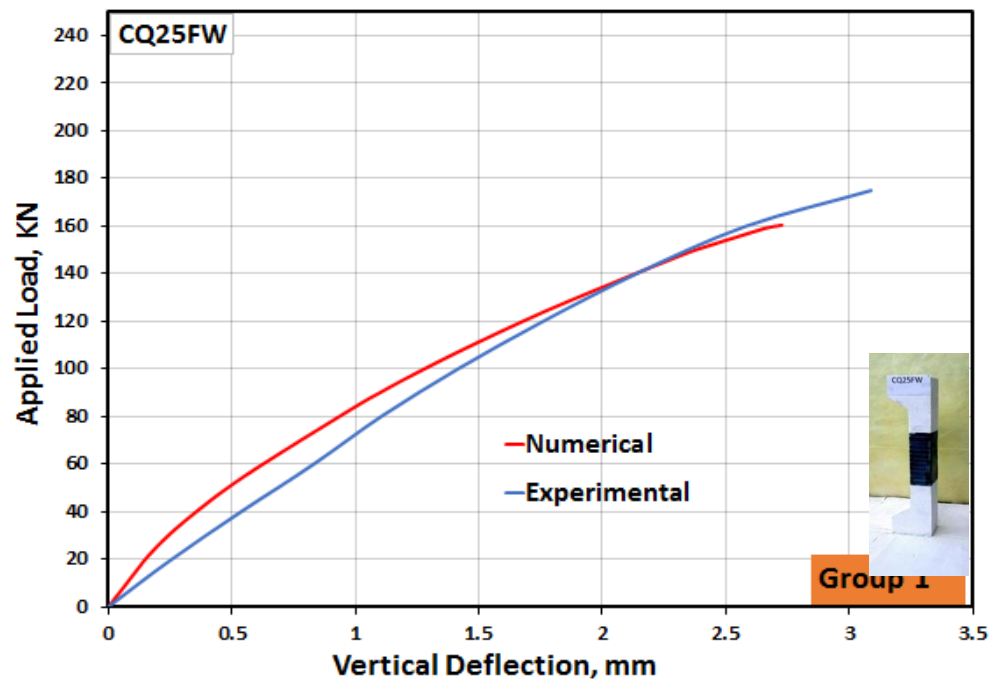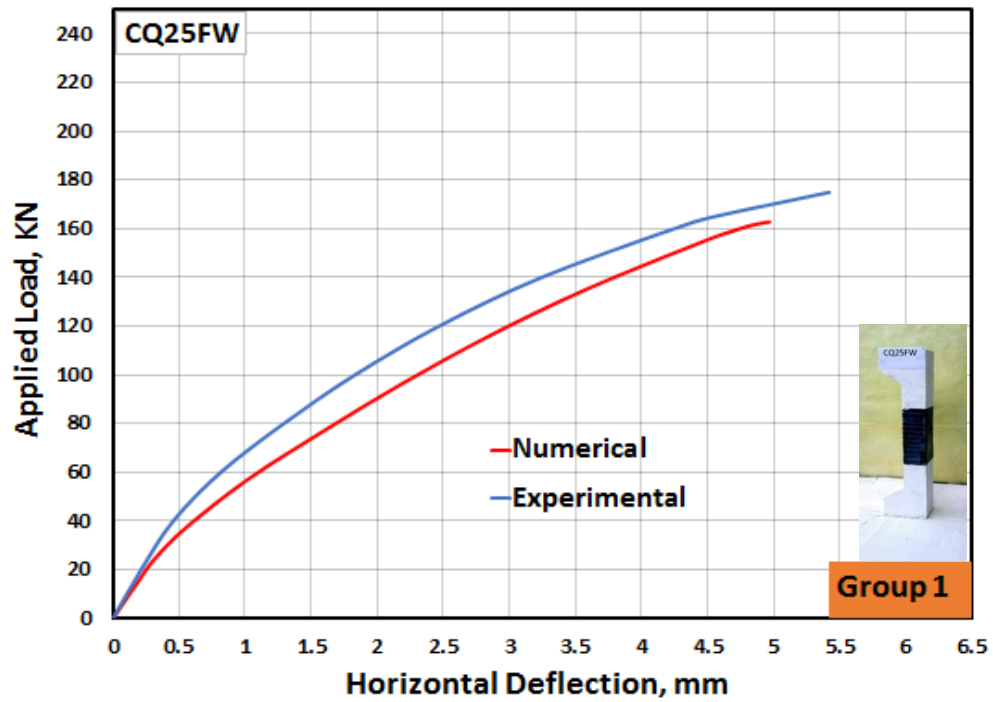
Fig. 5. 11. Numerical and experimental horizontal and vertical load-deflection curves for CQ25FW

101
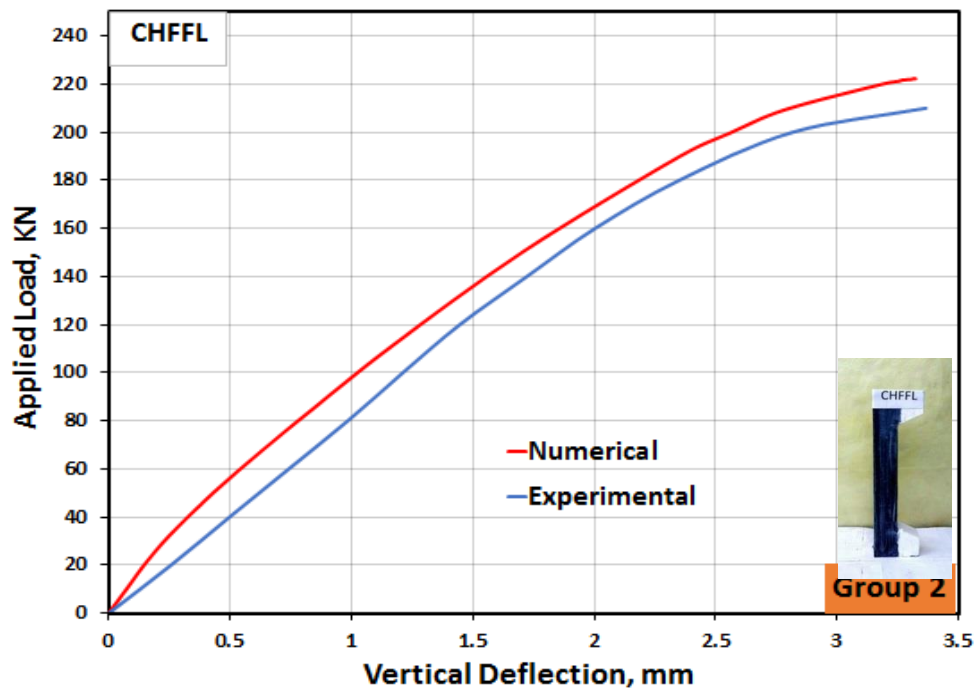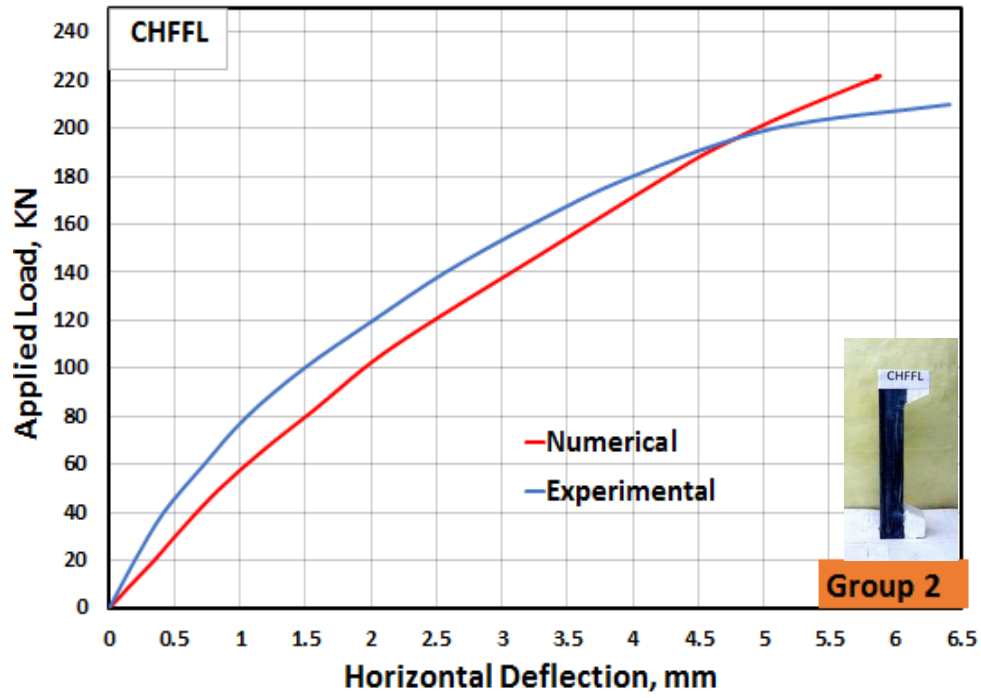
Fig. 5. 12. Numerical and experimental horizontal and vertical load-deflection curves for CHFFL
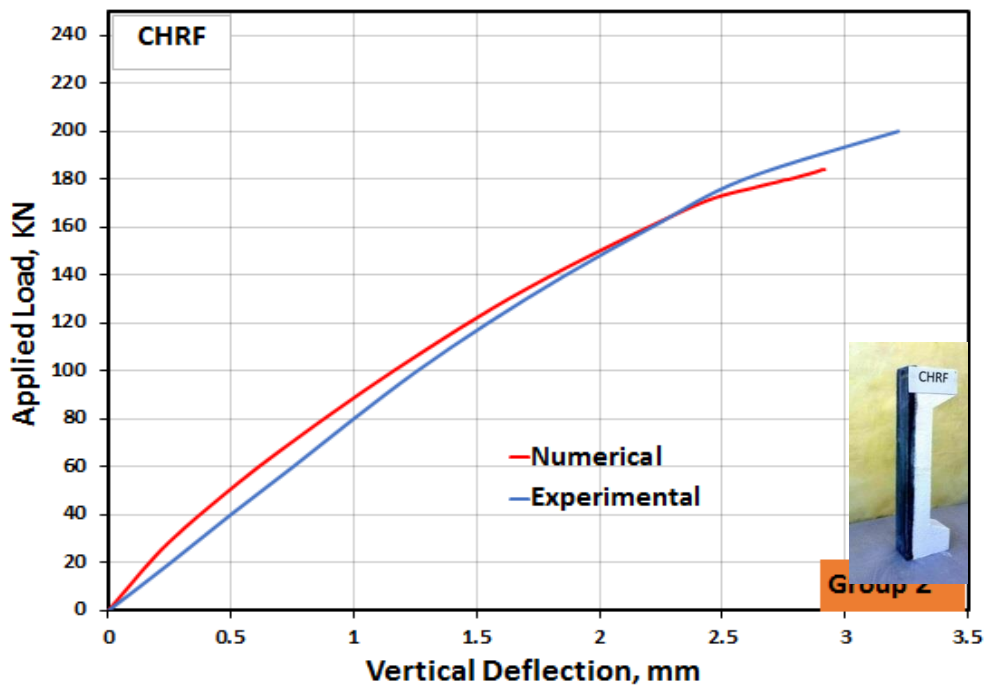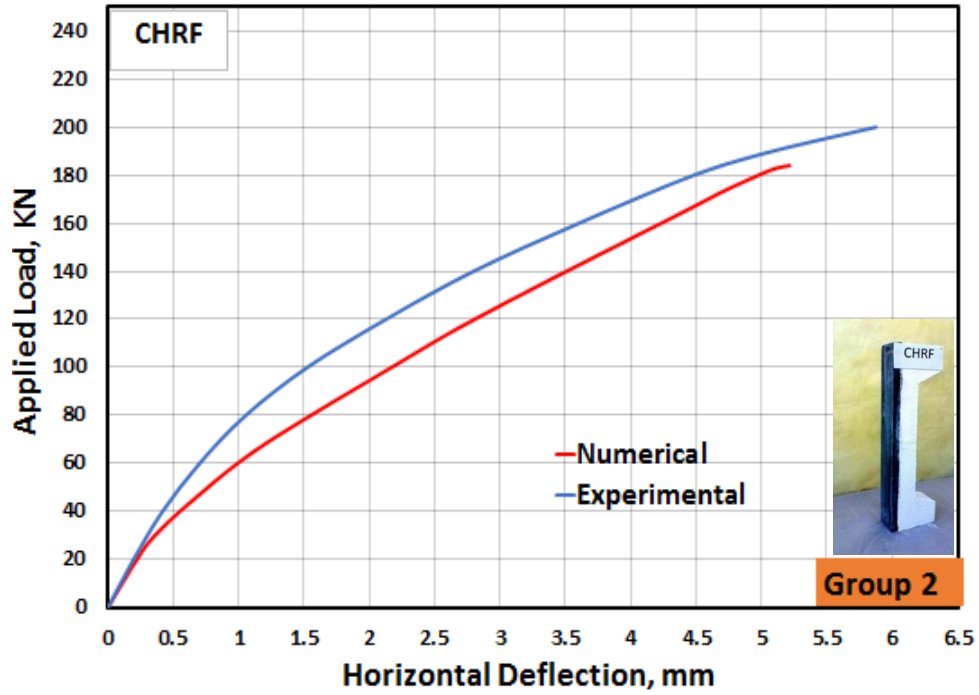
Fig. 5. 13. Numerical and experimental horizontal and vertical load-deflection curves for CHRF
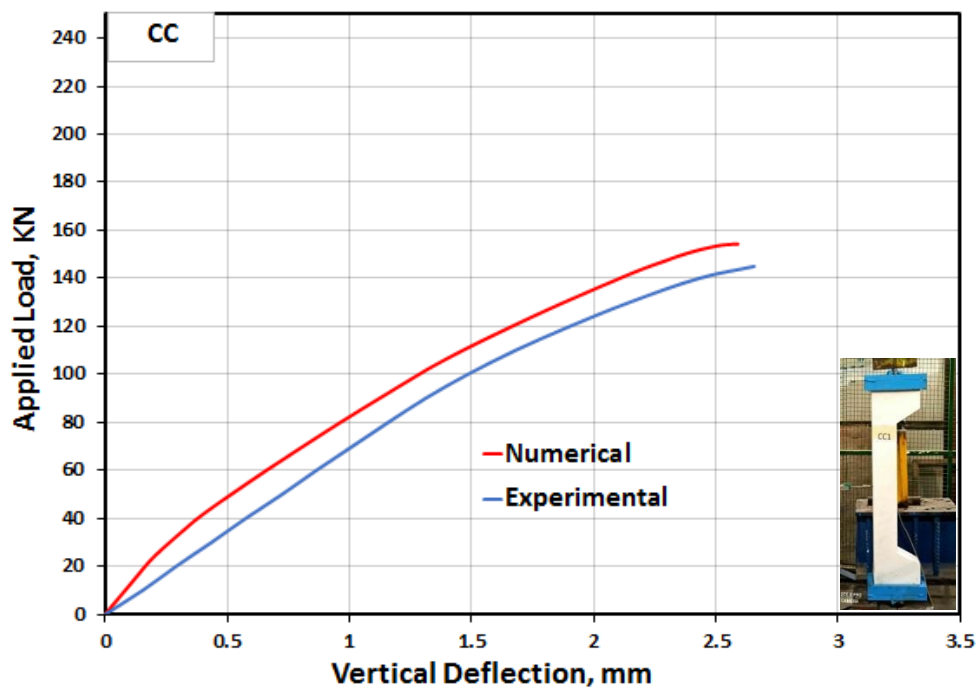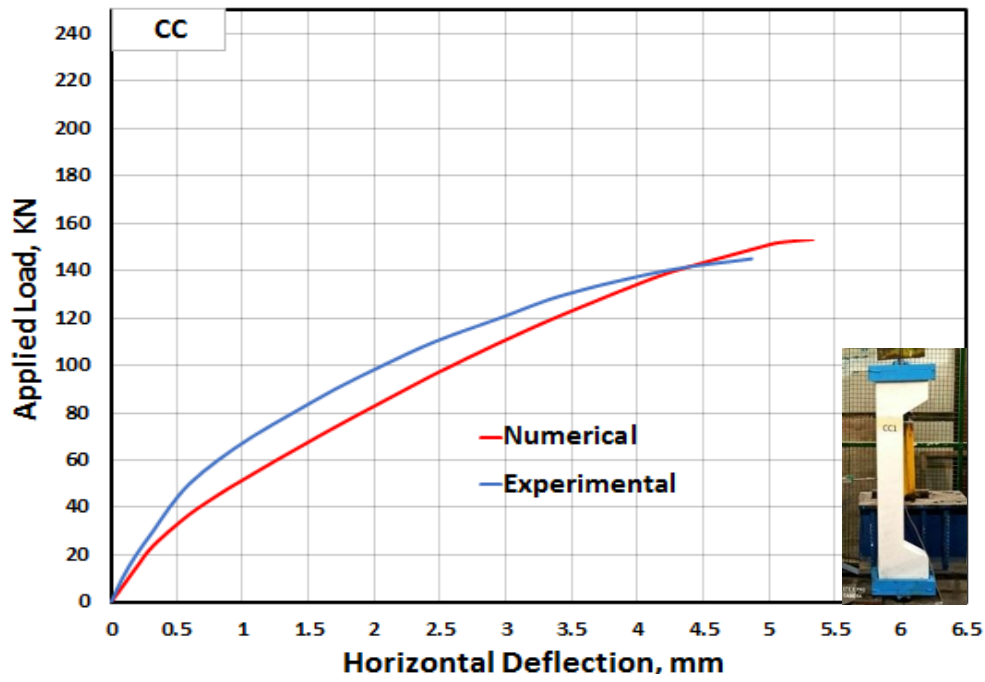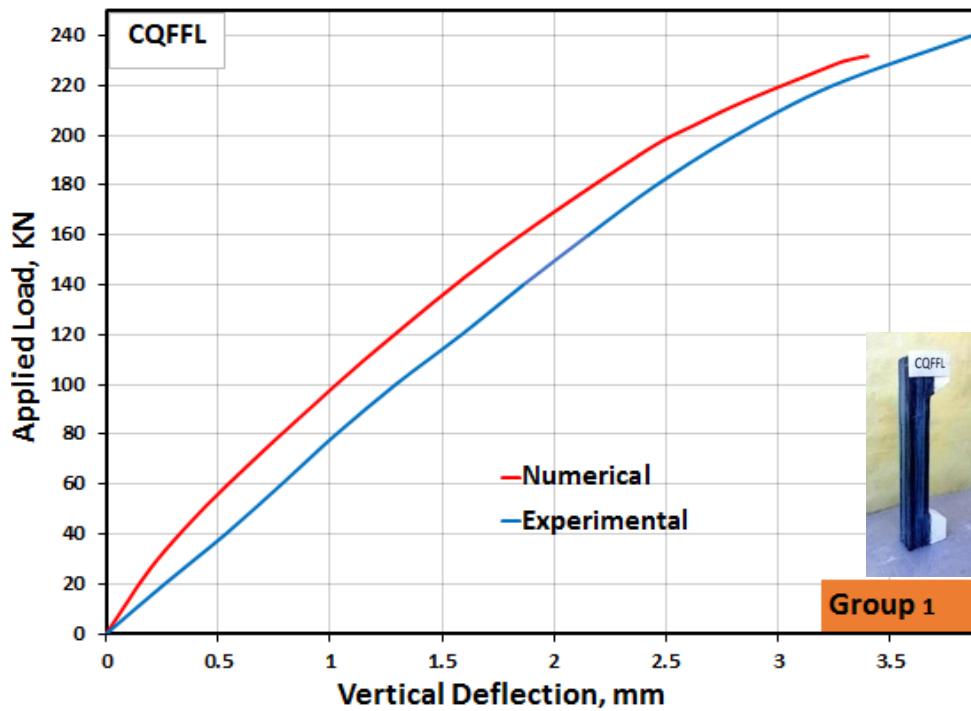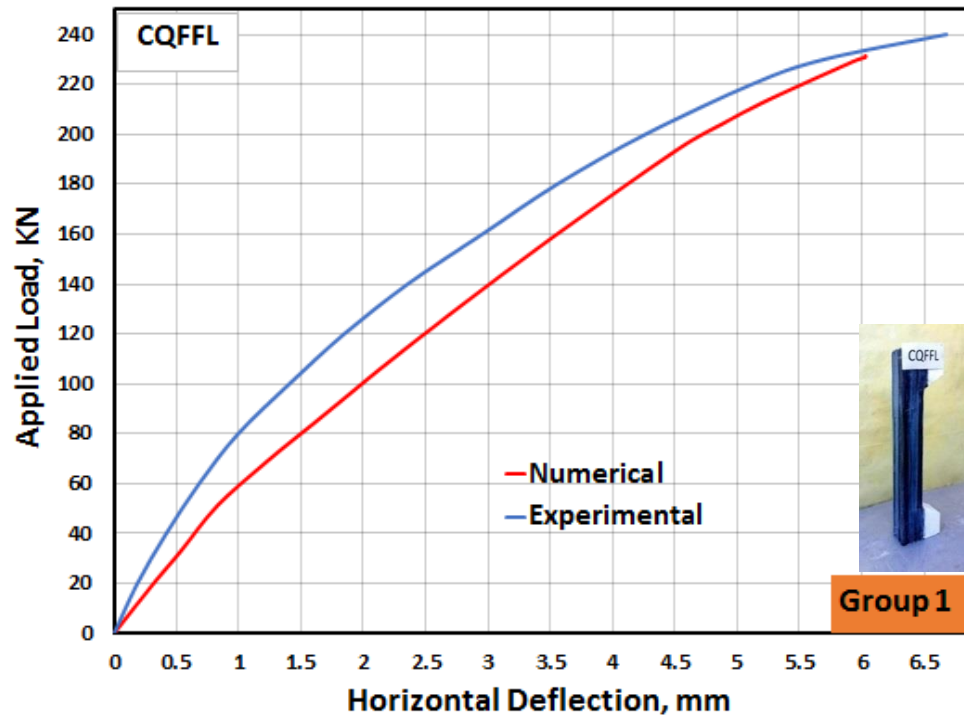
103
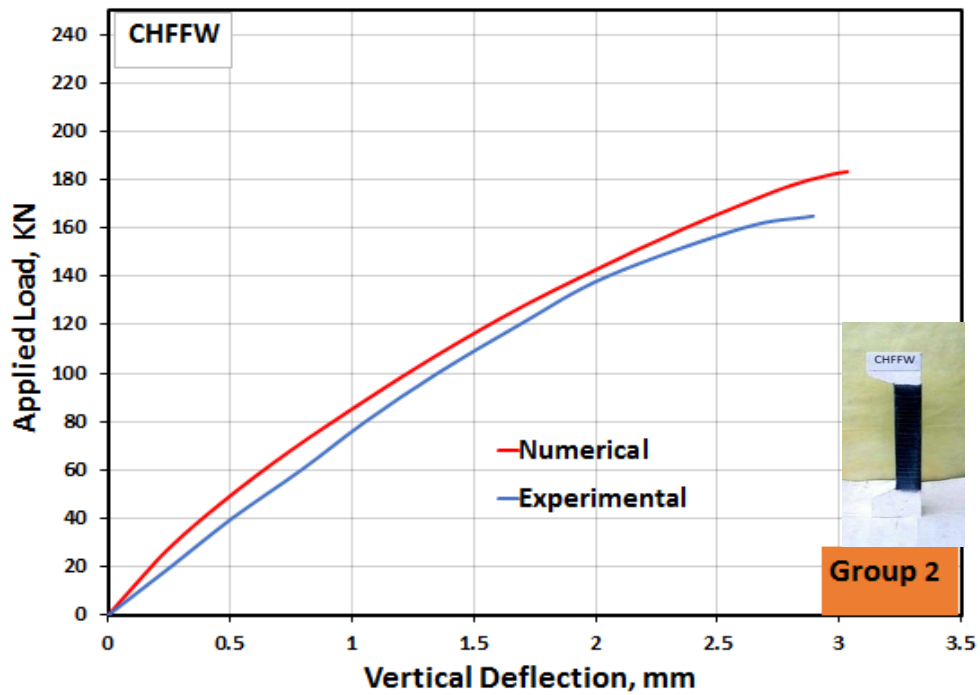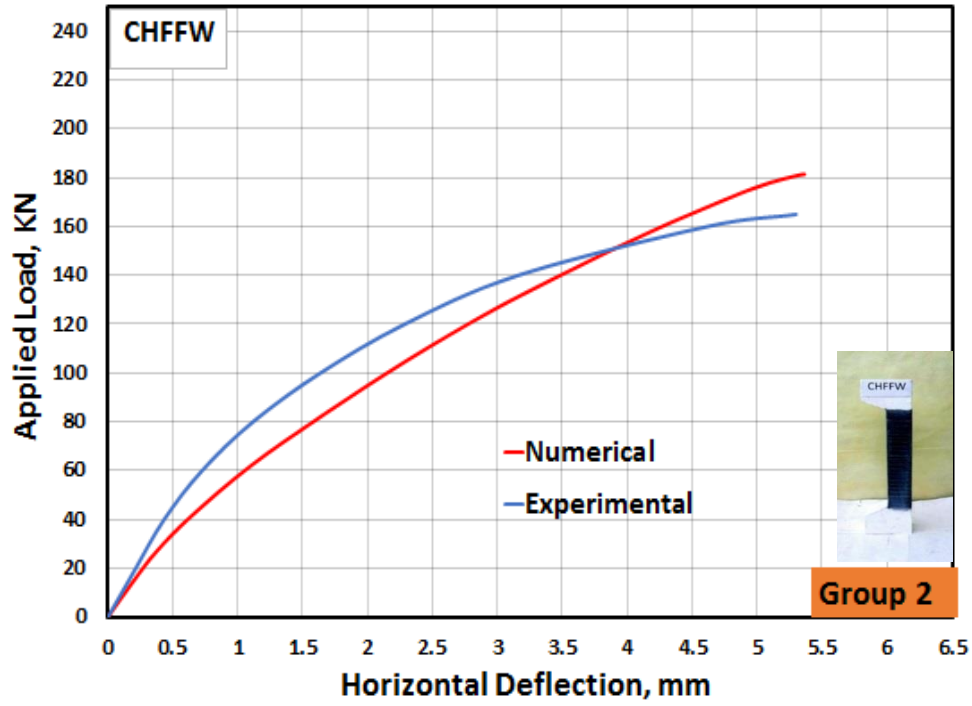
Fig. 5. 14. Numerical and experimental horizontal and vertical load-deflection curves for CHFFW

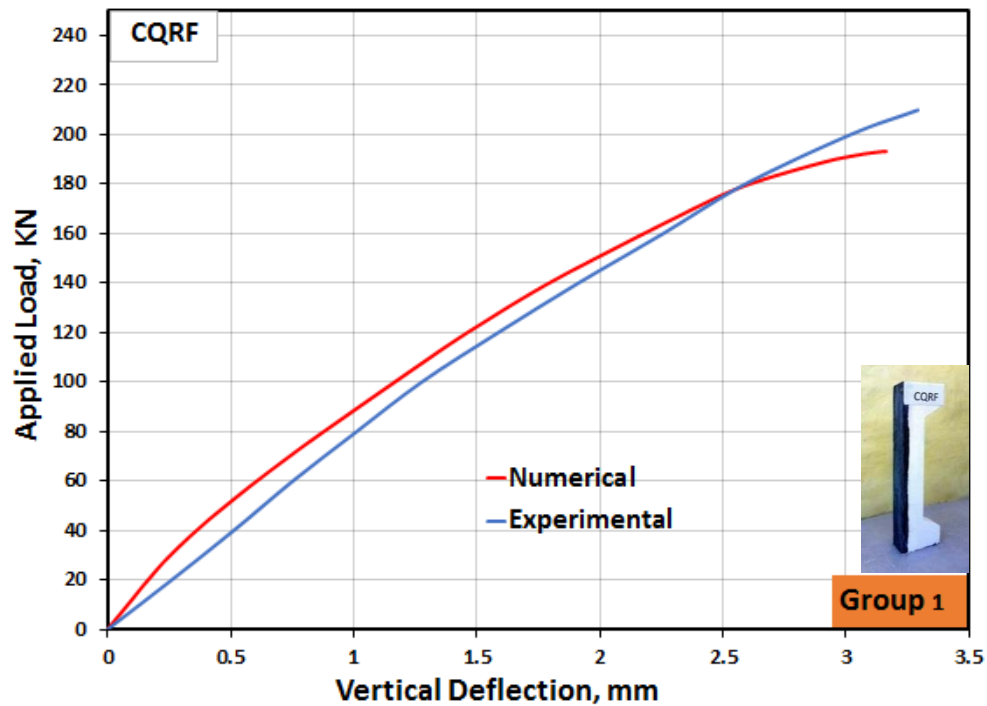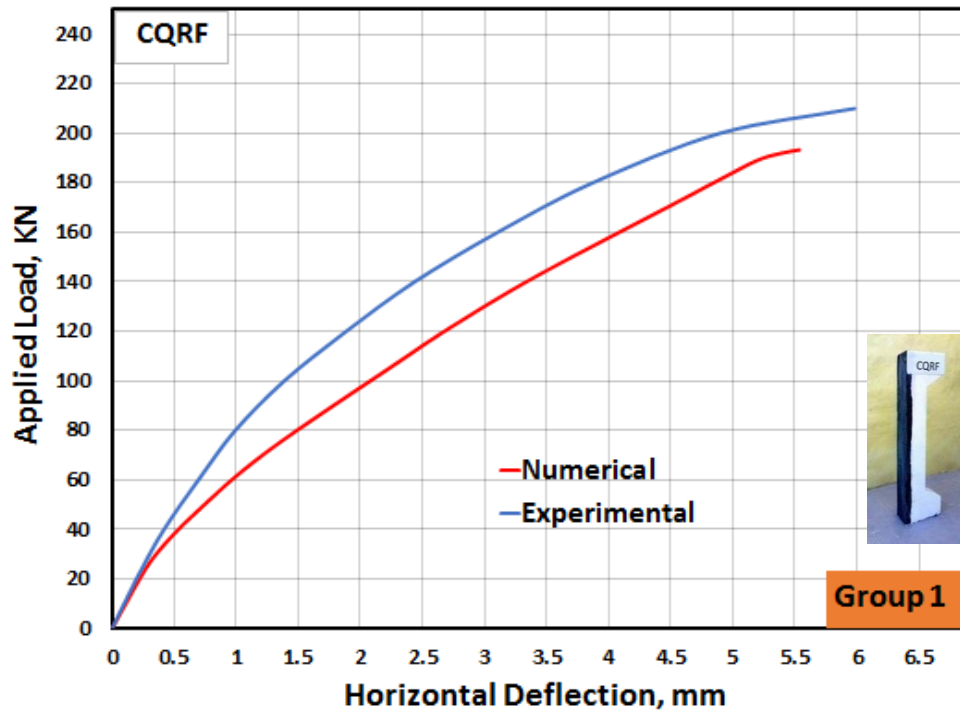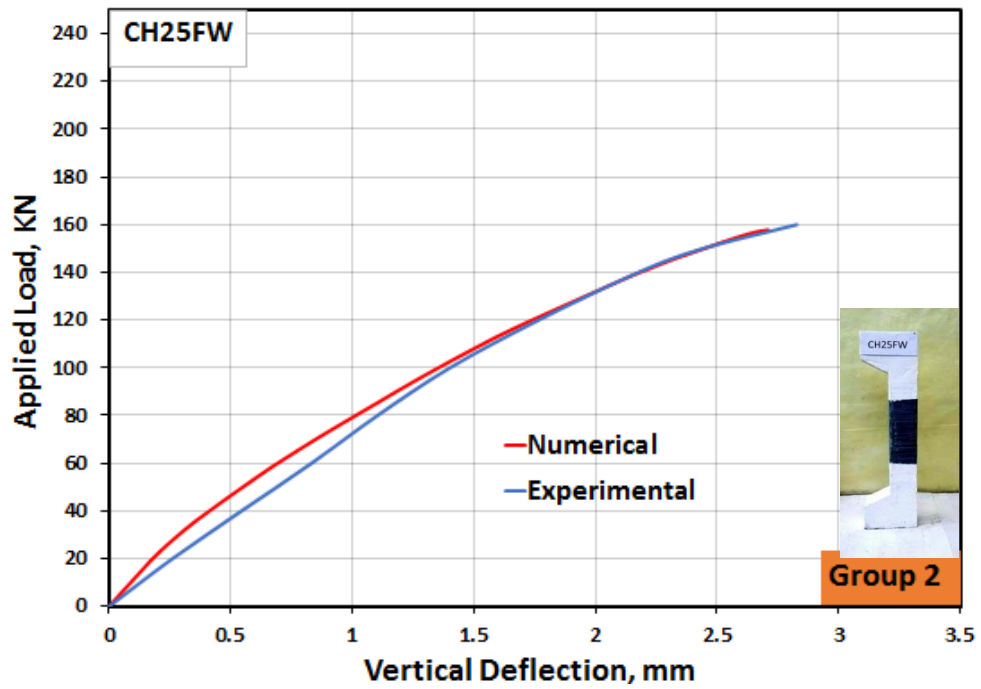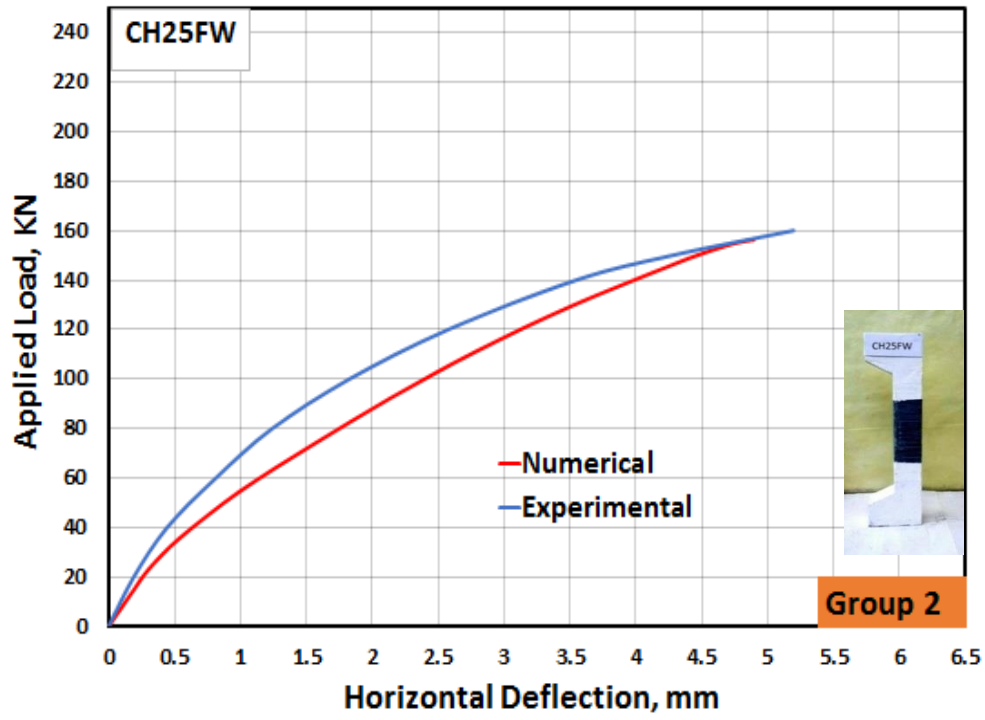**Fig. 5. 15. Numerical and experimental horizontal and vertical load-deflection curves for CH25FW**

5.6.2 Ultimate capacity and deflection

Table (5.5) compares the maximum experimental value of strength capacity and deflections with the numerical ultimate load capacity and horizontal and vertical deflections from the ABAQUS program. The maximum difference values for the ultimate load capacity and deflection between the experimental and the numerical results were 6.28%, 7.38% and 6.24, respectively. Therefore, an excellent convergence was recorded between the numerical and experimental results. For this reason, the proposed model could be considered accurate and can be used with confidence.

Table 5. 5 Theoretical and experimental results for tested columns

Group No.	Specimen symbol		Ultimate load (Pu) KN	Difference percentage	Horizontal deflection (Δv) mm	Difference percentage in	Vertical deflection (Δu) mm	Difference percentage in
	CC	EXP	145		4.86	9.69	2.65	
		FEA	153.17	5.63	5.33		2.59	2.36
	CQFFL	EXP	240		6.67	9.99	3.86	
		FEA	231.78	3.54	6.06		3.41	13.49
	CQRF	EXP	210		5.98	8.09	3.29	
Group 1		FEA	193.27	8.65	5.53		3.16	4.01
	CQFFW	EXP	180		5.49	0.71	3.15	
		FEA	188.45	4.69	5.45		3.06	0.41
	CQ25FW	EXP	175		5.42	9.20	3.08	
		FEA	162.78	7.51	4.96		2.73	12.27
	CHFFL	EXP	210		6.41	8.99	3.36	
		FEA	221.92	5.67	5.88		3.33	1.11
	CHRF	EXP	200		5.87	12.62	3.21	
		FEA	184.01	8.68	5.21		2.91	10.27
Group 2	CHFFW	EXP	165		5.30	1.12	2.89	
		FEA	181.36	9.70	5.36		3.03	8.37
	CH25FW	EXP	160		5.19	6.06	2.82	
		FEA	156.16	2.45	4.89		2.71	3.94
	Mean Diff.		-	6.28		7.38		6.24

5.7 Parametric study

Several vital parameters were proposed to be investigated numerically to study their impact on the behaviour of the partially damaged HSC columns under eccentricity loads by an eccentricity of 50 mm from the center (e/h = 0.5), and they can be summarised as follows:

1. Number of CFRP sheets layers;
2. Various eccentricity load e/h;
3. Different initial loading percentages;
4. Various sizes of CFRP sheets.

5.7.1 Number of CFRP sheets layers

The load-horizontal and vertical deflections for specimens CQFFL, CQFFW, CHRF, and CH25FW strengthened with one, two, and three layers of CFRP sheets are shown in Figs. (5.16) to (5.19), in which the figure increased the impact of increasing CFRP layers. There was a slight improvement in the load capacity and deflection, which is the primary observation from the specimens' figures, CHRF and CH25FW. On the other hand, the samples of CQFFL and CQFFW exhibited a remarkable improvement in their ultimate load capacity, Because of the effect of containment of concrete in the compressive and tension. with more than one layer of CFRP. The maximum load capacity values for CQFFL when using one, two and three layers of CFRP sheets were 231.78, 280.43, and 320.82 kN, respectively. Furthermore, the values of the load capacity for CQFFW when using one, two, and three layers of CFRP sheets were 188.45, 208.11, and 238.21 kN, respectively. Table (5. 6) shows the effect of the increase as the number of CFRP sheets layers. The stress of CFRP sheets was presented in Appendix C.

Table 5. 6. Effect of the number of CFRP layers

| Column symbol	Strengthening Scheme	Ultimate Load KN	Increment Ratio %	Horizontal deflection mm	Vertical deflection mm
	Full longitudinal wrapping with CFRP for all column faces - One layer	231.78	51.3	6.06	3.41
CQFFL	Full longitudinal wrapping with CFRP for all column faces - Two layers	280.43	83.08	7.165	3.94
	Full longitudinal wrapping with CFRP for all column faces - Three layers	320.82	109.45	7.954	4.48
	Full horizontal wrapping with CFRP for all column faces - One layer	188.45	23.03	5.45	3.05
CQFFW	Full horizontal wrapping with CFRP for all column faces - Two layers	208.11	35.86	5.6	3.47
	Full horizontal wrapping with CFRP for all column faces - Three layers	238.21	55.52	5.76	3.89
	Full longitudinal wrapping with CFRP for rear face only -One layer	184.01	20.13	5.24	2.91
CHRF	Full longitudinal wrapping with CFRP for rear face only - Two layers	213.95	39.68	5.32	3.33
	Full longitudinal wrapping with CFRP for rear face only -Three layers	226.85	48.10	5.51	3.86
	Horizontal wrapping with CFRP for 250 mm length at column mid-height -One layer	156.16	1.95	4.89	2.71
CH25FW	Horizontal wrapping with CFRP for 250 mm length at column mid-height - Two layers	173.66	13.37	5.18	3.02
	Horizontal wrapping with CFRP for 250 mm length at column mid-height - Three layers	188.13	22.82	5.44	3.38
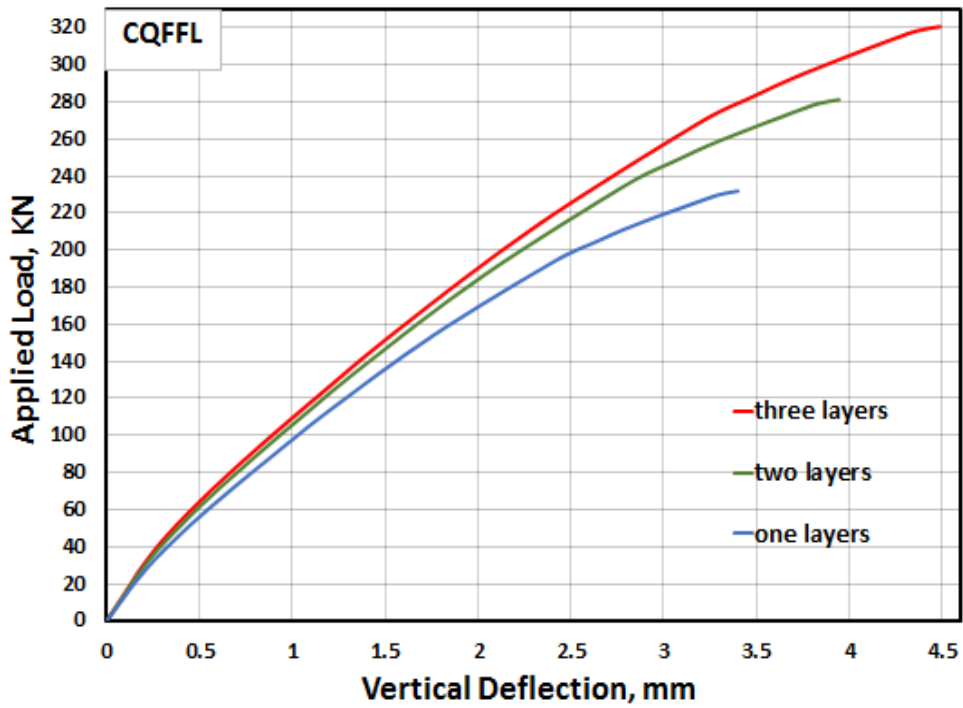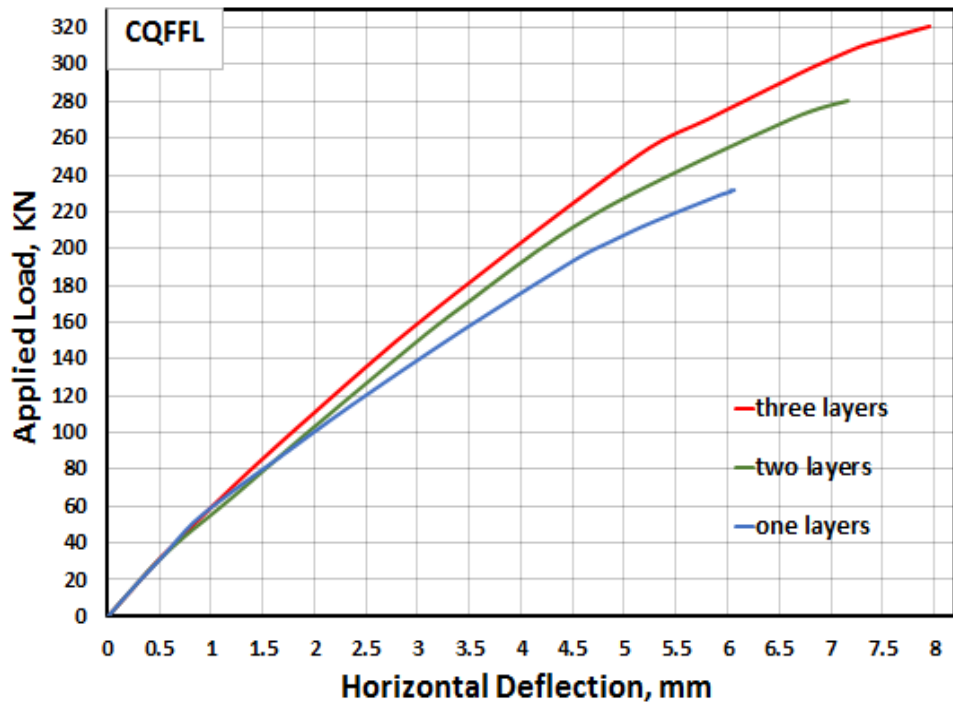
Fig. 5. 16. Impact the number of layers for CQFFL specimen
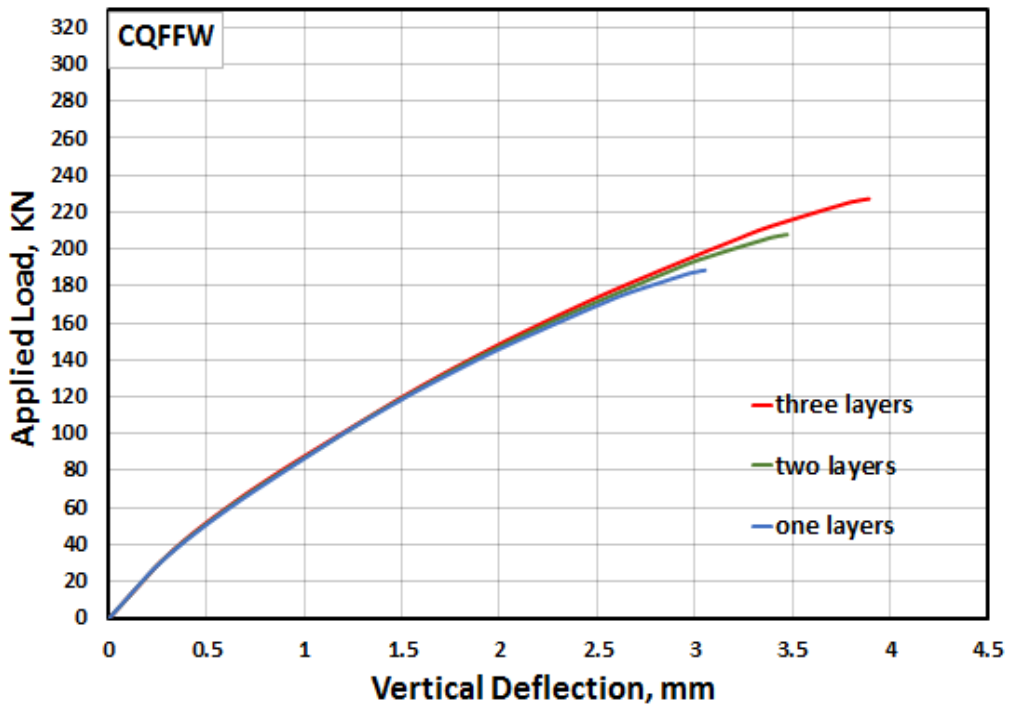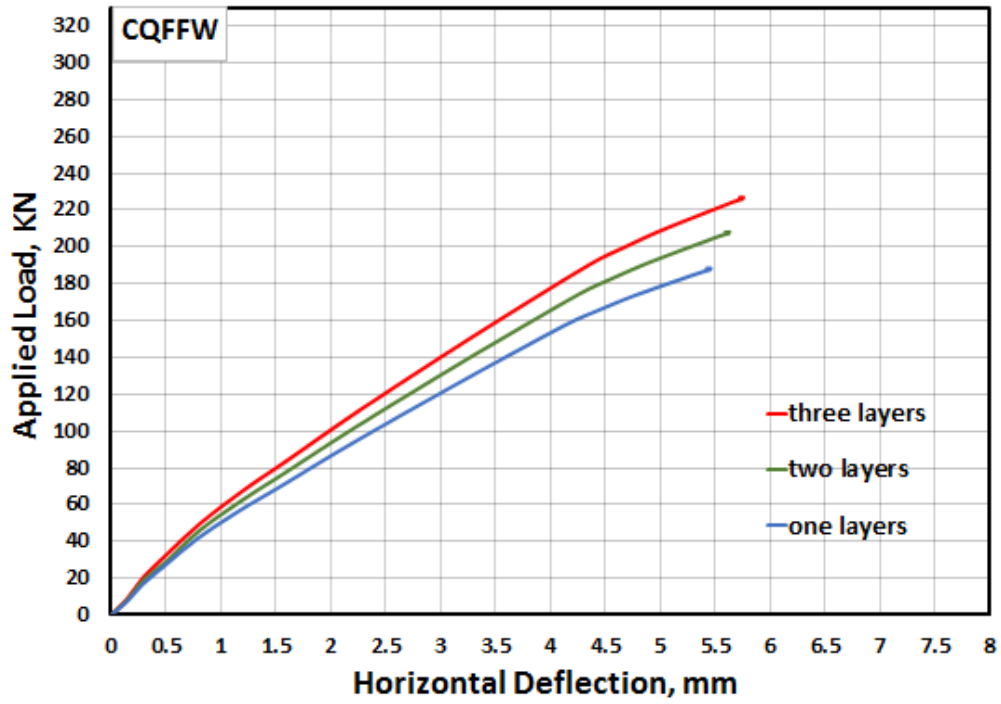
Fig.5. 17. Impact the number of layers for CQFFW specimen
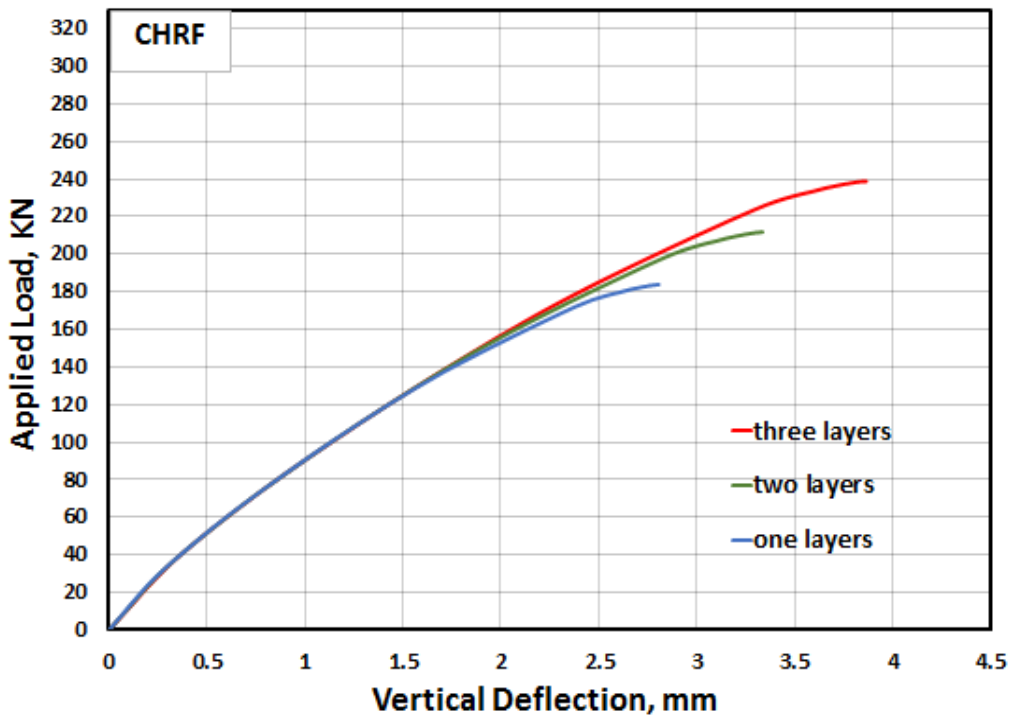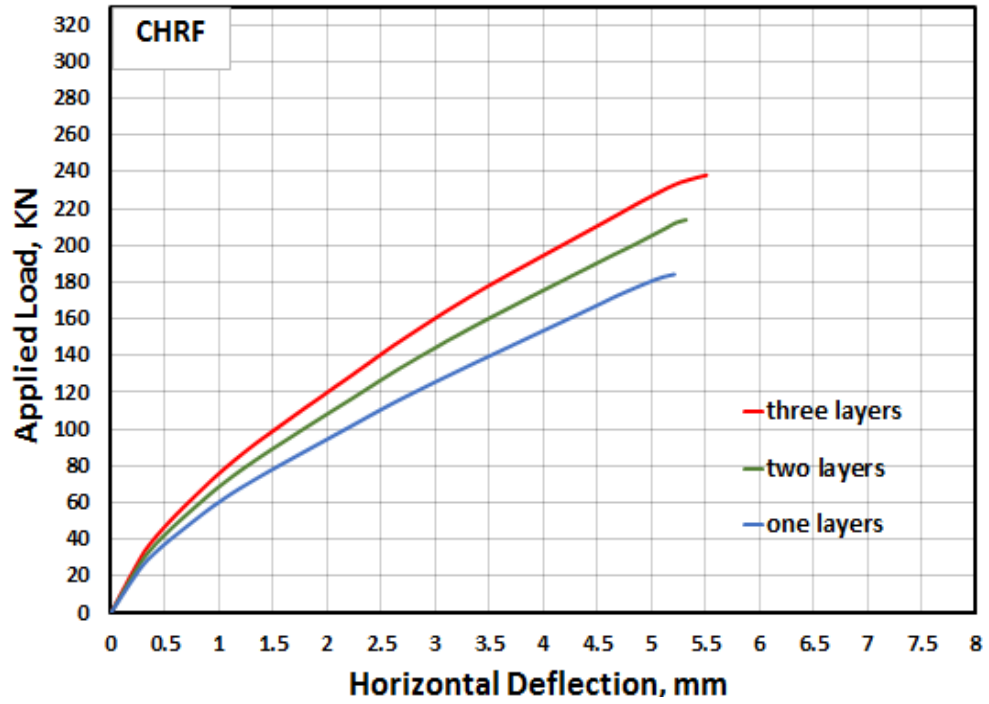
Fig.5. 18. Effect the number of layers for CHRF specimen
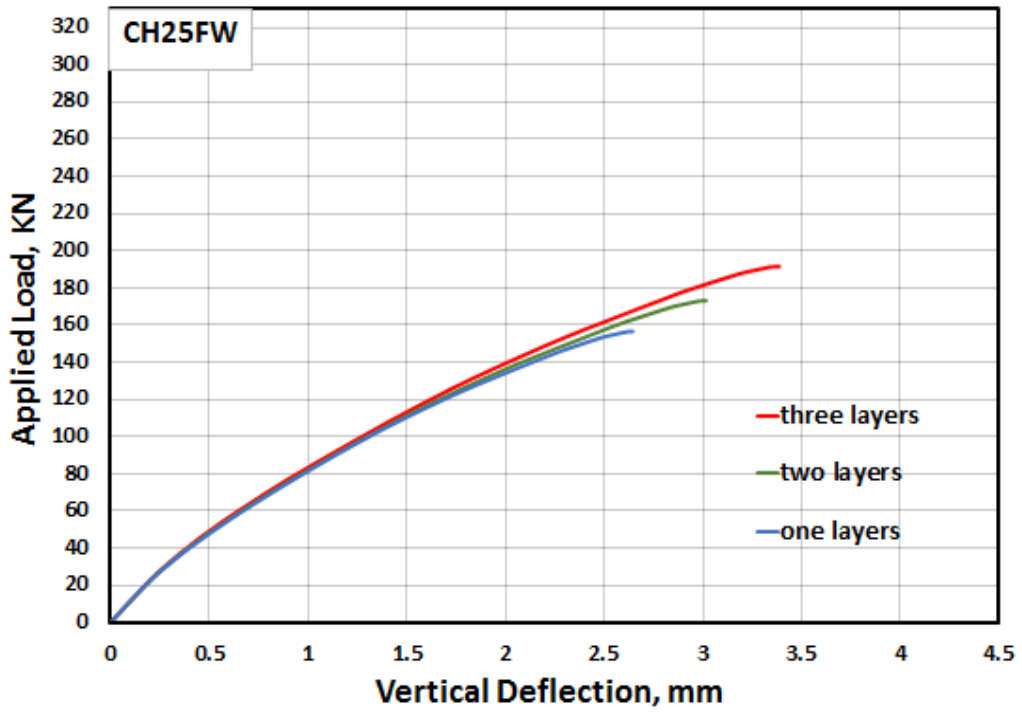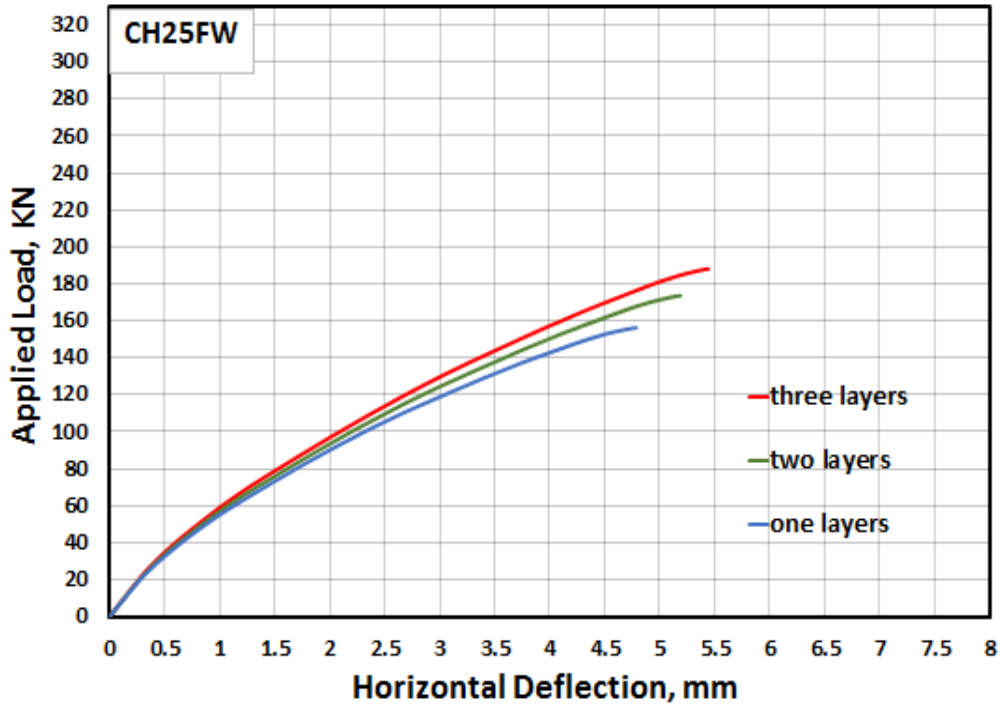
Fig.5. 19. Effect the number of layers for CH25FW specimen

5.7.2 Various eccentricity load e/h

The impact of changing the load eccentricity on the load capacity and load-horizontal and vertical deflection of square partially damaged HSC columns for the CC, CQFFL and CQRF were examined. The studied eccentricity load (e/h) were 0.35, 0.5, and 0.7 with fixed all other factors such as the number of CFRP layers and spacing between the CFRP sheets. Figures (5.20), (5.21), and (5.22) presented the vertical load-deflections for specimens with various eccentricity loads (e/h). Furthermore, changing the eccentric load of the sample CQFFL at a deflection of 0.35 increased the maximum amplitude compared to the deflections of e/h equal to 0.5 and 0.7 by 311.25, 231.78, and 119.78 kN, respectively, which result an increase in axial load with decrease in bending moment with a decrease in the eccentricity rate (e/h). Table (5. 7) presented the numerical results for the effect of eccentric load for the specimens CC, CQFFL and CQRF.

Table 5. 7. Effect of changing eccentricity load e/h for CC, CQFFL and CQRF

Column symbol	e/h	Ultimate load KN	Decreasing Ratio %	Horizontal Deflection (mm)	Vertical Deflection (mm)
CC	0.35	236.84	54.62	5.812	3.098
	0.5	153.17	……..	5.332	2.589
	0.7	93.46	-38.98	4.840	2.269
CQFFL	0.35	311.25	34.28	6.467	3.768
	0.5	231.78	……..	6.064	3.401
	0.7	119.78	-48.32	5.218	2.356
CQRF	0.35	249.52	29.10	6.204	3.227
	0.5	193.27	……..	5.532	3.162
	0.7	116.43	-39.75	4.973	2.625
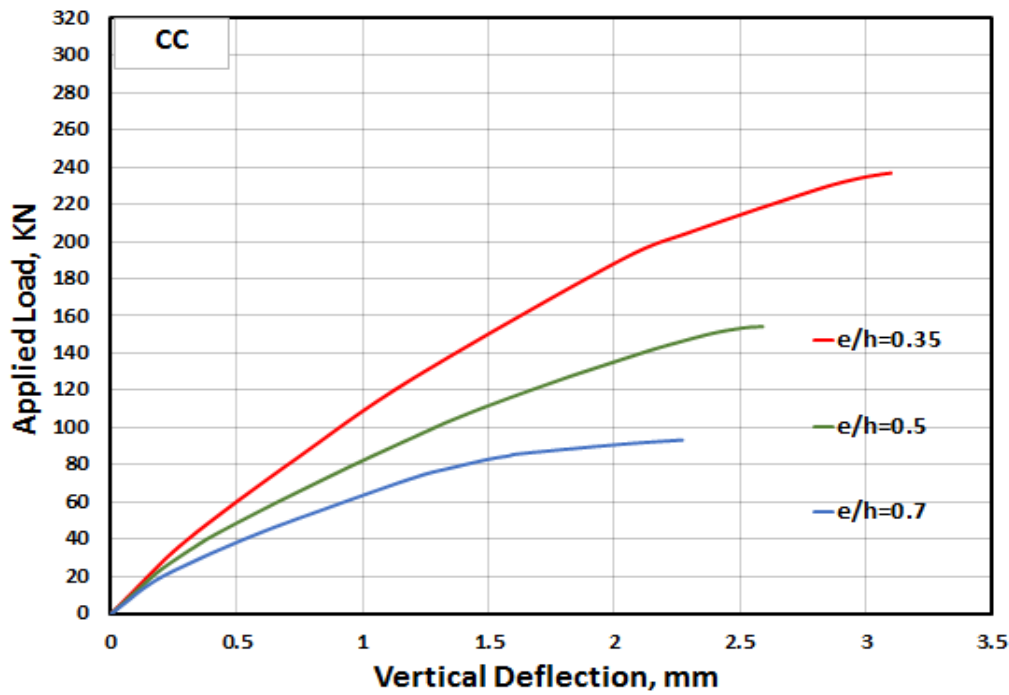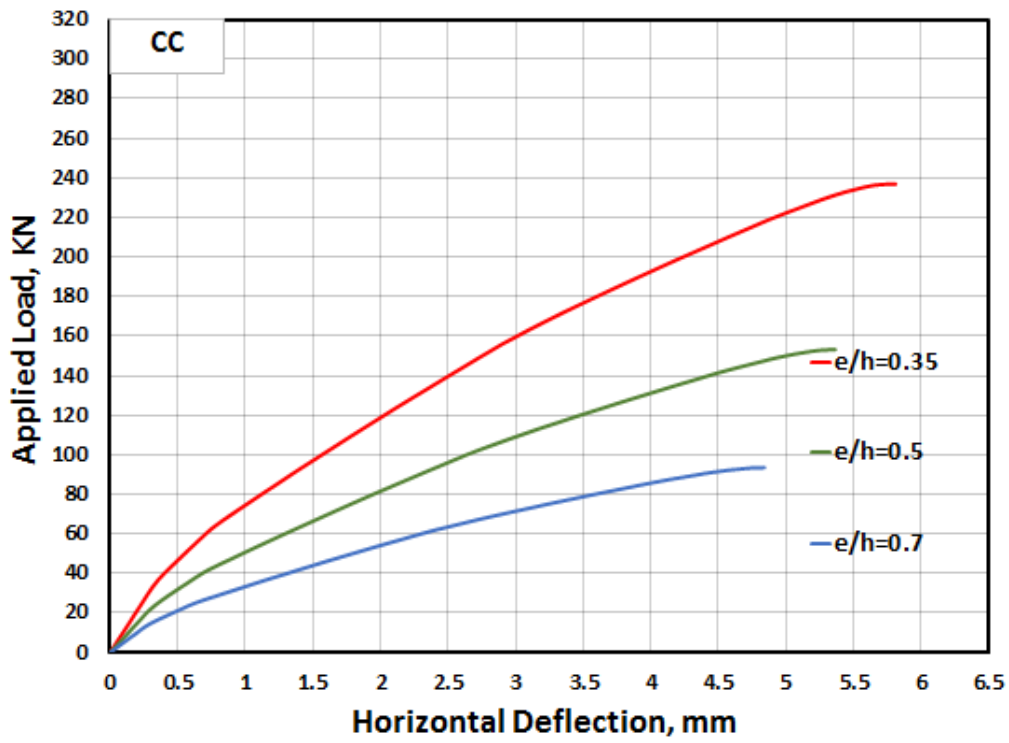
Fig. 5. 20. Effect of various eccentricity load e/h for the load- horizontal and vertical deflection curves for CC
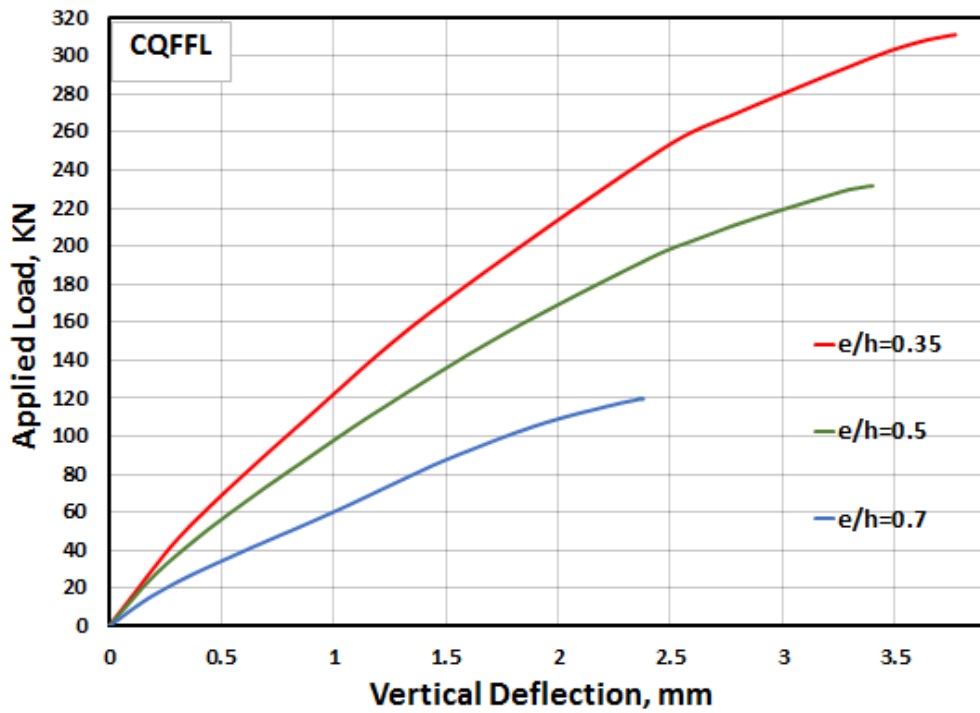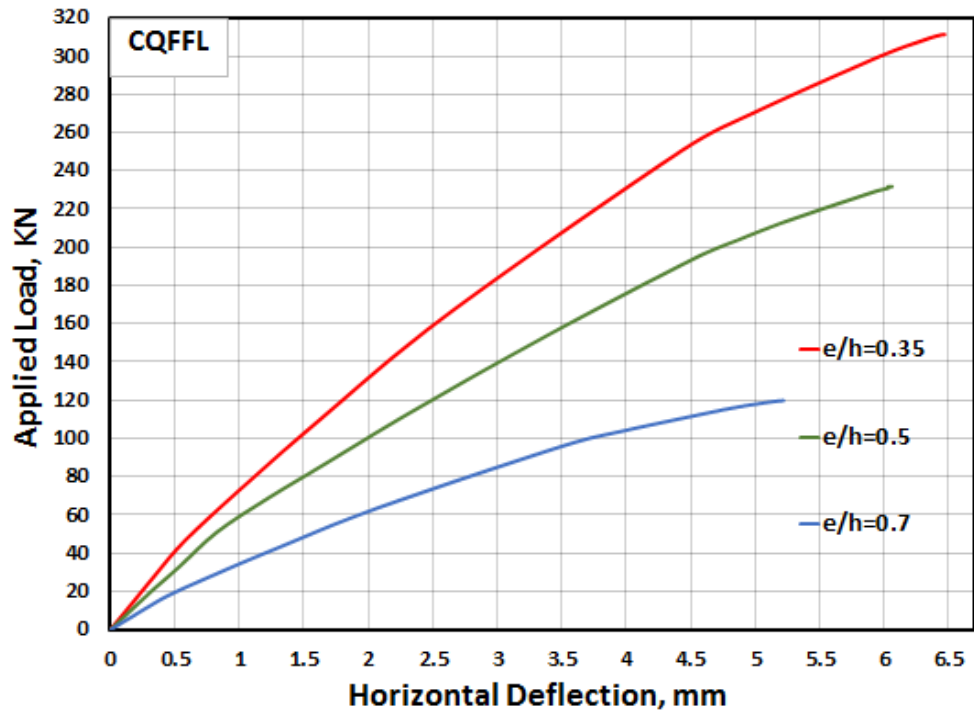
Fig. 5. 21. Effect of various eccentricity load e/h for the horizontal and vertical load-deflection curves for CQFFL

116
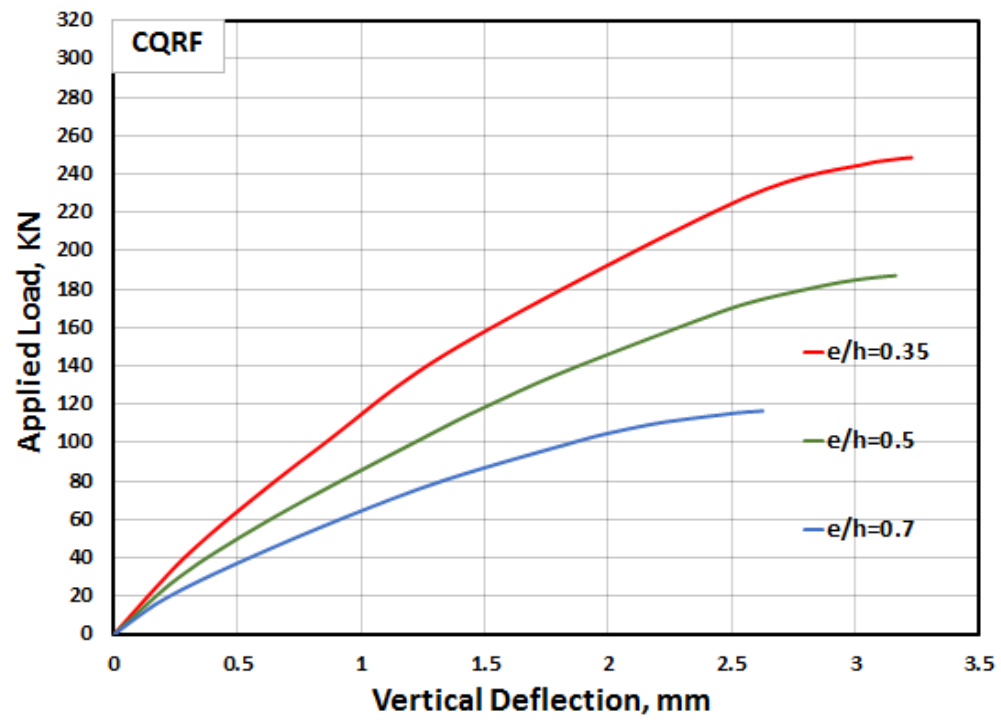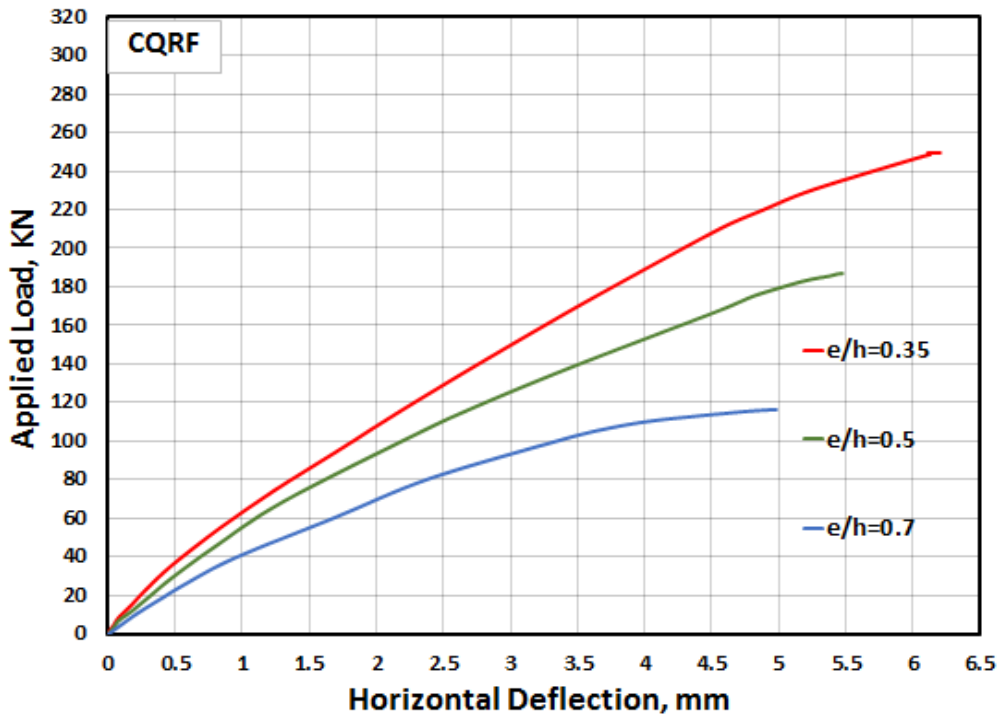
Fig. 5.22. Effect of various eccentricity load e/h for the horizontal and vertical load-deflection curves for CQRF

5.7.3 Various Initial Loading Percentage

The second loaded percentage was 50 % of the ultimate design load, which was changed to 60, 70, and 80 %. These percentages were studied for the specimens of CC and CQFFL. Figures (5.23) and (5.24) illustrated horizontal and vertical load-deflection curves for the impact of changing the percentage of loading for CC and CQFFL. From the results given in Table (5.8), increasing the initial loading rate from 50 to 80% led to a decrease in the values of the ultimate load capacity and deflection. As a result, the maximum load capacity for CC and CQFFL were 138.94 and 195.45 kN, respectively. In contrast, the horizontal load-deflection values decreased to 4.412 and 4.752 mm, respectively. While, the vertical load-deflection values fell to 1.738 and 2.309 mm, respectively, for the specimens mentioned above, as illustrated in Table (5.5).

Table 5. 8. Effect of various loading percentages for CC and CQFFL

Column symbol	Loading ratio %	Ultimate load KN	Decreasing Ratio %	Horizontal deflection (mm)	Vertical deflection (mm)
CC	0.5	153.17	……..	5.332	2.539
	0.6	148.66	2.94	5.053	2.389
	0.7	144.15	5.88	4.851	2.170
	0.8	138.94	9.23	4.412	1.738
CQFFL	0.5	221.92	…….	5.887	3.323
	0.6	212.05	4.43	5.593	2.855
	0.7	204.20	7.98	5.250	2.697
	0.8	195.45	11.92	4.752	2.309
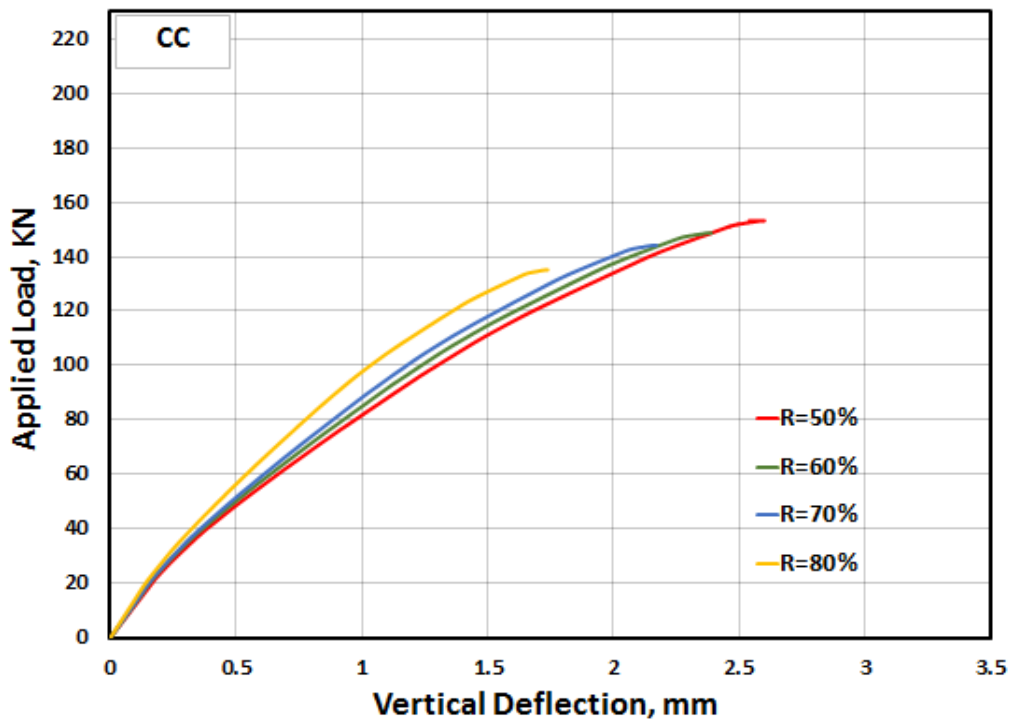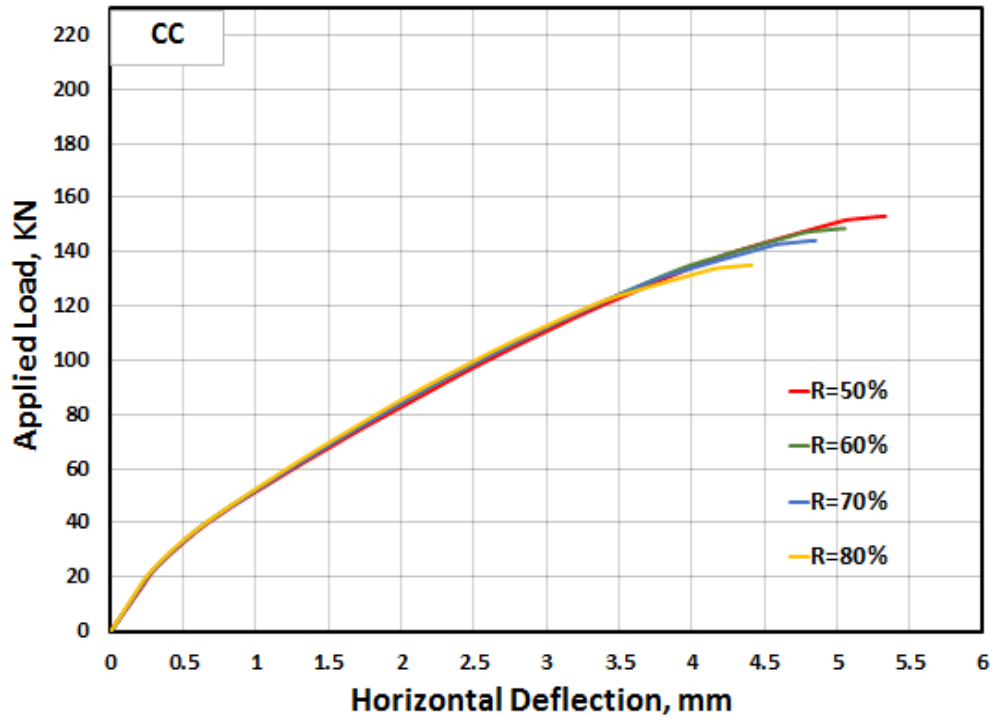
Fig. 5. 23. Impact of change the initial load ratio for CC
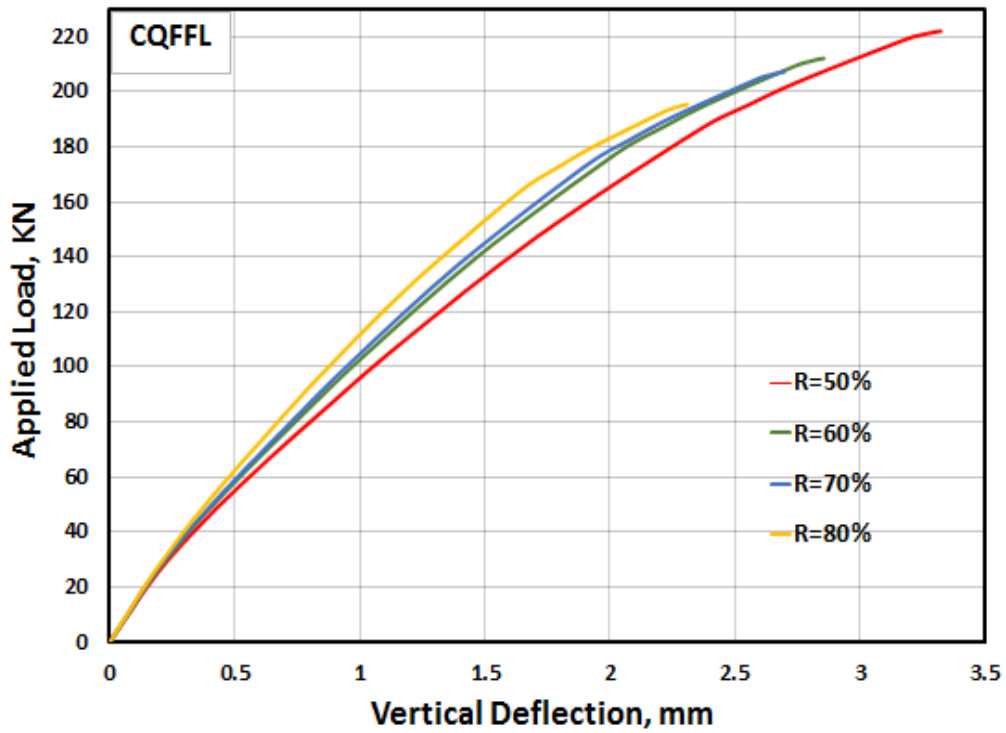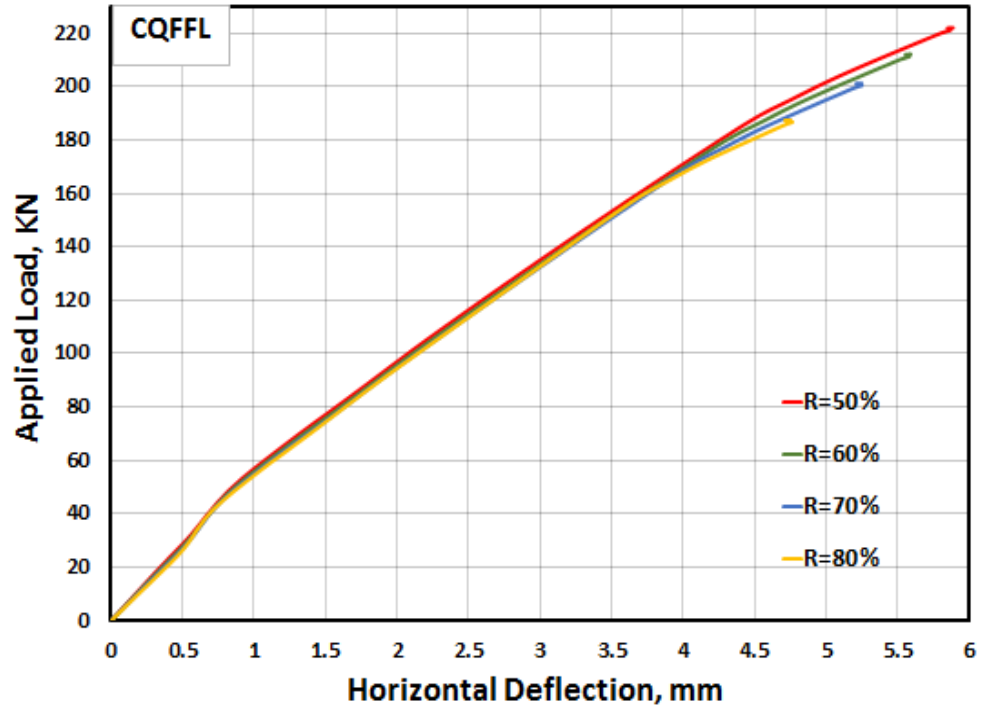
Fig. 5. 24. Impact of change the initial load ratio for CQFFL

5.7.4 Various width for CFRP sheets

Horizontal partial wrapping of CFRP sheets was carried out on sample CQ25FW, where the length of the CFRP sheet was 250 mm changed to lengths (300,400,500) mm to check the effect of changing the lengths of the carbon fiber reinforced polymer sheets. Increasing the lengths of CFRP sheets for the column from (250-500) mm increased the ultimate load of the columns. The horizontal and vertical load-deflection of specimens CQ25FW, CQ30FW, CQ40FW, and CQ50FW are shown in Figure (5.25), which shows that the ultimate goal is load and deflection increase with the increase in the lengths of the carbon fibre reinforced polymer sheets. The maximum load values for CQ50FW samples increased 188.45 kN compared to the sample CQ25FW (162.78 kN), as shown in Table (5.9)

Table 5. 9. Impact of reducing the spacing between CFRP sheets

Column symbol	Ultimate load KN	Increment Ratio %	Horizontal deflection (mm)	Vertical deflection (mm)
CQ25FW	162.78	6.27	5.457	2.730
CQ30FW	169.12	10.41	5.297	2.818
CQ40FW	176.85	15.46	5.115	2.939
CQ50FW	188.45	23.03	4.973	3.052
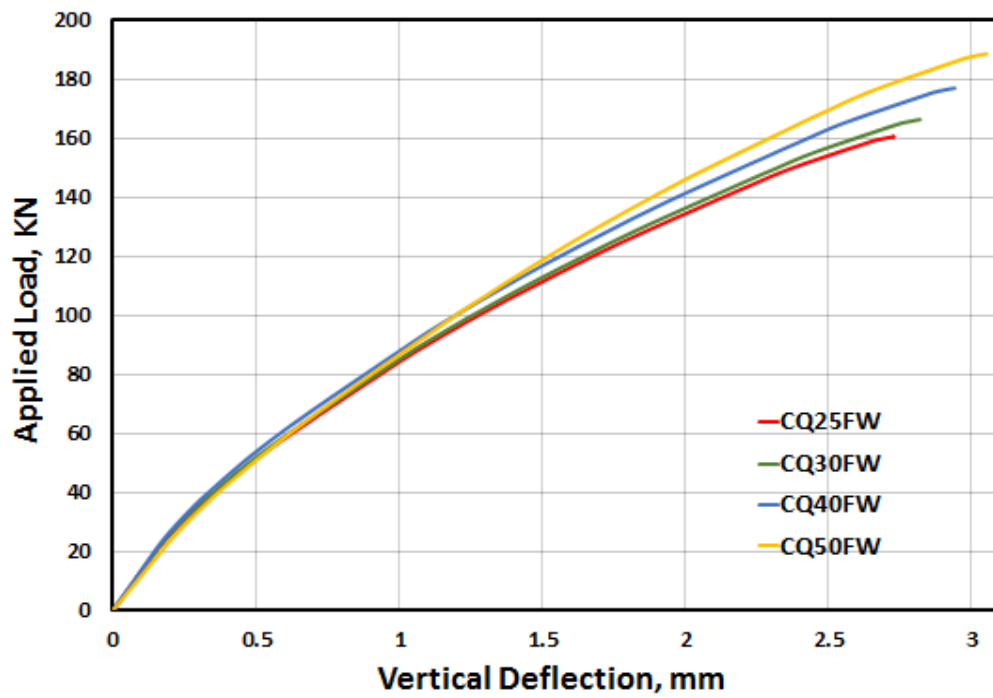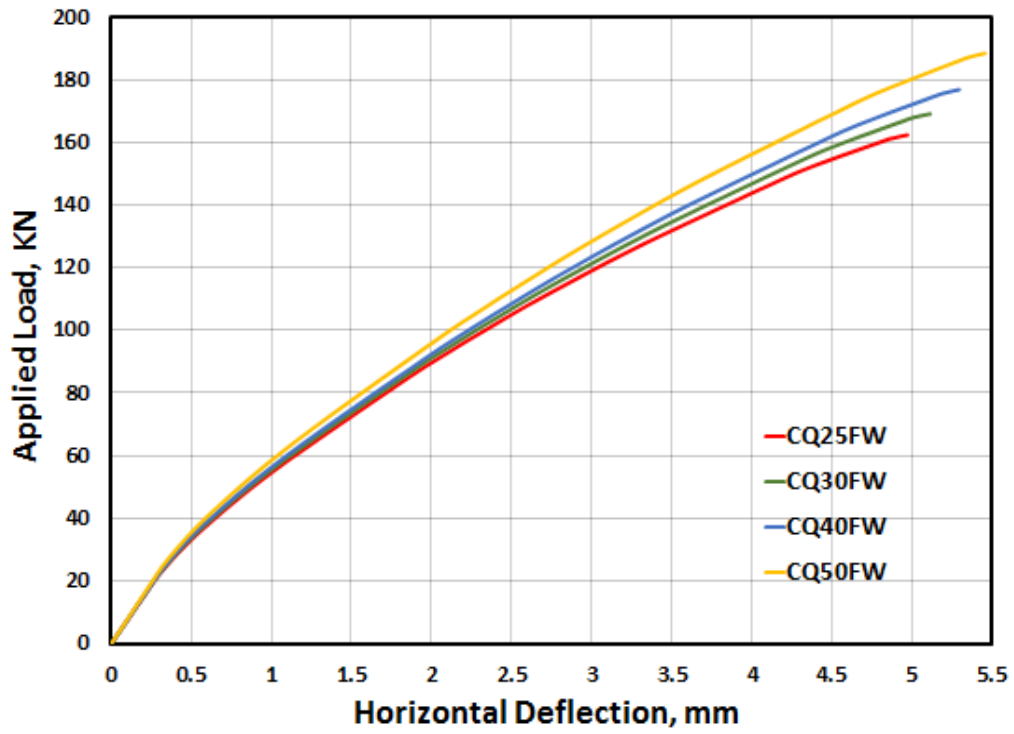
Fig. 5. 25. Impact of reducing the space between CFRP

5.8 Summary

1. By comparing the results of the ultimate load and the deflections for work experimental and numerical work , it was noted that they are identical, indicating that the numerical solution's results are valid.

2. Increasing the number of CFRP layers to two or three layers, presented in full longitudinal wrapping for all column faces, increased significantly the ultimate load capacity by 83.08% and 109.45%, respectively, compared with CC, Because of the effect of containment of concrete in the compressive and tension.

3. The ultimate load capacity increased with the decrease in the deflection ratio (e/h) from 0.5 to 0.35, which result an increase in axial load with decrease in bending moment.

4. A slight height in the ultimate load capacity was concluded when increasing the width for CFRP sheets for partial horizontal wrapping from 25 to 50 mm.

CHAPTER SIX
CONCLUSIONS AND RECOMMENDATIONS

6.1 Introduction

The behaviour of partially damaged HSC square cross-section short columns strengthened with the wrapping of CFRP sheets technique by various schemes was investigated in this work. The work involves experimental work and numerical study. The former dealt with testing strengthened columns experimentally, and the latter used a non-linear finite element (ABAQUS (2019) program to predict the overall behaviour for various cases. The conclusions obtained from the experimental and numerical results are illustrated in this chapter and the recommendation for future research.

6.2 Conclusions

This part presented the main conclusions noticed for each stage of the work (experimental and theoretical results obtained) for the partially damaged HSC columns strengthened with various schemes of wrapping by CFRP .

6.2.1 Experimental and Analysis Conclusions

1. Full longitudinal wrapping with CFRP for all column faces, increased the ultimate load capacity significantly by 65.55 and 44.83%, respectively, compared with CC. Also, both the ductility index and the stiffness increased to 1.78, 1.78, 53.17, and 52.31 according to the horizontal load-deflection data and 1.53, 1.52, 73.68, and 74.62 for the vertical load-deflection data, respectively;

2. Strengthening by using CFRP sheets wrapping, which is presented in full longitudinal wrapping with CFRP for tension side only, increased the ultimate load capacity by 44.82 and 37.93%, respectively, compared with CC, in addition to the increase that occurred to the ductility index and stiffness;

3. Full horizontal wrapping with CFRP for clear column height, increased the ultimate load capacity by 24.14 and 13.79%, respectively, in comparison to CC. Also, both the ductility index and the stiffness increased as well;

4. An increment in the ultimate load capacity by 20.69 and 10.34%, was recorded in partial horizontal wrapping with CFRP, respectively, compared with CC, in addition to an increase in the ductility index and stiffness;

5. The values of the horizontal load-deflection curves gave the highest ductility index for the samples strengthened with CFRP compared to the vertical load-deflection curves. In contrast, the vertical load-deflection curves showed higher stiffness values from horizontal load-deflection.

6. It was observed that strengthening the samples with CFRP in the longitudinal direction provides the highest strength ability repairing the damaged columns with the same material in the horizontal direction;

7. There was an increase in the stiffness and ductility index for all the strengthened specimens compared to the control column.

8. Crushing the concrete (compression failure of concrete) was the typical failure mode for specimens by partial CFRP wrapping . In contrast, the typical failure mode for specimens by fully wrapping of CFRP sheets was the rupture of CFRP.

9. An excellent convergence has been obtained between the experimental and theoretical results as the results were valid and agreed well with the experimental results.

10. The mean variation in the ultimate load efficiency and the overall load-horizontal and vertical deflection between FEA analysis and all specimens' experimental results were approximately 6.28%, 7.38% and 6.24 %, respectively, which confirmed the numerical solution's validity.

11. Increasing the number of CFRP layers to two or three layers, presented in full longitudinal wrapping with CFRP for all column faces, increased significantly the ultimate load capacity by 83.08 and 109.45%, respectively, compared with CC.

12. Increasing the number of CFRP layers to two or three layers to wrap CFRP sheets, presented in CHRF and CH25FW, improved the ultimate load capacity to 213.95, 226.85, 173.66, and 188.13 KN, respectively, in comparison with CC, which was 153.17 KN.

13. The ultimate load capacity for CC, CQFFL and CQRF increased with the decrease in the load eccentricity (e/h). The increments were 54.62%, 34.28% and 29.10%, respectively when in the eccentricity load (e/h) decreased from 0.5 to 0.35 while the strength ability for samples decreases as the eccentricity load (e/h) increases.

14. A slight reduction in the strength capacity was concluded when increasing the initial loading percentage for CC and CQFFL. However, the ultimate load capacity reduction reached 9.23% and 11.92%, for CC and CQFFL as the loading percentage increased from 50% to 80%, respectively.

15. A slight height in the ultimate load capacity was concluded when increasing the width for CFRP sheets for partial horizontal wrapping of CFRP sheets from 25mm to 50 mm.

6.3 Guidelines for Future Studies

1. Investigate the behaviour of partially short damaged self-compact concrete square cross-section columns using the same techniques of the current study under eccentric loads.

2. Study the behaviour of partially short damaged HSC square cross-section columns using the same techniques of the current study under impact loads.

3. Investigate the behaviour of partially short damaged columns using various types of concrete.

4. Consider studying the effect of higher volumetric stirrups reinforcement by changing the cross-section of the columns to increase the amount of the primary steel reinforcement under similar strengthening techniques.

5. Investigate the behaviour of short columns when using similar strengthening techniques without considering the damaged process on the columns.

References

ACI committe 318. (2019). Commentary on Building Code Requirements for Structural Concrete (ACI 318R-19).

ACI Committee 211. (2015), "Guide for Selecting Properties for High Strength Concrete with Portland Cement and Fly ash" ACI manual of concrete Practice (ACI 4R- 2015).

ACI Committee-363, "State of the Art Report on High Strength Concrete (ACI 363R-2019)", American Concrete Institute, Detroit, 2019.

Al-Nimry, H. S., and Al-Rabadi, R. A. (2019). Axial–Flexural Interaction in FRP-Wrapped RC Columns. International Journal of Concrete Structures and Materials, 13(1).

Alotaibi, K. S., and Galal, K. (2018). Experimental study of CFRP-confined reinforced concrete masonry columns tested under concentric and eccentric loading. Composites Part B: Engineering, 155, 257–271.

Alwash, N. A., and Jasim, A. H. (2015). Behaviour of Short Concrete Columns Reinforced By Cfrp Bars and Subjected To Eccentric Load. Technology, 6(10), 15–24.

ASTM C494: American Society of Testing Materials. (2013). Standard Specification for Chemical Admixtures for Concrete.

ASTM A615. (2016). Standard Specification for Deformed and Plain Carbon-Steel Bars for Concrete Reinforcement. American Society for Testing and Materials.

Ayub, T. Shafiq, N. and Nuruddin, M. F. (2014). Stress-strain Response of High Strength Concrete and Application of the Existing Models. Research Journal of Applied Sciences, Engineering and Technology, 8(10), 1174-1190.

BS 1881-116: (1983) 'Testing concrete — compressive strength of concrete cubes', British Standard Institution.

Buckle, I. G., and Friedland, I. M. (1994). Seismic Retrofit Manual for Highway Bridges. Lifelines and Highways, 249-258.

Chai, Y. H., Priestley, M. J. N., and Seible, F. (1994). Analytical Model for Steel-Jacketed RC Circular Bridge Columns. Journal of Structural Engineering, 120(8), 2358–2376.

Chellapandian, M. and Prakash, S. S. (2018). Rapid repair of severely damaged reinforced concrete columns under combined axial compression and flexure: An experimental study. Construction and Building Materials, 173, 368–380.

Chotickai, P., Tongya, P., and Jantharaksa, S. (2021). Performance of corroded rectangular RC columns strengthened with CFRP composite under eccentric loading. Construction and Building Materials, 268, 121-134.

Cusson, B. D., and Paultre, P. (1994). High-Strength Concrete Columns Confined by Rectangular Ties. California Institute of Technology, 120, 783–804.

El-Maaddawy, T., and El-Dieb, A. S. (2011). Near-Surface-Mounted Composite System for Repair and Strengthening of Reinforced Concrete Columns Subjected to Axial Load and Biaxial Bending. Journal of Composites for Construction, 15(4), 602–614.

Farghal, O.A., (2016). Structural performance of axially loaded FRP-confined rectangular concrete columns as affected by cross-section aspect ratio. HBRC Journal, 14(3).

Garzón-Roca, J., Adam, J. M., Calderón, P. A., and Valente, I. B. (2012). Finite element modelling of steel-caged RC columns subjected to axial force and bending moment. Engineering Structures, 40, 168–186.

Ghanim Jumah, G. (2019). Behaviour of High Strength Reinforced Concrete Hollow Circular Short Columns under Axial Loads. Diyala Journal of Engineering Sciences, 12(3), 95–102.

Hadhood, A., Mohamed, H. M., and Benmokrane, B. (2017). Experimental

Study of Circular High-Strength Concrete Columns Reinforced with GFRP Bars and Spirals under Concentric and Eccentric Loading. Journal of Composites for Construction, 21(2), 1-12.

Hadi, M. N. S. and Widiarsa, I. B. R. (2012). Axial and Flexural Performance of Square RC Columns Wrapped with CFRP under Eccentric Loading. Journal of Composites for Construction, 16(6), 640–649.

Hadi, M. N. S. (2006). Behaviour of FRP wrapped normal strength concrete columns under eccentric loading. Composite Structures, 72(4), 503–511.

Haji, M., Naderpour, H., and Kheyroddin, A. (2019). Experimental study on the influence of proposed FRP-strengthening techniques on RC circular short columns considering different types of damage index. Composite Structures, 209, 112–128.

Hassan, R. F., Sarsam, K. F., and Allawi, A. A. E. (2013). Behaviour of Strengthened RC columns with CFRP under Biaxial Bending. Journal of Engineering, 19(9), 1115–1126.

Hoshikuma, J. I. and Priestley, M. J. N. (2000). Flexural Behavior Of Circular Hollow Columns With A Single Layer Of Reinforcement Under Seismic Loading. STRUCTURAL SYSTEMS RESEARCH PROJECT, 13(59), 1–79.

Ibrahim, A. M., and Mahmood, M. S. (2009). Finite element modelling of reinforced concrete beams strengthened with FRP laminates. European Journal of Scientific Research, 30(4), 526–541.

Iraqi Specification No. 45, (1984)."Natural Sources for Gravel used in concrete and construction", Baghdad, Iraq.

Iraqi Specification No.5, (1984)."Portland Cement", Baghdad, Iraq.

Issa, M., Metwally, I. and Elzeiny, S. (2012). Performance of eccentrically loaded GFRP reinforced concrete columns. World Journal of Engineering, 9(1), 71–78.

Jiang, C., and Wu, Y. F. (2020). Axial strength of eccentrically loaded FRP-

confined short concrete columns. Polymers, 12(6), 32–41.

Kottb, H. A., El-Shafey, N. F., and Torkey, A. A. (2015). Behaviour of high strength concrete columns under eccentric loads. Housing and Building National Research Center Journal, 11(1), 22–34.

Kusumawardaningsih, Y., and Hadi, M. N. S. (2010). Comparative behaviour of hollow columns confined with FRP composites. Composite Structures, 93(1), 198–205.

Lignola, G. P., Prota, A., Manfredi, G., and Cosenza, E. (2007). Experimental Performance of RC Hollow Columns Confined with CFRP. Journal of Composites for Construction, 11(1), 42–49.

Lin, G., and Teng, J. G. (2016). Numerical simulation of cyclic/seismic lateral response of square RC columns confined with fibre-reinforced polymer jackets. 481–489.

Maaddawy, T. El. (2009). Strengthening of Eccentrically Loaded Reinforced Concrete Columns with Fiber-Reinforced Polymer Wrapping System: Experimental Investigation and Analytical Modeling. Journal of Composites for Construction, 13(1), 13–24.

Material Data Sheet. (2017a) 'Sikadur®-330', pdf Egypt-El Abour City (May), pp. 2–5.

Material Data Sheet. (2017b) 'SikaWrap ® -231 C Woven Unidirectional Carbon Fibre Fabric, (March), pp. 2–5.

Material Data Sheet.(2015)'Sika ViscoCrete® -5930.pdf' Egypt-El Abour City: Feb, pp. 1–2.

Material Data Sheet.(2015)'Sika® Fume S 92 D, "Concrete Additive Based on Silica Fume," Prod. Data Sheet Ed. 01.

Obaidat, Y. T. (2019). Evaluation for RC column confined partially with externally FRP wrapping sheet using nonlinear FE analysis. Materials Science Forum, 972, 129–133.

Olivova, K., and Bilcik, J. (2009). Strengthening of Concrete Columns With

CFRP. Slovak Journal of Civil Engineering, 1, 1–9.

Othman, Z. S., and Mohammad, A. H. (2019). Behaviour of Eccentric Concrete Columns Reinforced with Carbon Fibre-Reinforced Polymer Bars. Advances in Civil Engineering, 2019.

Ozbakkaloglu, T., and Saatcioglu, M. (2006). Seismic Behavior of High-Strength Concrete Columns Confined by Fiber-Reinforced Polymer Tubes. Journal of Composites for Construction, 10(6), 538–549.

Parvin, A., and Brighton, D. (2014). FRP composites strengthening of concrete columns under various loading conditions. Polymers, 6(4), 1040–1056.

Portolés, J. M., Romero, M. L., Bonet, J. L., and Filippou, F. C. (2011). Experimental study of high strength concrete-filled circular tubular columns under eccentric loading. Journal of Constructional Steel Research, 67(4), 623–633.

Pour, A. F., Ozbakkaloglu, T., Gholampour, A., and Zheng, J. (2017). FRP-confined high-strength concrete under eccentric compression. Proceedings of the 6th Asia-Pacific Conference on FRP in Structures, July, (1-5).

Sadeghian, P., Rahai, A. R., and Ehsani, M. R. (2010). Experimental Study of Rectangular RC Columns Strengthened with CFRP Composites under Eccentric Loading. Journal of Composites for Construction, 14(4), 443–450.

Sarafraz, M. E., and Danesh, F. (2012). New technique for flexural strengthening of RC columns with NSM FRP bars. Magazine of Concrete Research, 64(2), 151–161

Sharma, U. K., Bhargava, P., and Kaushik, S. K. (2005). Behaviour of confined high strength concrete columns under axial compression. Journal of Advanced Concrete Technology, 3(2), 267–281.

Christina, C., and Kent, G. (1998). SLENDER HIGH-STRENGTH CONCRETE COLUMNS SUBJECTED TO ECCENTRIC LOADING. J. Struct. Eng, 124, 233–240.

Taheri, A., Tasnimi, A. A., and Sarvghad Moghadam, A. (2020). Experimental

investigation on the seismic behaviour and damage states of reinforced high strength concrete columns. Structures, 27(May), 163–173.

Talaeitaba, S. B., Barati, E., and Eslami, A. (2020). Retrofitting of reinforced concrete columns using near-surface-mounted steel rebars and fibre-reinforced polymer straps under eccentric loading. Advances in Structural Engineering, 23(4), 687–701.

Torabian, D. M. and A. (2012). Experimental Study of Circular RC Columns Strengthened with Longitudinal CFRP Composites under Eccentric Loading: Comparative Evaluation of EBR and EBROG Methods. Journal of Composites for Construction, 16(0), 724–736.

Waleed A. Waryosh, Mohammed M. Rasheed, A. H. A. (2012). Experimental Study of Reinforced concrete Columns Strengthened with CFRP under Eccentric Loading Abstract : Journal of Engineering and Development, 16(3), 421–440.

Wu, Y. F., and Wei, Y. Y. (2010). Effect of cross-sectional aspect ratio on the strength of CFRP-confined rectangular concrete columns. Engineering Structures, 32(1), 32–45.

Yang, J., Wang, J., and Wang, Z. (2018). Rectangular high-strength concrete columns confined with carbon fibre-reinforced polymer (CFRP) under eccentric compression loading. Construction and Building Materials, 193, 604–622

Yazici, V. (2012). Strengthening hollow reinforced concrete columns with fibre reinforced polymers. University of Wollongong Thesis Collection, 153.

Yoshikawa, H., & Miyagi, T. (2001). Ductility and Failure Modes of Singly Reinforced Concrete Columns. Modeling of Inelastic Behavior of RC Structures Under Seismic Loads, 35–368.

Appendix A
Column Design

A. Design the ultimate load for the column

$a = 100\ mm, \qquad b = 100\ mm, \qquad d = 80\ mm, \qquad d' = 20\ mm$

$\dfrac{e}{h} = 0.5, \quad e = 50\ mm$

$fy = 380\ MPa, \qquad fc' = 70\ MPa,$

$Ag = Gross\ section\ area,$

$Ag = a * b = 10000\ mm^2,$

$As = \pi\, r^2\ , where,$

$As = As' = \pi\, 4^2 = 50.3\ mm^2$

$\rho = \dfrac{4 * \pi * 4^2}{10000} = 0.02 = 2\%$

clear cover=20 mm

4 Ø8 mm

Ø6 mm @ 100 mm

60

100

60

100
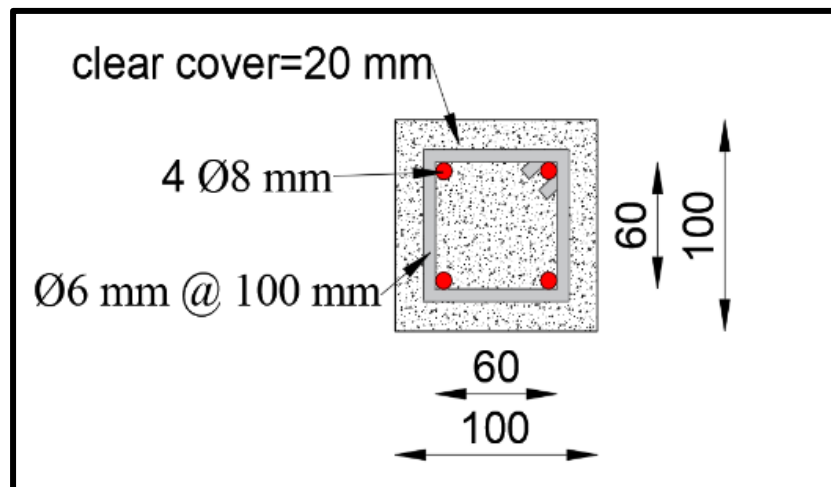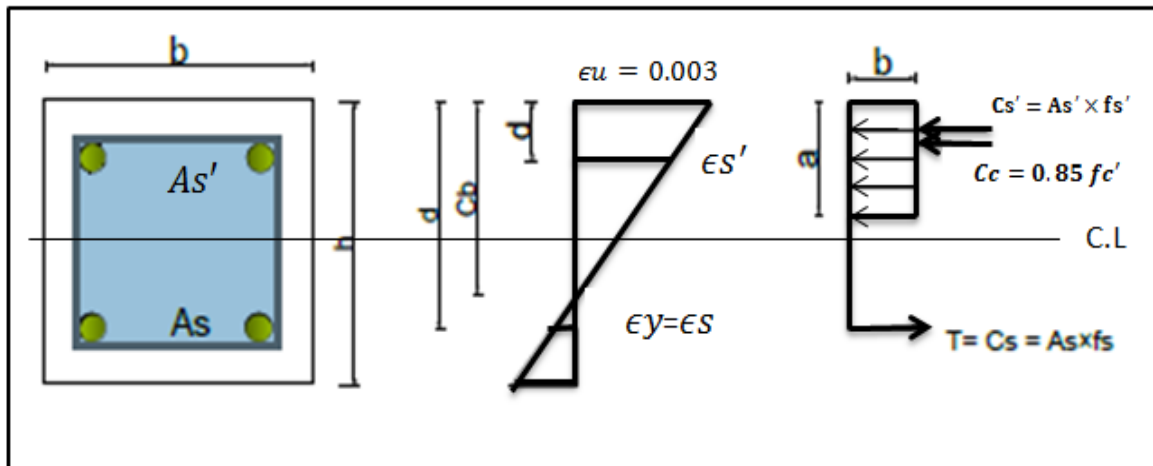
Fig. A. 1. Stress and strain distribution of the section

$$\frac{cb}{d} = \frac{\epsilon u}{\epsilon u + \epsilon y} \quad \rightarrow \quad \frac{cb}{d} = \frac{0.003}{(0.003 + fy)}$$

$$cb = \frac{600}{600 + 380}(80) = 49 \ mm$$

$$ab = \beta 1 \times cb = 0.85 \times 49 = 42 \ mm$$

$$fs' = \epsilon s' \times Es = \left(\frac{c - d'}{c}\right) \times \epsilon u \ Es = 200000 \times 0.003 \times \left(\frac{c - d'}{c}\right)$$

$$= 600\left(\frac{49 - 20}{49}\right) = 355 \ \text{Mpa} \ < fy = 380 \ \text{Mpa}$$

$$\therefore use \ fs' = 355 \ \text{Mpa}$$

$$fs = \epsilon s \times Es = \left(\frac{d-c}{c}\right) \times \epsilon u\, Es = 200000 \times 0.003 \times \left(\frac{d-c}{c}\right)$$

$$= 600\left(\frac{80-49}{49}\right) = 380 \text{ Mpa}$$

$$Cc = 0.85 \times fc' \times a \times b = (0.85 \times 70 \times 100 \times 42 \times 10^{-3}) = 249.9\, kN$$

$$Cs' = As' \times fs' = 100.5 \times 355 = 35.5\, kN$$

$$Cs = T = As \times fs = 100.5 \times 380 = 38\, kN$$

$$\sum FY = 0$$

$$Pnb = Cc + Cs' - Cs = 249.9 + 35.5 - 38 = 247.4\, kN$$

$$\sum M = 0$$

$$Mn = Cc\left(\frac{h}{2} - \frac{a}{2}\right) + Cs'\left(\frac{h}{2} - d'\right) + Cs\left(d - \frac{h}{2}\right)$$

$$Mn = 247.4(0.05 - 0.021) + 35.5(0.05 - 0.02) + 38(0.08 - 0.05)$$

$$= 9.38\, kN.m$$

$$eb = \frac{Mu}{Pu} = \frac{9.38}{247.4} = 38\, mm$$

$$but\,\frac{e}{h} = 0.5 \text{ , }(e)eccentrecity = 50\, mm\ > 38\, mm$$

$$assume\ C\ < Cb\ \ \rightarrow chosse\ C = 32mm\ < 49\, mm$$

$$ab = \beta 1 \times cb = 0.85 \times 32 = 27.2\, mm$$

$$fs' = 600\left(\frac{32-20}{32}\right) = 225\, Mpa\ < fy = 380 \text{ Mpa}$$

$$\therefore\ \text{use}\ fs' = 225 \text{ Mpa}$$

$$fs = 600 \left(\frac{80 - 32}{32} \right) = 900 \; Mpa \; > fy = 380 \; MPa$$

$\therefore use \; fs = 380 \; Mpa$

$Cc = 0.85 \times fc' \times a \times b = (0.85 \times 70 \times 100 \times 27.2 \times \; 10^{-3}) = 160.6 \; kN$

$Cs' = As' \times fs' = 100.5 \times 225 = 22.6 \; kN$

$Cs = T = As \times fs = 100.5 \times 380 = 38 \; kN$

$Pnb = Cc + Cs' - Cs = 160.6 + 22.6 - 38 = 145.2 \; kN$

$Mn = 145.2(0.05 - 0.0136) + 22.6(0.05 - 0.02) + 38(0.08 - 0.05)$

$$= 7.13 \; KN.m$$

$$eb = \frac{Mu}{Pu} = \frac{7.13}{145.2} = 49.2 \; mm \cong 50 \; mm$$

$\therefore at \; eccentrecity \; (e) = 50 \; mm$

$The \; specimen \; failure \; when \; ultimate \; load \; (pu) = 145.2 \; KN$

Appendix B
The properties of the materials

B-1 Cement

Table B. 1. Cement Chemical Properties*

Compound composition	Chemical composition	Weight (%)	Iraqi Limitations No. 5/1984
Lime	CaO	61.07	------------
Silica	SiO_2	20.24	------------
Alumina	Al2O$_3$	5.41	------------
Iron oxide	Fe2O$_3$	3.48	------------
Magnesia	MgO	2.49	$\leq 5\%$
Sulfate	SO_3	2.1	$\leq 2.5\%$ if C3A$<$ 5% $\leq 2.8\%$ if C3A$>$ 5%
Loss on ignition	L.O.I	1.43	$\leq 4\%$
Insoluble residue	I.R	0.68	$\leq 1.5 \%$
Lime saturation factor	L.S.F	0.83	0.66-1.02
Tricalcium aluminates	C_3A	8.78	------------
Tricalcium silicate	C_3S	41.33	------------
Diacalcium silicate	C_2S	29.1	------------
Tricalcium alumina ferrite	C_4AF	9.12	------------

* These results were performed in the Najaf construction Laboratory

Table B. 2. Cement Physical Properties*

Physical Properties	Test Result	Iraqi Limitations No. 5/1984, %
Setting Time, min,	132 Initial	≥ 45
	185 final	≤ 600
Fineness (Blaine), m^2/kg	354	≥ 230
Compressive strength at 3-days (MPa)	24.5	>15
Compressive strength at 7-days (MPa)	34.0	>23

* These results were performed in the Najaf construction Laboratory.

B.2 Sand (Fine Aggregate)

Table B. 2. Fine Aggregate Test Results *

Sieve size (mm)	Cumulative Passing %	Passing accumulated %Limits of Iraqi specifications No. 45/1984, zone(3)
10	100	100
4.75	97	90 - 100
2.36	91	85 - 100
1.18	85	75 – 90
0.60	76	60 – 79
0.30	45	12 – 40
0.15	10	0 – 10
Materials passing from sieve 75 µ %= 3.6% (specification requirements up to 5%)		
SO3 content=0.364% (specification requirements up to 0.5%)		

* These results were performed in the Najaf construction Laboratory.

B.3 Gravel (Coarse Aggregate)

Table B. 4. Coarse Aggregate Test Result*

Sieve size(mm)	passing %	Specification limits Iraqi specification No. 45/1984, %
37.5 (1.5 in)	----	-
19 (3/4 in)	100	100
12.5 (1/2 in)	98	90-100
10 (3/8 in)	62	50-85
4.75 (No. 4)	3	0 – 10
Mechanical wear =16.1% ((specification requirements up to 35%)		
Materials passing from sieve 75 µ %= 0.29% (specification requirements up to 3%)		
SO3 content=0.03% (specification requirements up to 0.1%)		

* These results were performed in the Najaf construction Laboratory.

B.4 Sika® Fume S 92 D (Silica fume)

Table B. 5. Sika ViscoCrete ® -5930 Chemical content*

Oxide	Content %
SiO2	Approximately 90% minimum
SO3	Approximately 0.2% maximum
CaO Approximately 0.8% maximum	Approximately 0.8% maximum
Cl-	Approximately 0.035% maximum

(*) The manufacturer provides this data

Table B. 6. Sika ViscoCrete ® -5930 Physical properties*

Physical properties	
Surface area	Approximately 24 000 – 28 000 m²/kg
Variation Average Fineness	Approximately 2% maximum
Pozzolanic Activity Index (28d)	Approximately 105% minimum
Grading – below 1μm	Minimum 90%

(*) The manufacturer provides this data

B.5 Sika ViscoCrete-5930 (Superplasticizer)

Table B. 7. Sika ViscoCrete ® -5930 Technical details*

Property	Description or Value
Basis	An aqueous solution of modified polycarboxylate
Appearance	Turbid liquid
Density (kg /lt)	1.095
Boiling	100 ^{0} C
PH	7-9
Recommended dosage	0.2-0.8 %, NC cement litter by weight
	0.8-2 %, NC cement litter by weight

(*) The manufacturer provides this data

B.6 Sika Wrap®-300 C

Table B. 8. Sika Wrap ® -300 C (Carbon Fiber Sheets) properties*

Fibre type	High strength carbon fibres
Fibre orientation	0∘ (unidirectional). The fabric is equipped with special weft fibres which prevent Loosening of the roving (heat-set process)
Dry Fiber Density	1.82 g/cm^3
Fabric design thickness	0.167 mm
Tensile strength of fibres	3500 MPa
Tensile modulus of fibres	230 000 MPa
Elongation at break	1.7 %
Fabric length/roll	≥ 100 m
Fabric width	500 mm

(*) The manufacturer provides this data

B.7 Epoxy Resin type (Sikadur-330)

Table B. 9. Sikadur-330 Properties ((Resin impregnated) *

Appearance	Comp. a: white Comp. b: grey
Density	1.31 kg/l (mixed)
Mixing ratio	A : B = 4 : 1 by weight
Open time	30 min (at + 35∘ C)
Viscosity	Pasty, not flowable
Application temperature	+ 15∘ C to + 35∘ C (ambient and substrate)
Tensile strength	30 MPa (cured 7 days at +23∘ C)
Flexural E-modulus	3800 MPa (cured 7 days at +23∘ C)

(*) The manufacturer provides this data

Appendix C
Ingredients used in ABAQUS Program

C. 1 Ingredients used in ABAQUS Program

Table C. 1. General Features of concrete

Column symbol	Compressive strength (MPa)	Young modules (MPa)	Poisson Ratio (v)
CC			
CQFFL			
CQRF	70	32000	0.18
CQFFW			
CQ25FW			
CHFFL			
CHRF			
CHFFW			
CH25FW			

Table C. 2. Damaged concrete plastics parameters

Dilation angle	Eccentricity	Fb0/fc0	k	Viscosity parameter
36	0.1	1.16	0.667	1E-07
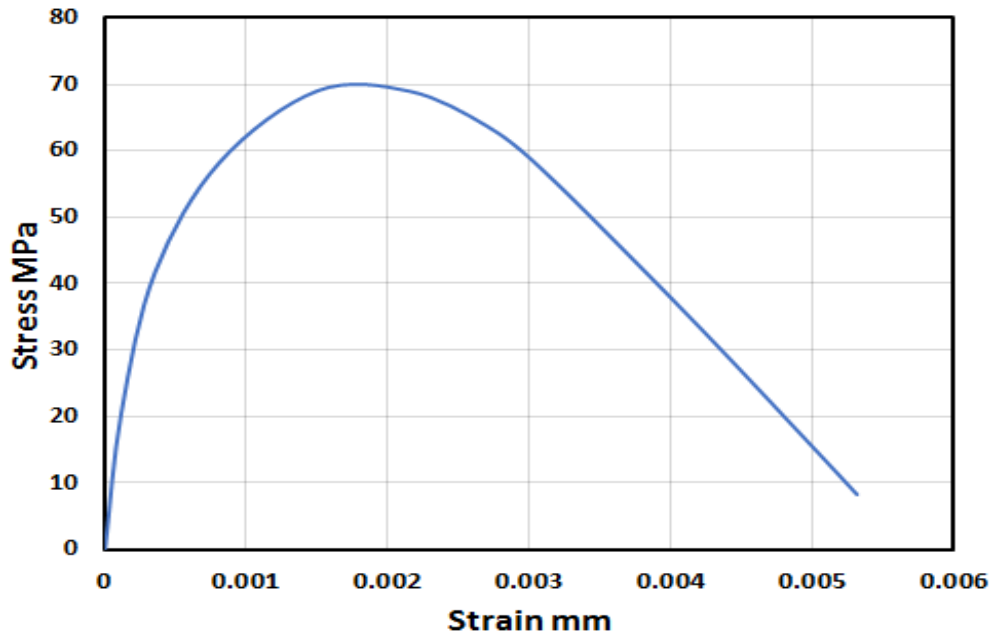
Fig. C. 1. Model of stress-strain relationship used in this research (Ayub, 2014)

Table C. 3. The stress-strain relationship used in this research

Number	Yield stress (MPa)	Plastic strain (mm)
1	0	0
2	20.48	0.0001141
3	41.65	0.0003521
4	58.25	0.0008094
5	69.02	0.001501
6	68.95	0.002154
7	63.55	0.002695
8	57.25	0.003085
9	35.54	0.004105
10	15.55	0.004995
11	8.25	0.005314

Table C. 4. Steel plastic properties

Ingredients	Diameter (mm)	Yield stress (MPa)	Plastic strain (mm)
Steel bar	6	360	0
		495	0.0056
Steel bar	8	380	0
		570	0.0085

Table C. 5. Technical data of CFRP sheets

Ingredients	Dry Fiber Modulus of Elasticity in Tension(MPa)	Dry Fiber Tensile Strength (MPa)	Laminate Nominal Thickness (mm)
CFRP	230 000	3500	0.167

Table C. 6. Epoxy (filling material) properties (Belal Almassri, 2013)

Ingredients	Compressive strength (MPa)	Tensile Strength (MPa)	Young modules (MPa)
Epoxy	80	30	3800

C. 2 Mises
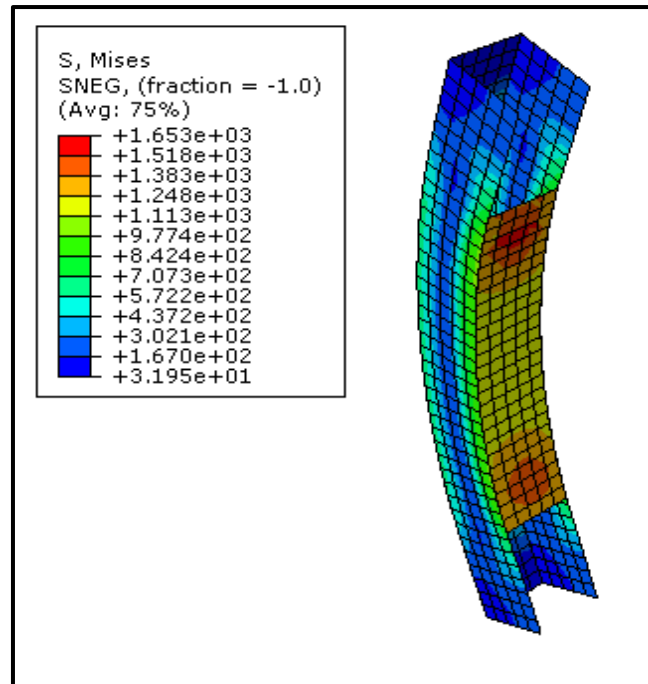
Fig. C. 2. The distribution of the stress of CFRP sheets for CQFFL specimen
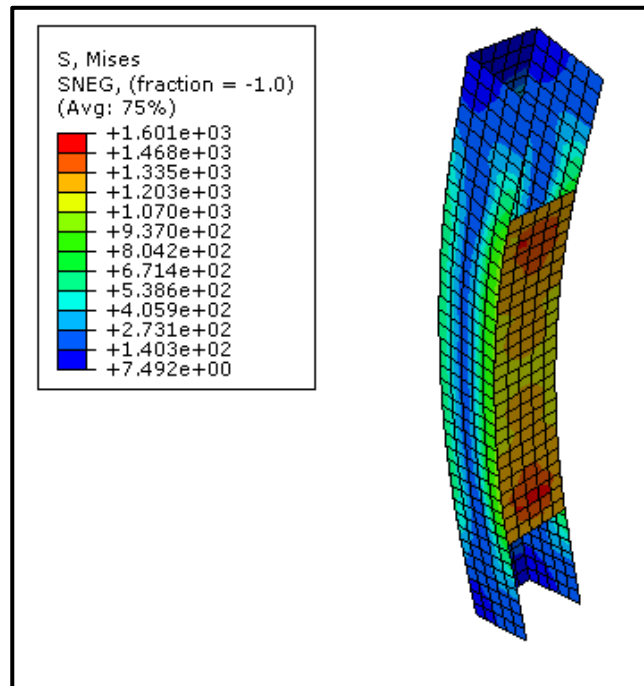
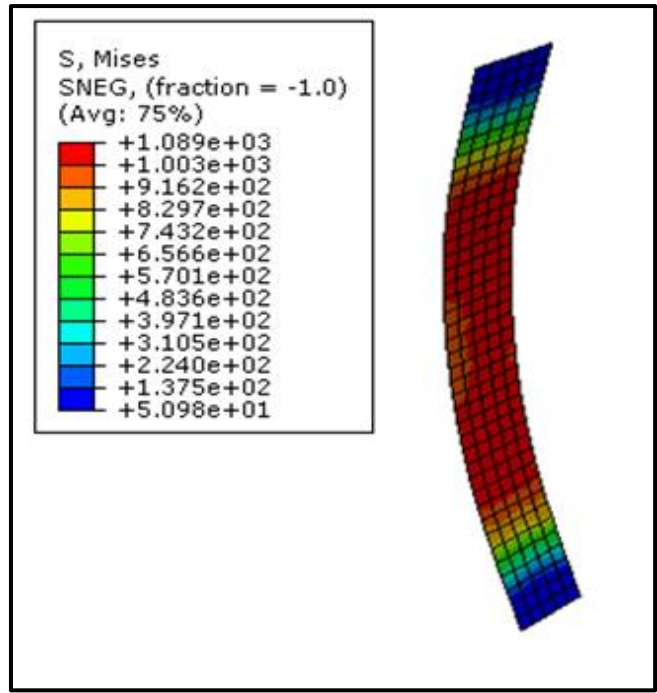**Fig. C. 3. The distribution of the stress of CFRP sheets for CHFFL specimen**

Fig. C. 4. The distribution of the stress of CFRP sheets for CQRF specimen
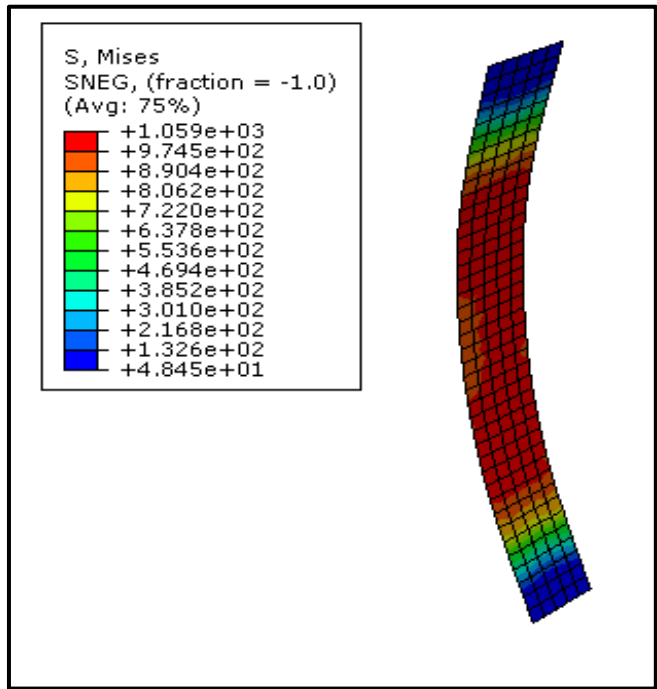

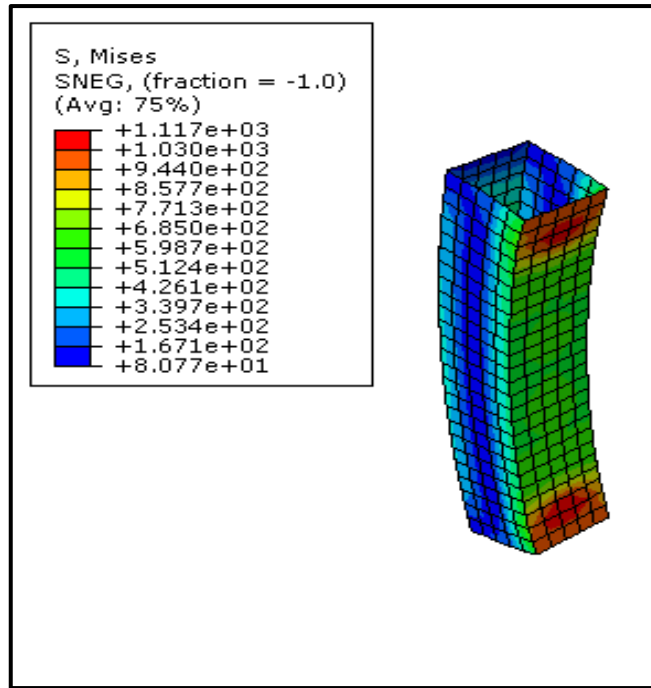**Fig. C. 5. The distribution of the stress of CFRP sheets for CHRF specimen**

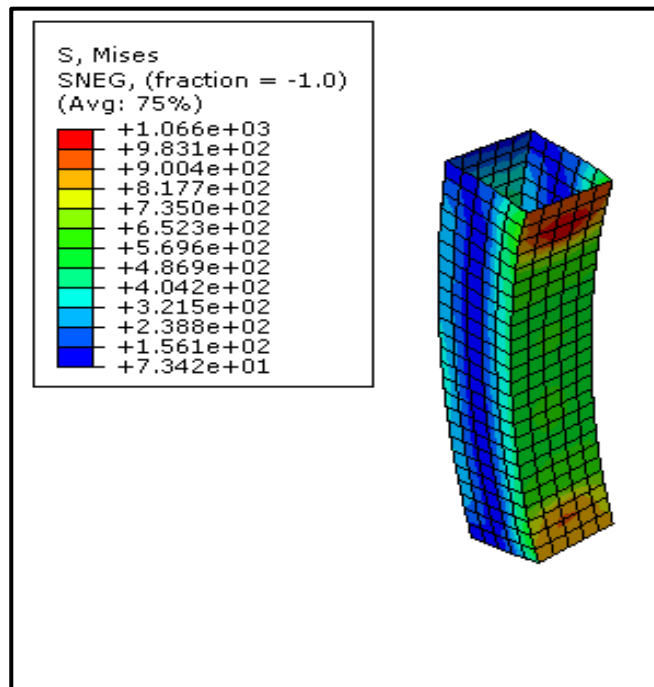**Fig. C. 6. The distribution of the stress of CFRP sheets for CQFFW specimen**

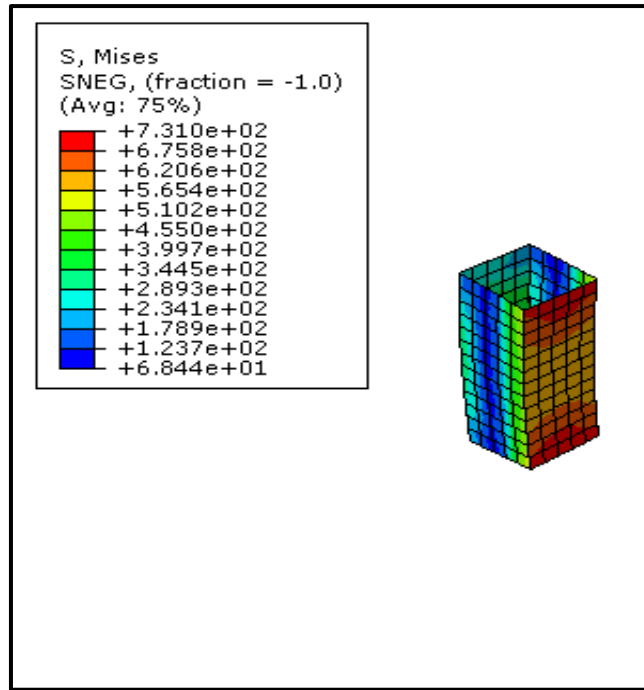**Fig. C. 7. The distribution of the stress of CFRP sheets for CHFFW specimen**

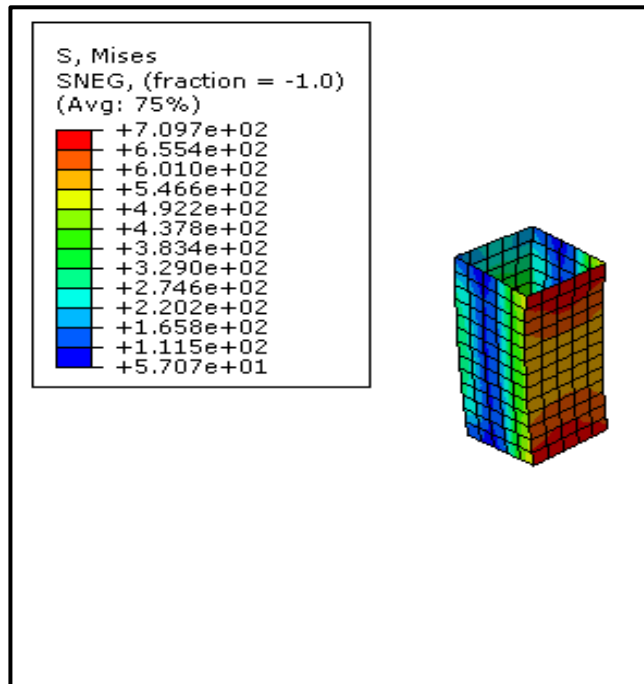**Fig. C. 8. The distribution of the stress of CFRP sheets for CQ25FW specimen**

Fig. C. 9. The distribution of the stress of CFRP sheets for CH25FW specimen
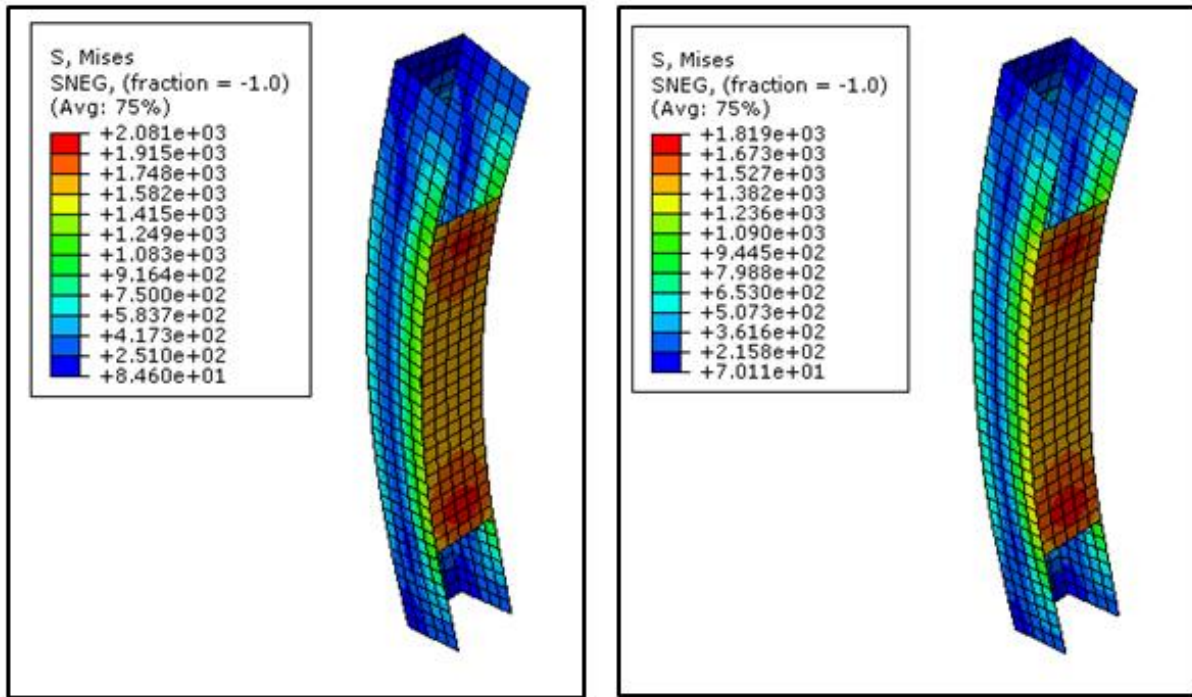
Fig. C. 10. The stress of CFRP for the impact of the number of layers on CQFFL. Two layers (right). Three layers (left)
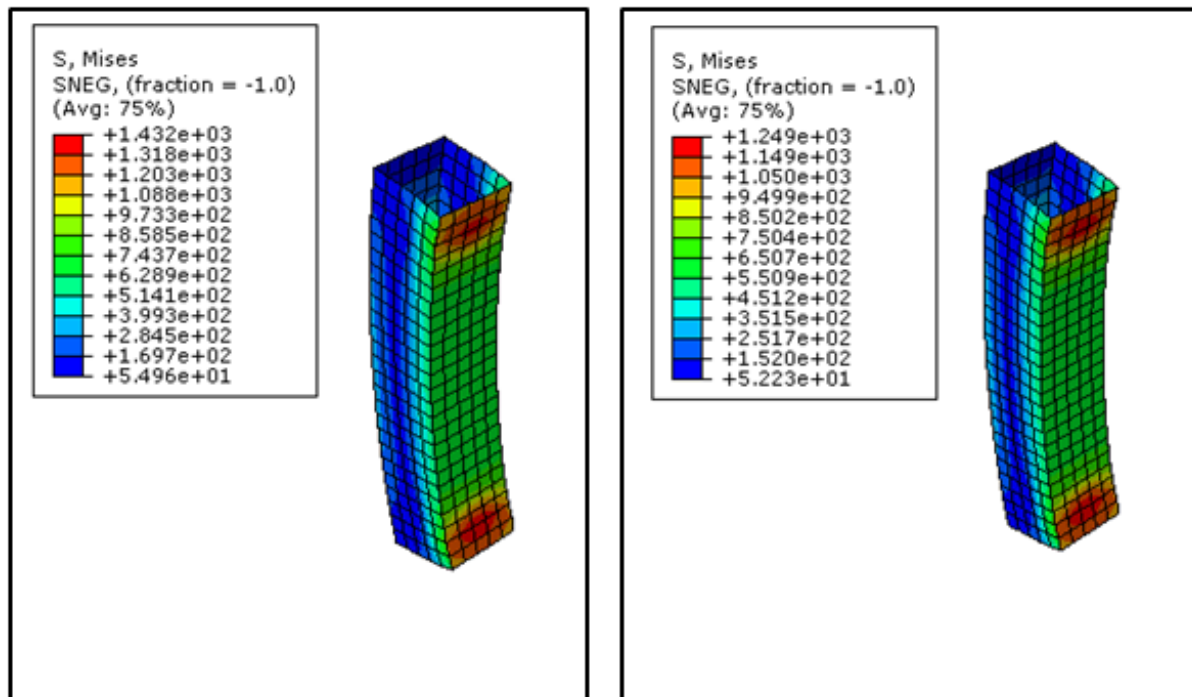

Fig. C. 11. The stress of CFRP for the impact of the number of layers on CQFFW. Two layers (right). Three layers (left)
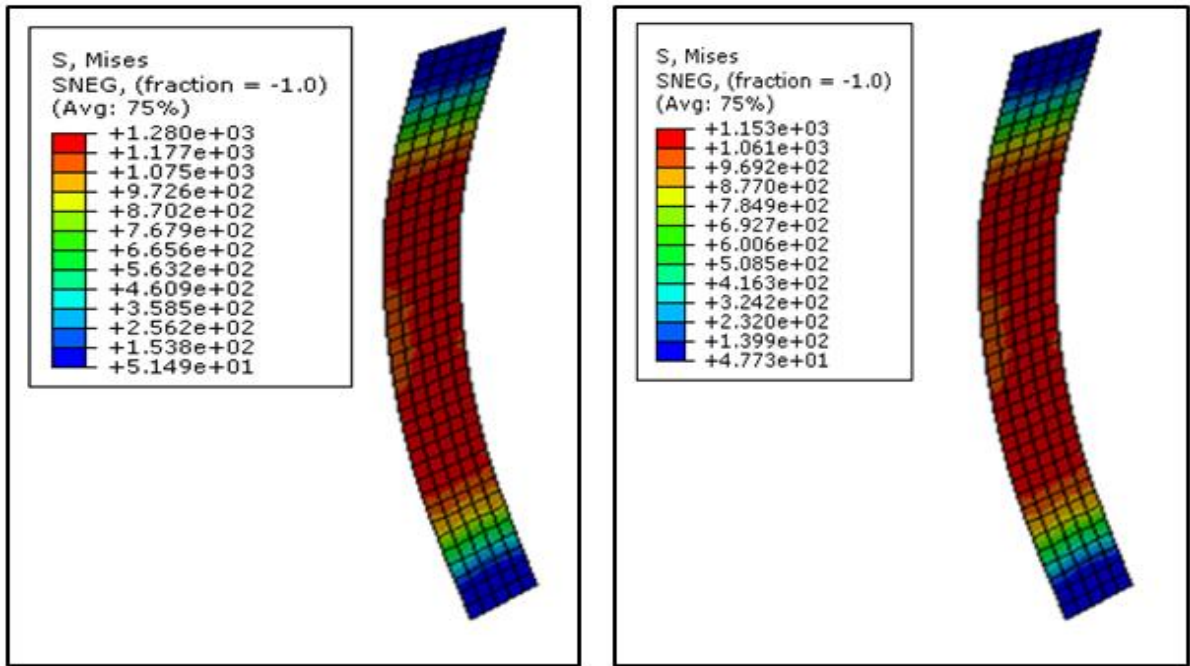
Fig. C. 12. The stress of CFRP for the impact of the number of layers on CHRF. Two layers (right). Three layers (left)
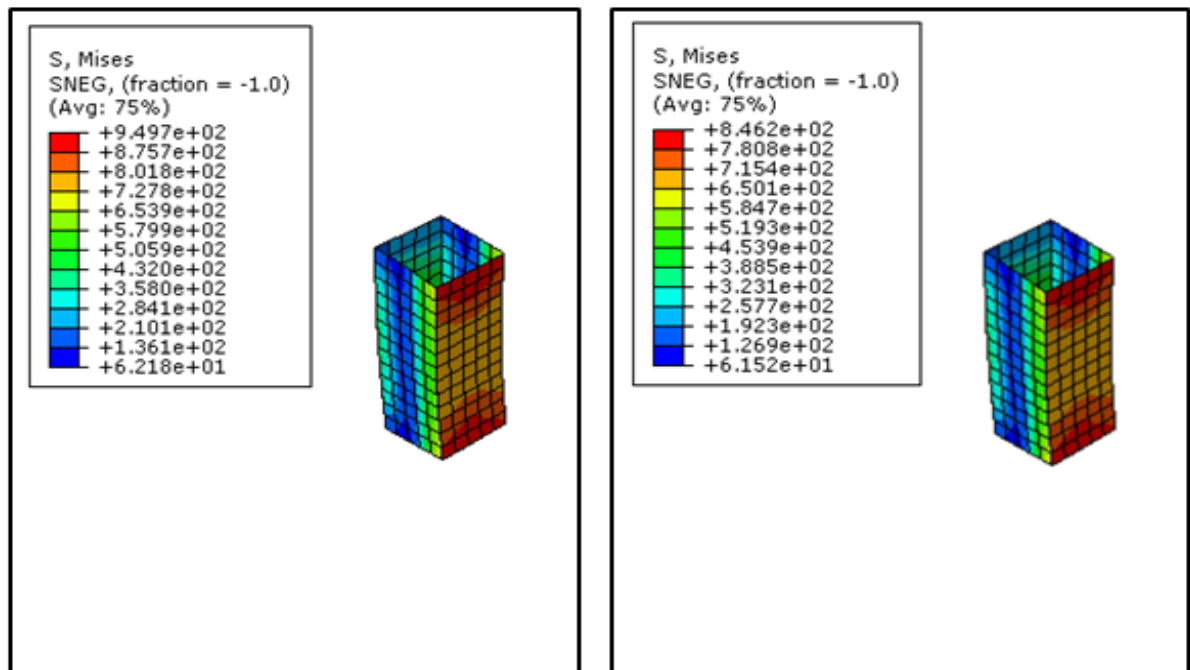

Fig. C. 13. The stress of CFRP for the impact of the number of layers on CH25FW. Two layers (right). Three layers (left)

الخلاصه

أصبحت عملية التقوية لأي عضو أنشائي ، مثل الأعمدة ، واحدة من أكثر الحلول القياسية لترميم المباني في العالم ، والتي يمكن تنفيذها لعدة أسباب ، بما في ذلك: التغيير في الاستخدام ، والفشل في حديد التسليح ، والأحمال الزائدة و / أو الظروف الجوية القاسية. يهدف هذا البحث إلى دراسة السلوك الإنشائي التجريبي والعددي للأعمدة الخرسانية القصيرة عالية القوة المحملة جزئياً والمقواة بشرائط CFRP. في هذه الدراسة ، تم تحضير تسعة أعمدة ذات مقطع عرضي مربع (١٠٠ × ١٠٠) ملم وارتفاع ٨٠٠ ملم برأسين كوربيل واختبارها تحت حمل لا مركزي مع انحراف ٥٠ ملم من المركز (0.5 = e / h) . تم اختبار أحد الأعمدة للفشل وتم اعتباره عمود تحكم ، والذي تم تحديده بـ CC ، . في المقابل ، تم تقسيم الأعمدة الثمانية الأخرى إلى مجموعتين من أربعة أعمدة متطابقة. تم تحميل المجموعة الأولى من الأعمدة بنسبة ٢٥٪ من أحمال التصميم النهائية ، بينما تم تحميل المجموعة الثانية بنسبة ٥٠٪. بعد ذلك ، تم تقوية جميع العينات المحملة جزئيًا في المجموعتين بمخططات مختلفة من CFRP بناءً على نسب التحميل الأولية ، والتي يتم تمثيلها على النحو التالي: التفاف كامل بالاتجاه الطولي مع CFRP لجميع جوانب العمود ، التفاف طولي كامل مع CFRP لجانب الشد فقط ، التفاف كامل بالاتجاه الافقي مع CFRP لارتفاع العمود الصافي والتفاف أفقي جزئي مع CFRP بطول ٢٥٠ ملم عند منتصف ارتفاع العمود.

النتائج التجريبية للعينات المقواة بلف كامل بالاتجاه الطولي من جميع الجوانب ولجانب الشد فقط للأعمدة في المجموعة الأولى سجلت زيادة في سعة الحمولة القصوى بنسبة ٦٥.٥٥٪ و ٤٤.٨٢٪ على التوالي ، مقارنة بـ CC. بالإضافة إلى ذلك ، زادت سعة التحميل القصوى للأعمدة المقواة في المجموعة الثانية بنفس المخططات المعززة بنسبة ٤٤.٨٣٪ ، ٣٧.٩٣٪ على التوالي ، مقارنة بـ CC. علاوة على ذلك ، زادت سعة الحمل القصوى للعينات المعززة بالتغليف الأفقي الكامل أو الجزئي للمجموعتين بنسبة ٢٤.١٤ و ٢٠.٦٩ و ١٣.٧٩ و ١٠.٣٤٪ على التوالي.

تم استخدام طريقة العناصر المحددة (ABAQUS) للتحقق من السلوك الإنشائي للأعمدة المربعة القصيرة عالية القوة المحملة جزئياً والمدعومة بشرائط CFRP ، والتي تم اختبارها تجريبياً في وقت سابق. أظهرت النتائج وجود توافق جيد بين النتائج التجريبية والعددية فيما يتعلق بسعة الحمل القصوى ومنحنيات الانحراف الأفقي والرأسي. كان متوسط الفرق في سعة الحمولة القصوى والحد الأقصى للانحراف الأفقي والرأسي (٦.٢٨٪ ، ٧.٣٨٪ ، ٦.٢٤٪) على التوالي ، مما يضمن دقة الحل العددي.

تم اقتراح معلمات إضافية ليتم فحصها عدديًا بواسطة النموذج الذي تم التحقق منه: تأثير زيادة طبقات CFRP ، وتأثير الانحرافات المختلفة للحمل (e / h) ، وتأثير معدلات التحميل الأولية المختلفة ، وتأثير زيادة العرض لـ CFRP. أوضحت النتائج العددية أن زيادة عدد طبقات CFRP إلى طبقتين أو ثلاث طبقات والمقدمة في غلاف طولي كامل مع CFRP لجميع أوجه الأعمدة زاد بشكل كبير من سعة التحميل القصوى بنسبة ٨٣.٠٨٪ و ١٠٩.٤٥٪ على التوالي ، مقارنة بـ CC. اضافة لذلك ، أدى انخفاض انحراف الحمل اللامركزي (e / h) من (٠.٥ إلى ٠.٣٥) إلى الحصول على حمولة نهائية عالية بنسبة ٥٤.٦٢٪ للعينات المقواة بالاتجاه الطولي بالكامل. من ناحية أخرى ، أدت زيادة نسبة التحميل الأولي من ٥٠٪ إلى ٨٠٪ إلى انخفاض طفيف في الحمل النهائي بنسبة ٩.٢٣٪ و ١١.٩٢٪ ، على التوالي ، لعمود التحكم والعينات المقواة بالكامل بالاتجاه الطولي بشرائط CFRP. علاوة على ذلك ، أدى زيادة عرض شرائط CFRP للتغليف الأفقي الجزئي إلى زيادة طفيفة في الحمل النهائي.

.

جمهورية العراق

وزارة التعليم العالي و البحث العلمي

جامعة كربلاء /كلية الهندسة

قسم الهندسة المدنية

السلوك الإنشائي للأعمدة الخرسانية المسلحة المتضررة عالية القوة التي تم إعادة تأهيلها بواسطة CFRP تحت التحميل اللامركزي

رسالة مقدمة الى

قسم الهندسة المدنية في كلية الهندسة /جامعة كربلاء

كجزء من متطلبات نيل شهادة الماجستير في علوم الهندسة المدنية –

مدني عام

من قبل

احمد حسن جبار

(بكالوريوس في الهندسة المدنية ـ جامعة الكوفة ـ ٢٠٠٣)

اشراف

أ.م.د .سجاد عامر حمزه

أ.م.د .وجدي شبر صاحب

٢٠٢١م

١٤٤٣هـ